

Republic of Iraq
Ministry of Higher Education and Scientific Research
University of Misan/Collage of Engineering
Department of Civil Engineering



NUMERICAL STUDY ON FLEXURAL BEHAVIOR OF SLABLESS REINFORCED CONCRETE STAIRCASES

By

Rafal Saeed Sabeh

B.Sc. civil engineering, 2020

A THESIS

Submitted in Partial Fulfillment of the

Requirements for the Degree of

Master of Science/Master of Structural Engineering

(in Civil Engineering)

Supervisor Name: Prof. Dr. Abdulkhaliq Abdulyimah Jaafar

بِسْمِ اللَّهِ الرَّحْمَنِ الرَّحِيمِ

{وَقُلْ رَبِّ زِدْنِي عِلْمًا}

[سورة طه، 114]

صدق الله العظيم

ABSTRACT

This study presents a comprehensive numerical investigation into the flexural performance of reinforced concrete (RC) slabless staircases. Initially, a finite element (FE) modeling strategy was developed and validated through a series of nonlinear simulations conducted using ABAQUS software. These simulations were benchmarked against experimental results from prior studies available in the literature. The validation outcomes confirmed a strong correlation between the FE models and experimental findings, particularly in terms of load–deflection behavior and crack propagation patterns. The main parameters investigated concrete compressive strength (f'_c), CFRP strengthening scheme, and type of reinforcing material. The results showed that various new triangular configurations for steel reinforcement provided different behavior. Placing triangular bars in zone S2 yielded a 29.2% increase in cracking load compared to 11.1% when placed in S1. For ultimate load, the increase ranged from 38.61 kN in ST to 40.47 kN in ST-M (an increase of 4.8%). When the triangular configuration was positioned in S2, the ultimate load increased by 18%, compared to 7.1% in S1. Models ST-L-R-1 and ST-L-R-4 demonstrated increases of 14.5% and 12.9%, respectively. Deflection increased by 78.2% in the S1 zone and by 69.2% in S2. In models ST-L-R-1 and ST-L-R-4, maximum deflection rose by 18.5% and 17.5% compared to ST. Removing planar bars decreased the cracking load by 30.1% in ST-M-WoP compared to ST-M, and by 19.2% and 30.9% in ST-L-WoP and ST-R-WoP, respectively. Ultimate load dropped by 5.5%, 2.1%, and 2.5% in the same models. Conversely, deflection increased by 10.9%, 8.9%, and 14.2%. Increasing concrete strength from 50 MPa to 70 MPa led to significant improvements. Cracking load increased by 58.3% in ST-M-70, 43.4% in ST-L-70, and 78.9% in ST-R-70. Ultimate load rose by 63.8%, 79.2%, and 109.5%, respectively. The impact of replacing steel with CFRP bars and

sheets was investigated. Using CFRP bars in S2 (ST-CRS2) raised the cracking load by 85.5% compared to ST-50, while simultaneous reinforcement in both S1 and S2 (ST-CRS1-2) increased cracking load by 103.7%. Full replacement of steel with CFRP bars (ST-CR) improved cracking load by 113.7%. For ultimate load, ST-CRS2 increased capacity by 62.2% over ST-50, and ST-CR improved by 72.36%. Replacing steel links between S1 and S2 with CFRP bars (ST-CRL) led to an 8.9% increase. Using CFRP sheets also provided significant gains. Models ST-CS-5, ST-CS-10, and ST-CS-15 showed cracking load increases of 28.9%, 31.84%, and 44.5%, respectively, while full wrapping (ST-CS-F) increased cracking load by 77.35% and ultimate load by 67.8%. Deflection decreased significantly by 48.2% with full wrapping. Adding a one-meter landing in the staircase midspan (ST-Ln) reduced cracking load by 19% and ultimate load by 29% compared to the reference slab without a landing. The highest ductility index (5.17) was found in ST. Increasing concrete strength reduced ductility by 14.4%, 44%, and 42.3% in ST-M-70, ST-L-70, and ST-R-70, respectively. Replacing steel with CFRP bars reduced ductility by 14.1% to 15.1%. CFRP sheets caused further reductions of 16.9% to 30.5%. Initial stiffness increased by 66.1%, 127%, and 142.25% as concrete strength rose to 50 MPa, and by 185% when CFRP reinforcement fully replaced steel with steel stirrups retained. This research concluded that the effectiveness of new reinforcement strategies particularly CFRP for improving the flexural capacity of slabless staircases, though with some reduction in ductility.

SUPERVISOR CERTIFICATION

I certify that the preparation of this thesis entitled " **Numerical Study on Flexural Behavior of Slabless Reinforced Concrete Staircases** " was presented by "**Rafal saeed sabeeh**", and prepared under my supervision at The University of Misan, Department of Civil Engineering, College of Engineering, as a partial fulfillment of the requirements for the degree of Master of Science in Civil Engineering (Structural Engineering).

Signature:

Prof. Dr. Abdulkhaliq Abdulyimah Jaafar

Date:

In view of the available recommendations, I forward this thesis for discussion by the examining committee.

Signature:

Assist Prof. Dr. Murtada Abass Abd Ali

(Head of Civil Eng. Department)

Date:

EXAMINING COMMITTEE'S REPORT

We certify that we, the examining committee, have read the thesis titled **(Numerical Study on Flexural Behavior of Slabless Reinforced Concrete Staircases)** which is being submitted by **(Rafal Saeed Sabeeh)**, and examined the student in its content and in what is concerned with it, and that in our opinion, it meets the standard of a thesis for the degree of Master of Science in Civil Engineering (Structures).

Signature:

Name: **Prof. Dr. Abdulkhaliq A. Jaafer**

(Supervisor)

Date: / /2025

Signature:

Name:

(Chairman)

Date: / /2025

Signature:

Name:

(Member)

Date: / /2025

Approval of the College of Engineering:

Signature:

Name: Prof. Dr. Abbas Oda Dawood

Dean, College of Engineering

Date: / /2025

Signature:

Name:

(Member)

Date: / /2025

ACKNOWLEDGEMENTS

First of all, all my thanks for **Allah** who led me during my way to complete this work.

I would like to express my cordial thanks and deepest gratitude to my supervisor **Prof. Dr. Abdulkhaliq A. Jaafer**, whom I had the honor of being under his supervision, for his advice, help, and encouragement during the course of this study.

I would like to extend my thanks to **Prof. Dr. Abbas O. Dawood** Dean of the college of engineering, and **Dr. Murtada Abbass** , the Head of Civil Engineering Department.

Special thanks go to **my father, mother** for their great efforts. Also, thanks go to **my husband, brothers, and sisters**.

Special thanks also go to **Asst. Lec. Ali Wathiq Abdulghani, Asst. Prof. Dr. Bahaa Hussain**, for their effort in helping me in ABAQUS program.

Rafal Saeed Sabeeh

2025

TABLE OF CONTENTS

Supervisor Certification	vi
EXAMINING COMMITTEE’S REPORT	vii
ACKNOWLEDGEMENTS	viii
TABLE OF CONTENTS.....	ix
LIST OF TABLES	xii
LIST OF FIGURES	xiii
LIST OF SYMBOLES.....	xvi
LIST OF abbreviations	xix
CHAPTER One: INTRODUCTION.....	1
1.1 General	1
1.2 Basic Structure	4
1.3 Slabless Staircases.....	5
1.4 Staircases Parameters and Loadings	7
1.5 Thesis Layout	10
CHAPTER Two: LITERATURE REVIEW.....	11
2.1 Introduction	11
2.2 Previous Studies	11
2.3 Summary	31
CHAPTER Three: Finite Element Formulation and Mathematical Modeling	32

3.1 General	32
3.2 Numerical Evaluation of Structures in a Nonlinear System	32
3.3 The Fundamentals of the Finite Element Theory	33
3.4 Material Modeling.....	34
3.4.1 Concrete Modeling.....	34
A) Plasticity Approach	34
B) Material Nonlinearity	35
C) Multilinear Relationship between Stress and Strain	36
D) Modelling for Cracks	39
E) Crushing Modeling	41
F) Steel Reinforcement Bars.....	42
3.5 ABAQUS Computer Program.....	43
3.5.1 Solution Technique.....	43
3.5.2 The Riks Method	44
3.6 ABAQUS Finite Element Model	46
3.6.1 Define Material Properties	46
3.6.2 Create Geometry	48
3.6.3 Element Mesh and Type.....	49
3.6.4 Contact Interaction and Boundary Conditions.....	52
3.6.4.1 Defining Contact Pairs and Properties of Contact.....	52
3.6.4.2 Boundary Conditions	54
3.6.5 Analysis Steps	56
CHAPTER Four: RESULTS AND DISCUSSION	58
4.1 General	58

4.2 Procedure of the Study	58
4.3 Verification Process	59
4.4 Finite Element Analysis of Slabless Staricases	62
4.4.1 Effect of Steel Reinforcement Configuration (Series One)	62
4.4.1.1 Results and Discussion Series One	66
4.4.2 Effect of CFRP Material (Series)Two.....	84
4.4.2.1 Results and Discussion	87
4.4.3 Series Three	100
4.4.3.1 Results and Discussion of Series Three	101
CHAPTER Five: CONCLUSION AND RECOMNDATIONS.....	108
Appendix : Experimental Model Specifications for Verification	111
REFERENCES	117

LIST OF TABLES

Table 1-1 Parameters Variations of Staircases according to IS: 875-1964 [10] and Residential Stair Guide 2018 [11].....	7
Table 2-1: Models of Staircases[23]	20
Table 4-1 The results of the validated comparison between the numerical study and the experimental study.	60
Table 4-2 Description of Specimens.....	63
Table 4-3 Test result of Speciment Tested.	66
Table 4-4 Description of Specimens.....	85
Table 4-5 Test result of Load Deflection Curve	87
Table 4-6 Description of Specimens.....	100
Table 4-7 Test result of Load Deflection Curve	102

LIST OF FIGURES

Figure 1-1 Staircases types [3].....	2
Figure 1-2 Staircases components[3].....	4
Figure 1-3 Slabless staircases in RC building [9].....	6
Figure 1-4 Staircases Conditions [12].	8
Figure 2-1: (a) Prototypes of wooden staircases being subjected to a comprehensive static load test; (b) a three-dimensional finite element analysis model of a wooden staircase[13].	12
Figure 2-2. Slabless staircases specimens of Baqi and Mohammad [22].....	19
Figure 2-3 . Slabless staircases specimens of Özbek et al. [25].	22
Figure 2-4 : The cement fibre board internal staircase structure collapse [26].....	24
Figure 2-5: modeled slabless staricases[27].	25
Figure 2-6 Tested staircases presented by Zhang [29]	29
Figure 2-7 staircases tested by Wang. [30].....	30
Figure 3-1 Finite element discretization [32].	33
Figure 3-2 a) Nonlinear elastic material response b) Nonlinear plastic material response [35].....	36
Figure 3-3 Various concrete strengths are represented by a uniaxial compressive strain curve [36].	37
Figure 3-4 Simplified stress-strain for NSC [39].	39
Figure 3-5(a) Stress-strain method; (b) fracture behavior after failure [40].....	40
Figure 3-6 The concrete's uniaxial tensile stress-strain behavior [40].	41
Figure 3-7 Modeling of reinforcing bars [44].....	42
Figure 3-8 Typical unstable static response [46].....	44

Figure 3-9 Arc length and arc length increment[46] .	45
Figure 3-10 Properties of concrete in Abaqus	47
Figure 3-11 Properties of reinforcement in Abaqus.	48
Figure 3-12 Solid element conditions [47].	49
Figure 3-13 T3D2 element description [47]	50
Figure 3-14 Mesh size of slabless staircases.	51
Figure 3-15 Properties of contact between concrete and reinforcement .	53
Figure 3-16 Variables of Contact.....	54
Figure 3-17 a) Boundary conditions and applied loading conditions were considered. b) The bottom support c) The top support.....	55
Figure 3-18 Appropriate analysis type in abaqus.	57
Figure 4-1 Load-deflection curve of experimental vs. numerical data.....	61
Figure 4-2 Demonstrations of geometry tests.....	64
Figure 4-3 Cracking and ultimate load results for first group.	67
Figure 4-4 Cracking and ultimate load results.....	68
Figure 4-5 Load deflection relationship of ST-M, ST-L and ST-R slabless staircases models.....	69
Figure 4-6 Load deflection relationship of ST-L-R-1 and ST-L-R-4 slabless staircases models.....	69
Figure 4-7 Cracking and ultimate load results.....	70
Figure 4-8 Load deflection relationship of ST-M and ST-M-Wop slabless staircases models.....	71
Figure 4-9 Load deflection relationship of ST-L and ST-L-Wop slabless staircases models.....	71
Figure 4-10 Load deflection relationship of ST-R and ST-R-Wop slabless staircases models.....	72

Figure 4-11 Ultimate load and Cracking results.....	73
Figure 4-12 Load deflection relationship of ST-M and ST-M-70 slabless staircases models.....	74
Figure 4-13 Load deflection relationship of ST-L and ST-L-70 slabless staircases models	75
Figure 4-14 Load deflection ST-R and ST-R-70 slabless staircases models.	75
Figure 4-15 Ductility Index.	77
Figure 4-16 Ductility Index.	78
Figure 4-17 Initial stiffness of the slabless staircases	79
Figure 4-19 Cracks pattern for slabless staircases of ST ,ST-M , ST-L and ST-R.	81
Figure 4-22 Demonstrations of geometry tests.....	86
Figure 4-24 Cracking and ultimate load results.....	92
Figure 4-25 Load-deflection curve of slabless staircases.	92
Figure 4-26 Ductility index of the slabless staircases.	95
Figure 4-27 Initial stiffness of the tested slabless staircases.	97
Figure 4-28 Cracks pattern for slabless staircases Series Two.....	99
Figure 4-31 Load-deflection curve of ST-Ln-60 , ST-Ln-70 and ST-Ln slabless staircases.	104
Figure 4-32 Ductility of slabless staircases of Series Three.....	105
Figure 4-33 Initial Stiffness of of slabless staircases Series Three	105

LIST OF SYMBOLES

Symbol	Description	Unit
A	Cross-sectional area	mm^2
b	Beam width	mm
d	Effective depth.	mm
E	Modulus of elasticity	MPa
E_c	Modulus of elasticity of concrete	MPa
E_s	Modulus of elasticity of reinforcing bars	MPa
E_T	Strain hardening modulus	
F	Function of principal state ($\sigma_{xp}, \sigma_{yp}, \sigma_{zp}$)	
f_t	Ultimate uniaxial tensile strength of concrete	MPa
f_r	Modulus of rupture of concrete	MPa
f_{cb}	Ultimate biaxial compressive strength	MPa
f_l	Ultimate compressive strength for a state of biaxial compression superimposed on hydrostatic stress state	MPa
f_c'	Compressive strength of concrete cylinder	MPa
f_y	Yielding stress of steel reinforcement	MPa
f_2	Ultimate compressive strength for a state of uniaxial compression superimposed on hydrostatic stress state	MPa
f_c	Concrete ultimate uniaxial compressive strength	MPa
f_y	Steel yield strength and	MPa
f_u	Steel ultimate tensile strength	MPa

f_{cr}, ε_{cr}	Cracking stress and strain	MPa
h	Height of the cross section	mm
L	Span length of the beam	mm
Le	Effective length	mm
P and V	Any applied force on the structure	kN
P_{cr}	Cracking load	kN
P_u	Ultimate load	kN
u, v, w	Displacement components in x,y and z coordinates	mm
W_{ext}, W_{int}	External and internal work	
x, y, z	Global coordinate	
α	Haunch angle with horizontal line	Degree
β	Shear transfer coefficient	
B_t, β_c	Opened and closed shear transfer coefficient	
$\gamma,$	shear strain	
ε	Strain	
ε_o	Strain at ultimate compressive stress f'_c	
ε_u	Ultimate strain	
ζ, η	Local coordinates	
σ	Stress	MPa
σ_h^a	Ambient hydrostatic stress state	MPa

τ	Shear stress	MPa
ν	Poisson's ratio	
$[A]^T$	Transpose of matrix $[A]$	
$[A]^{-1}$	Inverse of matrix $[A]$	
$[B]$	Strain-displacement matrix	
$[D]$	Constitutive matrix	
$[J]$	Jacobian matrix	
$[K]$	Overall stiffness matrix	
$[K]_e$	Element stiffness matrix	
$[L]$	Differential operator matrix	
$[N]$	Matrix of shape functions	
$[T]$	Transformation matrix	
$\{a\}$	Nodal displacement vector	
$\{F^a\}$	Vector of applied loads	
$\{f\}$	Load vector	
$\{u\}$	Displacement vector	
$\{\varepsilon\}$	Strain vector	
$\{\sigma\}$	Stress vector	

LIST OF ABBREVIATIONS

Symbol	Description
ACI	American Concrete Institute
BS	British Standards (BSI: British Standards Institute)
CFRP	Carbon Fiber Reinforced Polymer
FE	Finite Element
FEA	Finite Element Analysis
FEM	Finite Element Method
HSC	High Strength Concrete
NSC	Normal Strength Concrete
RC	Reinforced Concrete

CHAPTER ONE: INTRODUCTION

1.1 General

Structural systems are essential components of engineering that provide support and stability to buildings and other constructions. The design and analysis of these systems involve understanding various structural elements such as beams, columns, frames, and slabs, which work together to carry loads safely and efficiently. Structural engineers apply principles of mechanics and material science to ensure that structures can withstand forces such as gravity, wind, and seismic activity while maintaining serviceability and safety. In the context of modern architectural design, the evolution of structural systems has led to innovative solutions that not only fulfill functional requirements but also enhance aesthetic appeal. Among these innovations are various types of stairs including traditional and contemporary designs, each serving essential roles in accessibility and circulation within buildings. A staircase is a series of stairs that connects different levels or floors. There is a significant amount of engineering involved in selecting a standard size from a manufacturer [1]. The majority of stairs are specifically engineered to comply with mandated design criteria. Stairs are often constructed using steel, concrete, or a combination of both materials[2].

Reinforced Concrete (RC) slabless staircases represent a unique approach to staircase design that eliminates traditional slab components, offering a more streamlined and aesthetically pleasing solution. These staircases are characterized by their use of cantilevered treads that extend from a supporting wall or structure, creating an open and airy appearance. Stairs can be classified into different types based on their structural configuration as revealed in Fig. (1-1) :a) Straight Stair Spanning Longitudinally which this design features horizontal treads and vertical

risers in a straight line, commonly used for its simplicity and efficiency. b) Straight Stair Spanning Horizontally whereas similar to the longitudinal version but oriented horizontally, this design leads to landings and is effective in wider spaces. c) Slabless Staircases which these stairs have cantilevered treads extending from a wall without a traditional slab, which called sawtooth or ortho-polygonal staircases [4]. d) Free Standing Stairs that having a free-standing stairs serve as visual focal points and require careful stability considerations. e) Helical Stair with Curve strut around a central axis, helical stairs are ideal for compact spaces and enhance visual interest. f) Spiral Staircases forming a winding strut around a central pole, spiral stairs are efficient in tight areas but require attention to safety.

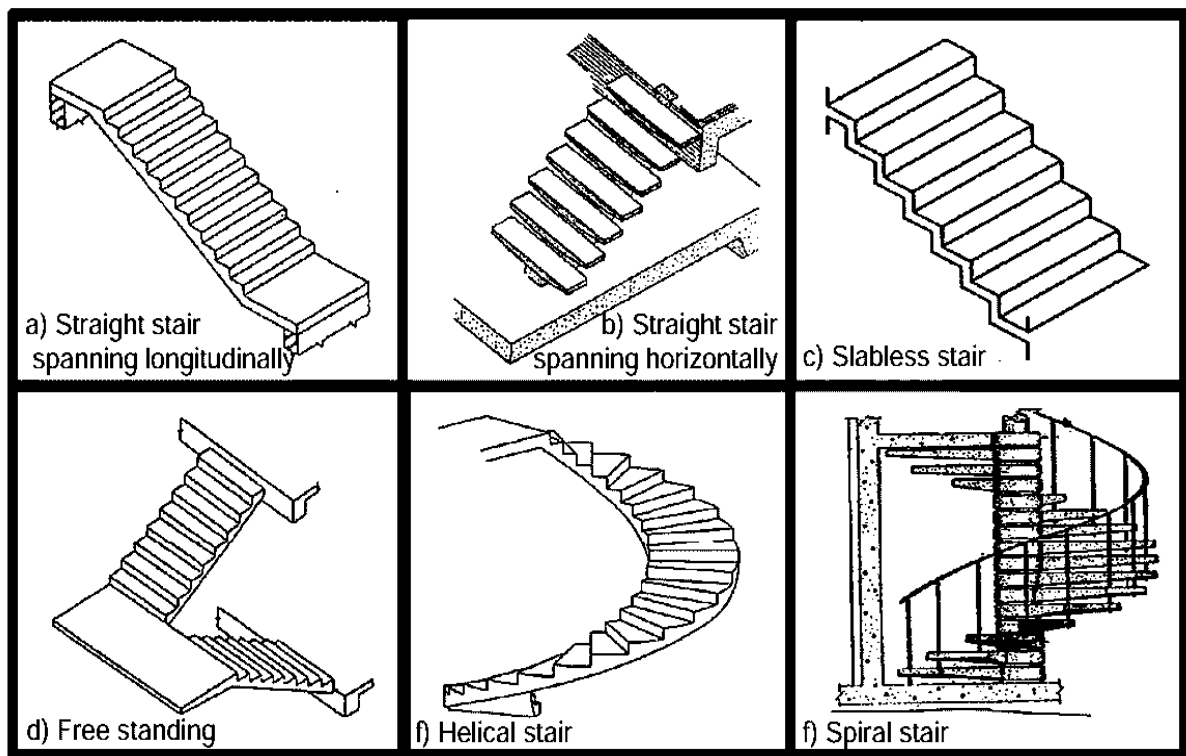


Figure 1-1 Staircases types [3].

The sections of buildings with staircases exhibit enhanced rigidity compared to the remainder of the structure due to the inclusion of sloped pitch that provide

support for the staircases. It is important to mention that in the sections of the structures where staircases are located, there are also lift pits. These pits are made of reinforced concrete, which help to increase the rigidity of the structure because it helps make the structure stiffer and more resistant to bending or deflection. Stairs are essential for safely exiting a structure in the event of an earthquake. Staircases with cantilever steps, which belong to the first group of staircases in the aforementioned classification, are not affected by earthquakes. In other cases, the impact of the earthquake on the staircases could pose a risk to the overall safety of the structure. For instance, the significant difference in position between the ends of the staircase located on various floors creates a substantial amount of strain and should be considered during the design phase of the building, [3]. If the strength and stiffness of a structure in the stairway area are enhanced, it will affect the seismic torsional distress of the structure and might potentially cause shear failure in the staircase or other parts of the structure. It is worth mentioning that during two recent earthquakes in New Zealand [5]. The staircases in at least four tall buildings completely collapsed, while several others sustained significant damage. Due to significant damage to staircases made of both reinforced concrete and metal, authorities have made revisions to the applicable rules for designing new staircases and evaluating the performance of existing ones during earthquakes [6]. The significance of the relationship between staircases and their structures has led to extensive research in the field of earthquake engineering. Recent research indicates that the inclusion of stairs has modified the mode shapes of the structure, resulting in the torsional mode shape becoming the primary one in numerous instances. In frame-type constructions, the columns and beams near the staircases are particularly susceptible to damage. The primary reason for failure in this area is shear stress, especially in small columns created within the staircases [6].

1.2 Basic Structure

The stairs constitute an orthopolygonal configuration on a flat surface. A plane orthopolygonal structure is a geometric shape that lies within a two-dimensional plane and is composed of a continuous broken line. The line segments of this shape are arranged in such a way that they create approximately right angles with each other. The steps may exhibit varying support and terminal conditions[7]. Typically, the ends of a stair between two flights are anchored in the walls, allowing them to be considered as fixed ends. However, this is not always the case. If a hard beam is present at the start of the landing or if there is a thick slab at the ends, it is also possible to consider the ends as fixed. If the ends of the steps are supported by a bearing wall, then it can be assumed that the ends are hinged. Fig. (1-2) illustrate the component of the staircases.

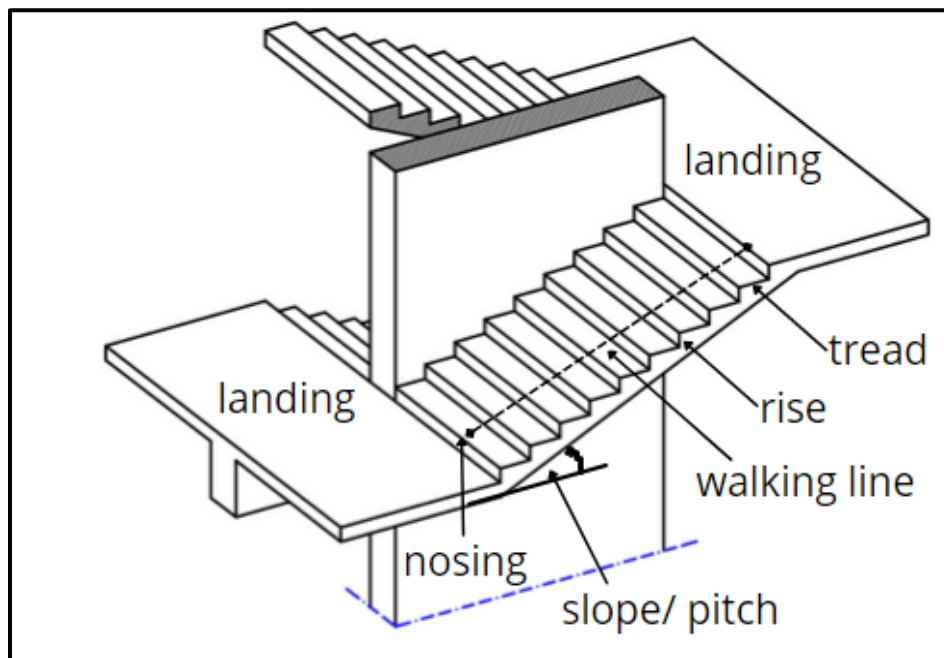


Figure 1-2 Staircases components[3]

Typically, a concrete beam is placed underneath the landing to give support. This particular situation is referred to as an intermediately supported staircase. An

unsupported stair is one in which the support beam is absent. Indeed, in cases when support is provided, the bending moments, which are the primary factor in design considerations, experience a large reduction. To simplify the process of structural analysis using traditional methods, certain types of stairs are considered as fixed or continuous beams [7].

1.3 Slabless Staircases

Traditional reinforced concrete stairs support the force of gravity by utilising waist slabs located beneath the steps as seen in Fig.(1-3). Conversely, slab-less reinforced concrete staircases support the loads solely through the use of treads and risers. Put simply, this action has a strong resemblance to folded plates. Slabless staircases are alternatively referred to as sawtooth or orthopolygona staircases. The slabless staircase is not a cost-effective construction method compared to standard stairs due to the challenges in formwork and reinforcing. However, it still appeals to architects because of its trendy and aesthetically pleasant design. Slabless stairs are designed in the shape of a folded plate. Thorough examination of folded plates necessitates the use of challenging and time-consuming techniques, such as the standard semi-analytical finite strip method and the spline finite strip method. Additionally, finite strip methods employing calculated shape functions and modified Fourier series are also employed [8] .

A Slabless tread-riser stair is a type of staircase where the external loads are solely supported by the treads and risers. A construction composed of straight lines forming a polygon with right angles as seen in Fig.(1-3). The light and slim design of these steps has captured the attention of numerous architects and engineers. As a result, they have been widely adopted for use in the construction of modern commercial and residential buildings.

The design of traditional stairs assumes that the waist slab, also known as the slab, bears all types of loads. In these stairs, the reinforcement is placed in the slab. However, in slabless tread-riser stairs, the loads are carried by the treads and risers. As a result, the reinforcement is provided in the treads and risers in the form of loops. Orthopolygonal stairs have several advantages compared to ordinary steps. They are aesthetically superior, provide greater headroom, and require less concrete and reinforcement. However, there are some drawbacks, including difficulty in laying them out, the need for unique shuttering, and the requirement for expert labour.



Figure 1-3 Slabless staircases in RC building [9].

1.4 Staircases Parameters and Loadings

In stair design, two types of loads are taken into account: dead load and living load. According to IS: 875-1964 [10] and Residential Stair Guide 2018 R311.7 stairway [11] in residential buildings, business buildings, and similar structures where overcrowding is not expected, the live load for stairs can be assumed at 3 (kN/m²). For any other public building, the live load can be assumed to be 5 (kN/m²). The dead load consists of the weight of the treads, risers, and landings themselves. The load is uniformly distributed, but for the sake of precision, it can be approximated as a series of equivalent point loads focused at the riser. The design parameters of a slabless tread riser steps are illustrated in Fig. (1-4). The typical changes of these values are as follows according to IS and Residential Stair Guide 2018 shown in Table (1-1):

Table 1-1 Parameters Variations of Staircases according to IS: 875-1964 [10] and Residential Stair Guide 2018 [11]

Variable	IS: 875-1964 [10]	Residential Stair Guide 2018 [11]
Landing (L)	1200 mm	915 mm
Tread (T)	250 mm	263.5mm
Rise (R)	190 mm	193.7mm
Thickness of Tread (th)	100 – 150 mm	-
Thickness of Riser(v)	100 – 150 mm	-

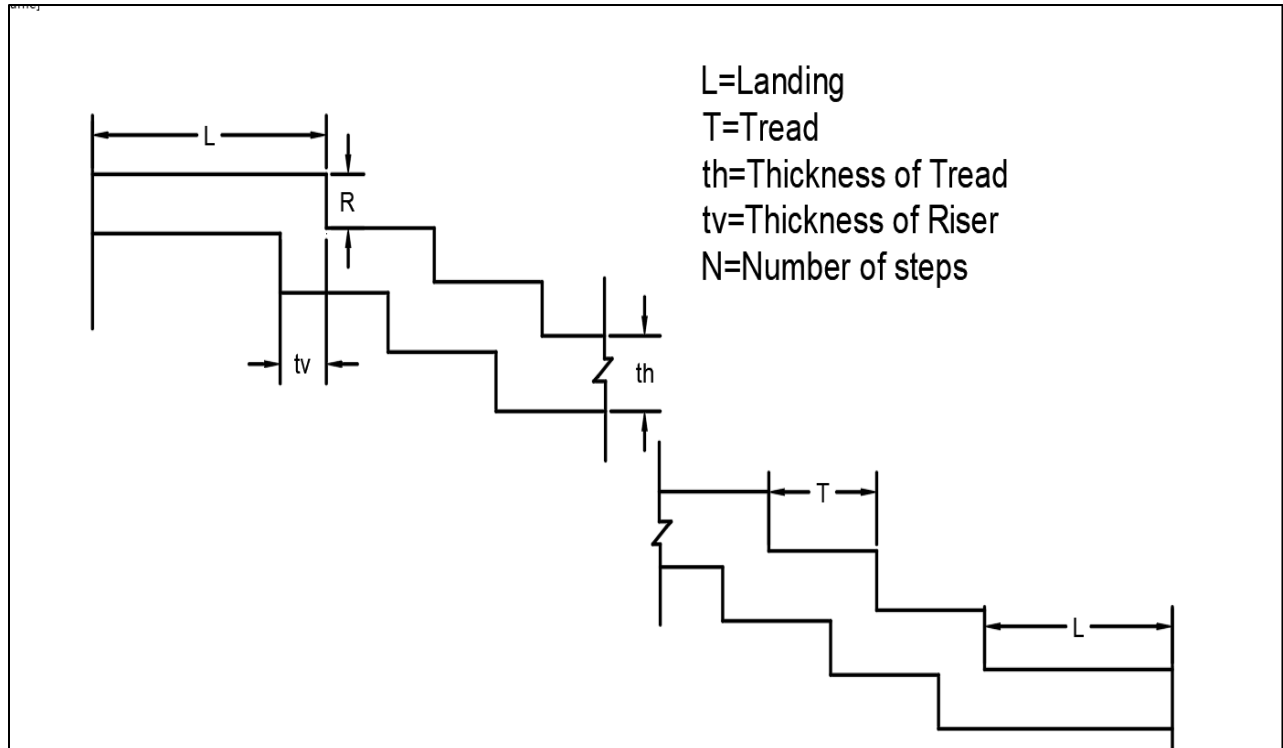


Figure 1-4 Staircases Conditions [12].

1.2 Aim of the Study

The primary aim of this study is to investigate and enhance the structural performance of slabless reinforced concrete staircases through advanced numerical modeling and innovative reinforcement techniques. The research seeks to explore the effectiveness of different reinforcement configurations, materials, and geometric modifications in improving the load-carrying capacity, stiffness, ductility, and overall structural behavior of slabless staircases. By validating finite element models against experimental data, the study aims to establish reliable predictive tools and design recommendations for safer and more efficient slabless staircase systems.

1.3 Objectives of the Study

To achieve this aim, the following specific objectives are defined:

1. Model Development and Validation

- Develop three-dimensional finite element models for slabless reinforced concrete staircases using ABAQUS software.
- Validate numerical models against existing experimental data in terms of load-deflection behavior, cracking patterns, ultimate loads, and failure modes.

2. Study of Steel Reinforcement Configurations

- Investigate the influence of various steel reinforcement configurations, including triangular arrangements and staggered layouts, on the structural performance of slabless staircases.
- Analyze their effects on cracking loads, ultimate loads, deflection behavior, initial stiffness, and ductility index.

3. Evaluation of CFRP Strengthening Techniques

- Examine the effectiveness of incorporating Carbon Fiber Reinforced Polymer (CFRP) bars as partial or full replacement of traditional steel reinforcement in slabless staircases.
- Assess the impact of externally applied CFRP sheets of varying widths and wrapping schemes on structural performance parameters.

4. Impact of Concrete Compressive Strength

- Study the influence of different concrete compressive strengths ranging from 20 MPa to 70 MPa on the flexural behavior and ductility of slabless staircases.

5. Geometric Modifications

- Evaluate the effect of adding geometric features, such as intermediate landings, on the overall structural behavior and load capacity of slabless staircases.

6. Analysis of Failure Mechanisms

- Analyze crack patterns, stress distributions, and failure mechanisms in various reinforcement and material scenarios to identify critical factors affecting the structural integrity of slabless staircases.

1.5 Thesis Layout

This thesis consists of five chapters which can be summarized as follows:

- 1) Chapter one introduces an introduction to the subject. Stairs, their structure, design parameters and objectives.
- 2) Chapter two introduces a general outline of previous work performed on RC staircases.
- 3) Chapter three, presents the analytical phase of the thesis, including the theory formulation and solution techniques.
- 4) Chapter four analysis of the results produced from the analysis of the RC staircases is discussed, and a comparison is made between the results gained through experimentation and those obtained through analysis.
- 5) Chapter five provides a summary of the findings and suggestions for further research.

CHAPTER TWO:LITERATURE REVIEW

2.1 Introduction

This section synthesizes existing research, theories, and methodologies related to the design, behavior, and reinforcement of slabless staircases, as well as the application of numerical modeling techniques, particularly presented in previous studies. In recent years, has been a growing interest in innovative staircase designs that enhance both aesthetic appeal and functional performance. Slabless staircases, characterized by their cantilevered treads and minimalistic structure, represent a significant advancement in architectural engineering. This literature review will explore various studies that examine the structural integrity, load-bearing capacities, and failure mechanisms of slabless designs. Furthermore, the review will delve into the different reinforcement strategies employed to optimize the performance of slabless staircases, highlighting both internal and external retrofitting methods. By evaluating previous research findings, this chapter will identify gaps in the current literature, provide context for the study's objectives, and establish the relevance of the research within the broader field of structural engineering.

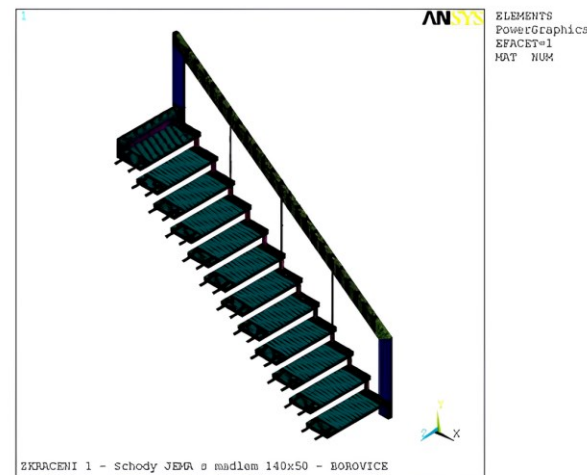
2.2 Previous Studies

In 1995, Bishop, Willford, and Pumphrey[13] investigated the behavior of slender staircases subjected to human-induced dynamic forces. Willford, and Pumphrey combined both experimental and numerical methodologies. The primary purpose of the study was to investigate the challenges associated with designing modern slender staircases subjected to human-induced dynamic forces. variables in the study included the loading characteristics caused by a single person's footprint, the effects of multi-person loading on dynamic responses, and the acceptance levels

for vibration and user comfort. The study also examined factors influencing loading variability, such as walking speed and individual gait. The findings revealed that the loading characteristics of individual footfalls were more complex than previously understood, with significant variability based on multiple factors. Additionally, multi-person loading could amplify dynamic responses, which standard design practices fail to adequately account for. The investigation highlighted that current vibration acceptance criteria were insufficient for slender staircases, potentially compromising user comfort and structural integrity. In conclusion, the study emphasized the need for updated design guidelines that specifically address the unique dynamic behaviors of slender staircases. The authors advocated for evolving existing practices to better accommodate the complexities of human-induced loading, ensuring both safety and comfort for users as seen in Fig. (2-1).



(a)



(b)

Figure 2-1: (a) Prototypes of wooden staircases being subjected to a comprehensive static load test; (b) a three-dimensional finite element analysis model of a wooden staircase[13].

In 1996, Saenz and Martin[14] explored the design methodologies for slabless staircases. Their study aimed to simplify the design process by substituting

distributed gravitational forces with concentrated loads positioned along the risers. This approach allowed for a clearer structural analysis, assuming the staircase was immovably fixed at both ends. The study focused on key parameters, including the effectiveness of the column analogy and second difference techniques in structural analysis. The findings indicated that both methods yielded equivalent results, reinforcing the validity of the analytical approaches. Additionally, the research included reinforcement detailing specific to slabless staircases, where despite variations in bending moments along the staircase, each step received uniform reinforcement. Principal bars were arranged longitudinally, formed into closed stirrups, which provided additional support. The study emphasized that this closed-loop configuration not only facilitated the necessary development length and resistance against negative moments at support regions but also enhanced shear capacity and ductility through confinement across the structure. This innovative reinforcement strategy proved essential, especially in partially restrained scenarios.

In 2000, Solanki [15] conducted an investigation into the behavior of freestanding slabless staircases, which included an upper flight, a lower flight, and a uniform thickness landing slab. Utilizing the finite element method (FEM) for analysis, the study aimed to explore the structural performance and load distribution characteristics of these unique staircases. However, the research faced significant limitations, as further investigation into this innovative design was ultimately abandoned. This highlighted a critical gap in the existing literature regarding slabless staircases. Despite employing FEM, the findings lacked comprehensive exploration due to a restricted scope of variables considered in the analysis. Solanki noted that, to the best of their knowledge, no prior studies had empirically investigated slabless staircases, indicating a remarkable absence of experimental data to support theoretical findings.

The variations between floor loading and stair loading caused by humans were studied by Kerr and Bishop [16] in 2001. These distinctions have not always been well-defined, which has proven problematic for the designers of contemporary flexible stairs. It was discovered throughout the inquiry that some constructions only showed signs of dynamic responsiveness after they were already built, which resulted in expensive repairs. The scientists were able to make conclusions regarding the differences that should concern staircase designers by comparing data gathered from several force plate trials with existing experimental data.

In 2001, Kerr and Bishop [17] investigated the influence of human loads on staircases, motivated by the inadequacy of existing design guidance. The study noted that staircase designers often relied on experience drawn from footbridge and floor designs, despite the significant differences in footfall rates and harmonic amplitudes between these structures and staircases. The primary objectives of their research were to analyze the discrepancies between the loading forces encountered on staircases versus those on floors and bridges, and to establish standard vibration tolerability levels for staircase occupants, which were previously nonexistent. The impact loads produced by subjects walking within a horizontal surface and descending or ascending a staircase were assessed using force plate testing in the study. Utilizing Fourier analysis techniques, they calculated the harmonic amplitudes and frequencies linked to the two loading circumstances in order to analyse the data. Their findings revealed that the footfall forces and harmonic responses on staircases significantly differed from those observed on floors or bridge slabs, emphasizing the unique dynamics involved in staircase design. A critical aspect of their research was the accurate prediction of a staircase's natural frequency. Kerr and Bishop warned that failing to predict this frequency could lead to serious vibration issues. Based on experimental data, the study provided recommendations

for conditions that should raise concerns for staircase designers. Notably, they proposed a minimum natural frequency tolerance level of 10 Hz for staircases, indicating that frequencies below this threshold could result in unacceptable vibration levels for occupants.

In 2008, Kim et al. [18]. conducted an experimental assessment of the vibration serviceability of stair systems, focusing on both steel and reinforced concrete stairs. The motivation for this study arose from the critical role of serviceability in design considerations and the increasing trend in the construction industry toward lighter steel staircase systems. The researchers aimed to evaluate the dynamic performance of various stair types and compare them against established serviceability criteria, referencing guidelines from Murray, Allen, and Ungar (1997), AISC (1997), and Bishop et al. (1995). Multiple stair layouts were considered in the study, including those made of reinforced concrete, laminated tread boards, and steel with reinforced concrete treads. Each stair flight was analyzed individually, connecting a floor to a mid-story landing. To assess the dynamic properties, Kim et al. employed heel-drop tests alongside accelerometers to measure the natural frequency and damping characteristics of each staircase. Additionally, they analyzed the behavior of human walkers traversing the stairs at various speeds to determine the peak acceleration experienced by the stair structures. The findings revealed a significant disparity in the dynamic responses between the two materials. Specifically, steel stair systems exhibited much higher dynamic responses compared to reinforced concrete staircases. As a result, reinforced concrete stairs were found to be more capable of meeting serviceability standards than their steel counterparts. This outcome highlights the importance of material choice in staircase design.

In 2008, Cosenza, et al[19]. conducted a numerical investigation into the seismic performance of existing buildings, focusing specifically on moment-resisting frame

structures and the critical role of stair members, including columns, beams, and slabs. Their research addressed the dual nature of stair systems in structural design: while they enhance the overall strength and stiffness of a building, they can also become points of vulnerability during seismic events. The study highlighted how stair systems can attract significant seismic forces, which may lead to failures in short columns, slabs subjected to high shear forces, or inclined beams supporting the steps that experience elevated axial forces. To assess the performance of stair systems in gravity-load-designed structures, the authors explored various structural solutions and design practices, aiming to establish a clear geometric definition of stair systems to better understand their behavior under seismic loading. The analysis involved both linear and nonlinear numerical modal push-over analyses conducted on a representative reinforced concrete building that adhered to the materials and design criteria of its time. Two types of stair configurations were examined: cantilever steps constrained by inclined beams and stairs composed of simply supported slabs. The modal analysis revealed distinct modal behaviors when accounting for the stairs, indicating that their presence significantly influences the dynamic response of the structure. By employing nonlinear lumped plasticity models, the researchers conducted nonlinear push-over analyses to identify key failure mechanisms within the stair systems. The findings emphasize the importance of considering stair systems in seismic design, highlighting both their contributions to structural integrity and their potential vulnerabilities.

Davis and Murray [20] conducted an analytical and experimental examination of slender monumental stairs in 2009. The study aimed to address specific enquiries regarding stair vibrations and provide additional guidance for designers. The increased utilisation of stairs, which function as prominent architectural features, was the primary impetus for their inspiration. They indicated that the architectural

requirements of these staircases frequently lead to slender structures with extended clear spans, which may create serviceability issues. Narrow stringers, thick treads, and guardrails in steps are more prone to low natural frequencies and vibration issues under walking stimulation, necessitating adherence to tougher design rules. Elucidated the methodologies utilised to determine the vibration characteristics of the staircase via analytical and experimental approaches. The researchers employed modal and walking tests to ascertain the structure's damping characteristics and fundamental natural frequency. The experimental data was utilised for prediction by finite element modelling. We employed traditional eigenvalue analyses to predict the natural frequencies and mode shapes of the stairs. They predicted the harmonic associated with the fundamental frequency and implemented adjustment factors based on occupant numbers following their research, subsequently proposing a method for assessing the footfall forces of the design.

In the year 2013, Tegos and colleagues [21] conducted research on all different kinds of staircases, focussing on two primary aspects: Theoretical analysis focused on the critical role that the vertical component of earthquake acceleration plays in determining the structure's performance. Throughout the study, The researchers examined stair behavior and the crucial role that stairs serve as seismic linkages in the response and activity of space buildings. The outdoor staircases that connect structurally independent multistory systems were the subject of particular attention within this project. An examination was conducted on a multistory exterior stairway that connected buildings in an area with a high seismic activity occurrence. Staircases that present unique design issues due to gravity and earthquake loadings were also explored as part of this effort. These staircases included helical staircases and staircases with a free landing. This work, the authors remarked, may prove to be useful to practicing engineers, as it covers (nearly) all forms of staircases and their

structural considerations, particularly in the context of seismic design and the interaction with the surrounding building frame. This is in addition to the fact that this work is of theoretical relevance.

In 2013, Baqi and Mohammad [22] presented a theoretical study focused on the behavior of U-Turn reinforced concrete dog-legged stair slabs with mid-landings. Two stair slab layouts were studied using the FEM method: one with landings on both sides and supported at the ends by a wall, and another with many flights and six alternative support systems. In order to characterise the behavior of these stair slabs, including the positions of critical moments and deflections, the study examined characteristics such as stresses, strains, and deflections that were acquired from the FE analysis. We compared the critical moment values found using FE analysis to those found using more traditional analytical approaches. According to the findings, crucial moments are often located close to the "kinks," or the points where the mid-landing and inclined waist slabs meet. Because the material is continuous in the transverse direction across the two adjacent landings, adding extra stiffness, the dog-legged stair slab's behavior changes. Traditional approaches to design, however, tend to ignore this detail as seen in Fig.(2-2).

An investigation of the impact of staircases on the seismic performance of RC frame buildings was carried out by Kumbhar et al. [23] in the year 2015. A numerical analysis had been carried out in order to investigate the impact that disregarding staircases as part of the modeling and design process for RC frame buildings

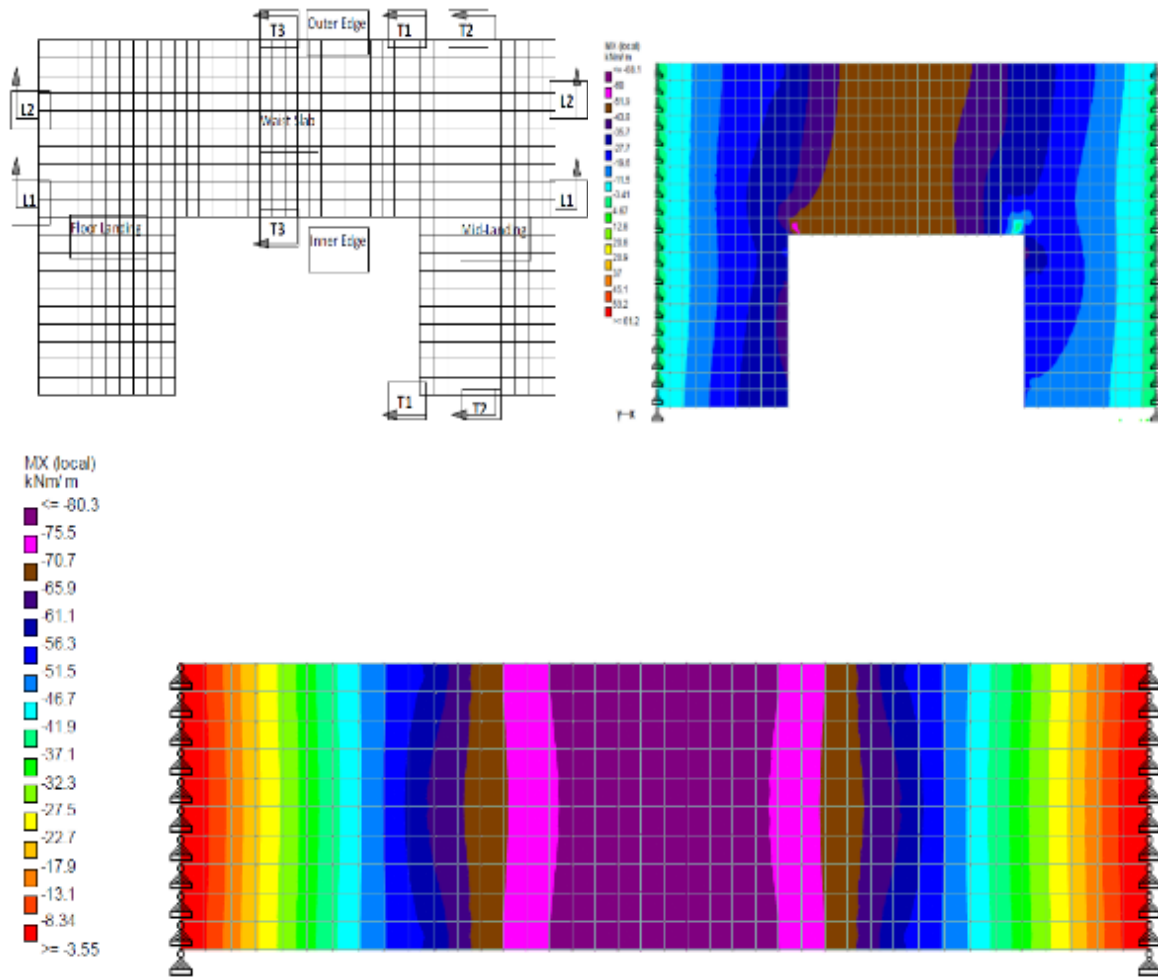
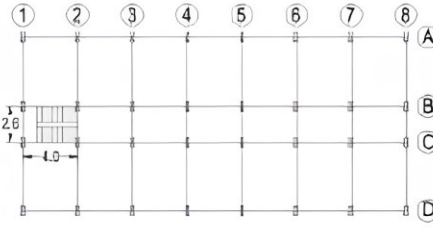
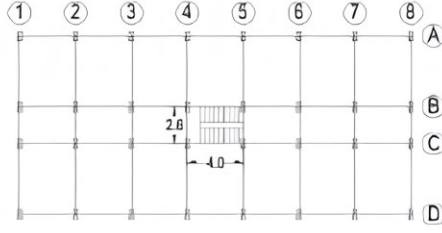
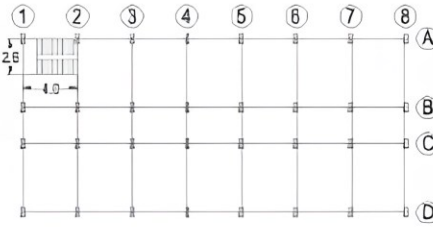
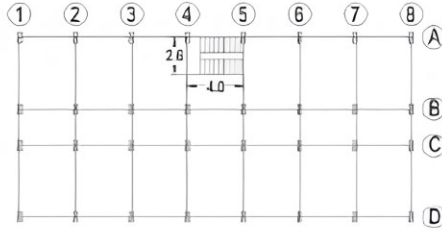
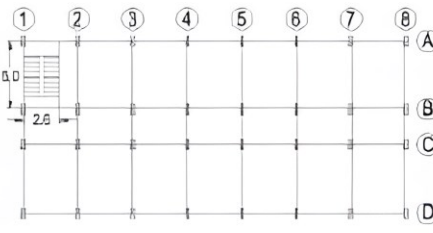
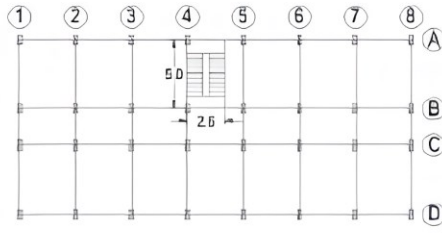


Figure 2-2. Slabless staircases specimens of Baqi and Mohammad [22]

A six storey building with plan representing a typical office or public building has been modeled and designed for three grades of concrete (with nominal characteristic strength of 20 MPa, 30 MPa and 60 MPa) without considering staircase as seen in Table 2.1. Further six building model plans (each considering three grades of concrete) by inserting single staircase at different location and orientation, in the model without staircase has been developed. It has been observed from modal analysis that insertion of staircase not only affect the fundamental period of vibration significantly, but also the appearance of mode changes i.e., in some cases second translational mode changes to torsional mode. Moreover, the effect of same staircase placed at different locations and in different orientations, significantly affects modal

characteristics i.e., the variation of fundamental period of vibration for single staircase ranges from 7 to 22% and for two staircase model it reduces up to 35% for different models. In order to estimate seismic performance of aforementioned models capacity curves have been developed using NSP as per FEMA 356/ASCE 41-06 guidelines. Superior performance of building model without staircase has been drastically reduced due to inclusion of staircase

Table 2-1: Models of Staircases[23]

Model Description	Figure	Model Description	Figure
Model-1: Analysis model with staircase located at first bay along longer side and second bay along shorter side, parallel to longer side		Model-2: Analysis model with staircase located at fourth bay along longer side and second bay along shorter side, parallel to longer side	
Model-3: Analysis model with staircase located at first bay along longer side and third bay along shorter side, parallel to longer side		Model-4: Analysis model with staircase located at fourth bay along longer side and third bay along shorter side, parallel to longer side	
Model-5: Analysis model with staircase located at first bay along longer side and second bay along shorter side, parallel to shorter side		Model-6: Analysis model with staircase located at fourth bay along longer side and second bay along shorter side, parallel to shorter side	

As a result of the collapse of columns that supported inserted staircases, certain building models that received a higher grade of concrete exhibited brittle failure. As a result of the presence of the staircase, it has been discovered that the ductility capacity of the building model with low strength concrete (20 MPa) can decrease by as much as 70 percent. Moreover, in most of the cases early development of plastic hinge in short column which is created due to inclusion of staircase lead to pushing the building to collapse level. It has also been observed that location and orientation of staircase plays an important role in deciding the performance of building. Based on the findings of the study, it is possible to draw the conclusion that if the contribution of the staircase is ignored in the structural modelling and design of the building under consideration, it may result in excessive damage or even collapse in the event of a seismic event.

During the year 2018, Wang and Hutchinson[24] conducted an investigation into the high-fidelity finite element models in an effort to increase their understanding of the seismic steel stairs under pseudo-static displacement loading, which is typical of earthquake-induced building motions. The first step in implementing any new modelling strategy was checking it against existing experimental data. After that, it's expanded into a parametric analysis to add more stair designs and features. Geometry, story height, connection and landing features, and their effects on the system's behavior are the main foci of the investigation. Parametric analysis has shown that the aforementioned critical design elements have a significant impact on the stairs' static force and displacement response. Strong seismic performance and, by extension, continuous stair operation, depend on the ability of stair-to-building connections to maintain connectivity during earthquakes. Sideways displacement loading places substantial stress and strain loads on these connectors.

In 2021, Özbek et al. [25] presented experimental research to investigate the flexural behavior of slabless staircases. For testing under six-point monotonic loads, twelve specimens that were two-thirds scaled were constructed, each with a unique combination of four reinforcement configurations and three tread/riser thicknesses (Fig. (2-3)).

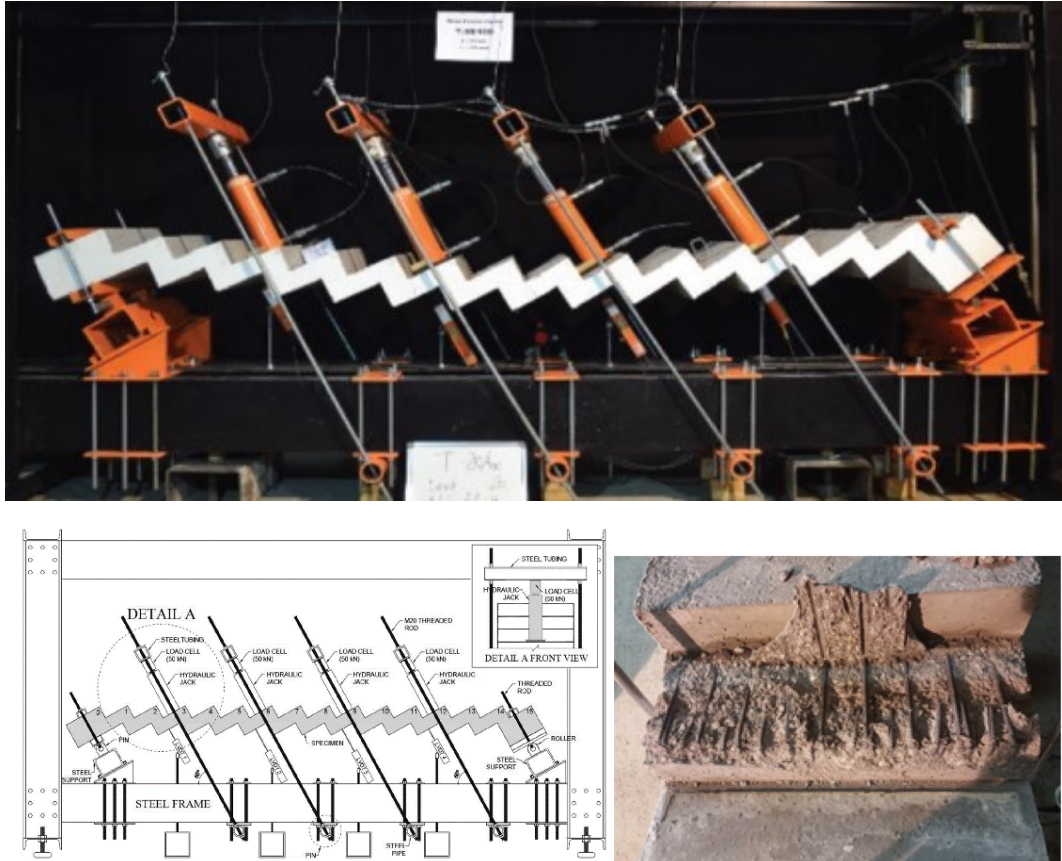


Figure 2-3 . Slabless staircases specimens of Özbek et al. [25].

The results demonstrated that slabless staircase behavior is greatly influenced by tread thickness and not riser thickness. Planar reinforcement has also been shown to significantly enhance behavior and forestall bonding issues. While reducing the thickness of the riser had no effect on the behavior and strength, decreasing the thickness of the tread led to a considerable drop in strength and concentrated damage and cracks on the treads. It is believed that the system's behavior was influenced by

possible arch action, which was produced along the very small span of risers. As a result, it is strongly suggested that the tread thickness be greater than or equal to the thickness of the riser. The analytical approaches that were developed for slabless staircases with basic supports were able to generate estimates for strength and deflection that were pretty comparable to the values that were obtained through experimentation. It is important to ensure that the tread and riser thicknesses are same if you want your measurements to be more accurate.

In 2021, Nespěšný et al. [26] examined the mechanical properties of cement fiber boards (CFBs) on the staircases behavior, particularly focusing on their strength and toughness in relation to fiber orientation. Experimental variables include the material type, specifically CFBs reinforced with cellulose fibers compared to traditional materials like wood. Load conditions encompass various static loads applied during testing, including initial, gradual, and maximum loads, with a total applied load at collapse of 2100.6 kg and a surface loading of 9.26 kN/m² as seen in Fig.(2-4). Deformation measurements focus on permanent deformations recorded after each loading cycle, along with initial and subsequent vertical displacements, such as 4.096 mm before the first crack. The duration of loading breaks and their effects on structural relaxation are also considered, with recommendations for break intervals to ensure displacement changes remain within 0.5%. Structural parameters involve the configuration and dimensions of the staircase, as well as the connection methods and their impact on performance. Results indicated that the CFB staircase meets technical standards for static load capacity, demonstrating the viability of CFBs produced via the Hatschek process for load-bearing applications. Key findings reveal that initial loading leads to significant permanent deformations, attributed to production inaccuracies and the activation of connecting elements. Comparisons with wooden staircases show comparable

permanent deformation values. Notably, a recommendation is made for initial partial loading to activate the structure before full loading. The staircase ultimately collapsed under a total load of 2100.6 kg, exceeding standard surface loading requirements by 131.5%. The study emphasizes the importance of loading breaks for structural relaxation, suggesting optimal break durations to stabilize vertical displacements. Furthermore, a numerical verification using ATENA software yielded minimal discrepancies between simulated and experimental results, indicating that material imperfections may influence performance. This research contributes valuable insights into the potential of CFBs in construction, advocating for further investigation into optimal design practices for staircase applications.

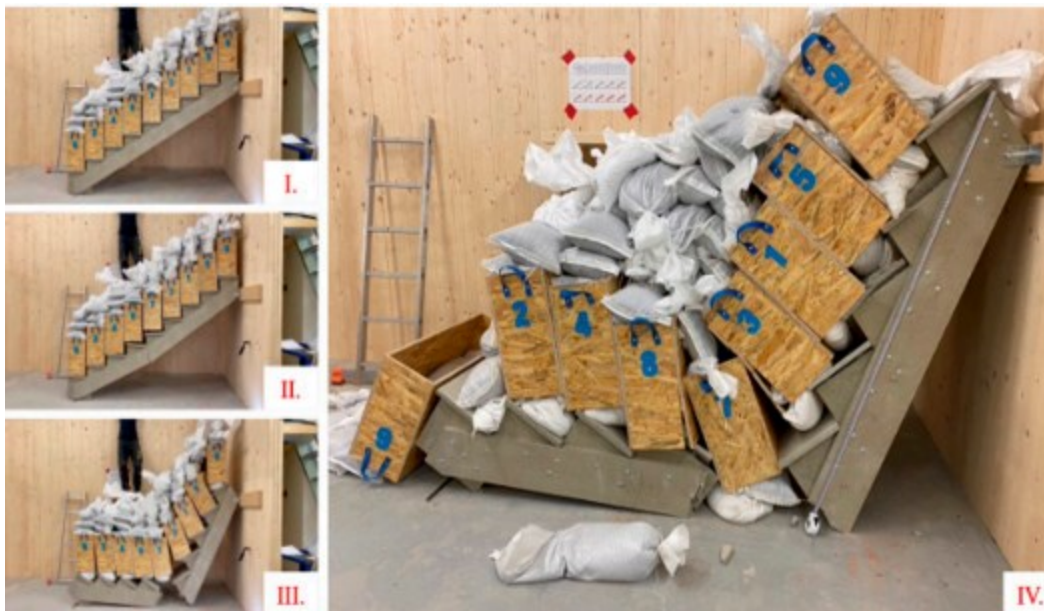


Figure 2-4 : The cement fibre board internal staircase structure collapse [26].

In 2022, Olivieri et al.[27] explored the influence of concentrated loads on masonry open-well spiral staircases as seen in Fig.(2-5) . The research revealed that the application of concentrated loads can significantly alter the compressive stress regime and stress distribution within these staircases, potentially leading to

undesirable torsional effects on the steps. The study highlighted that the stability of spiral stairs could be compromised based on various factors, including geometry, materials, and construction techniques. A notable gap in the existing literature was identified, as most studies had primarily focused on uniformly distributed loads, neglecting the implications of localized or concentrated loads.

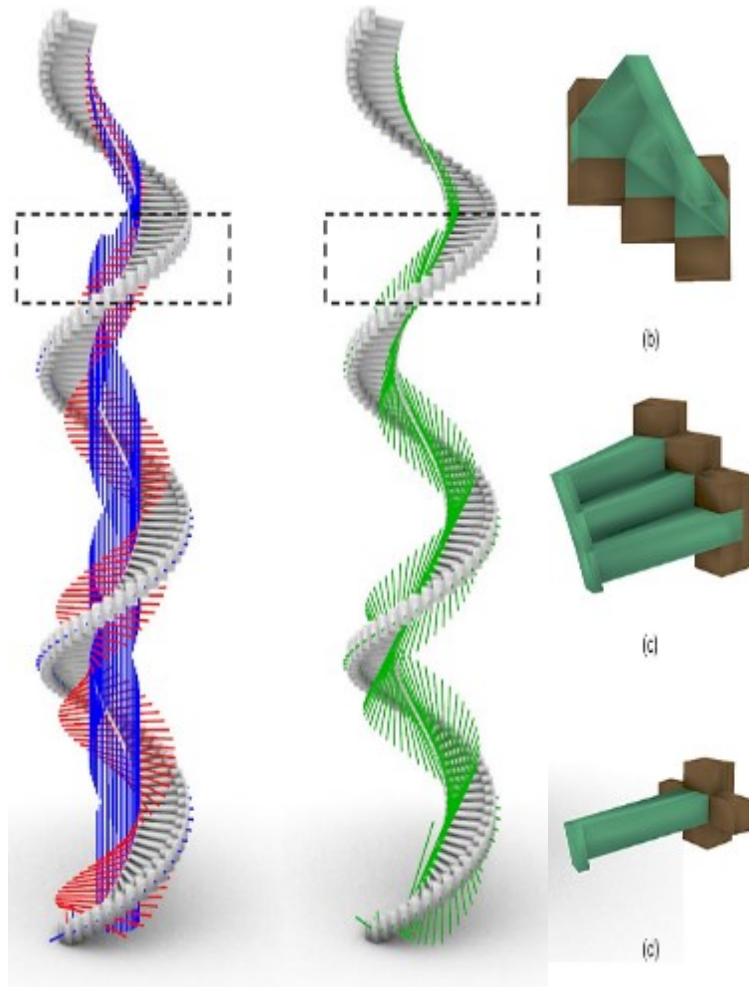


Figure 2-5: modeled slabless staircases[27].

Olivieri et al. used a simpler analytical technique known as the Linear Arch Static Analysis (LASA) approach to address this issue. This method was recently created for the purpose of analysing the structural behavior of open-well spiral stairs when they were subjected to constant stresses. A thorough parametric study of staircases

with elliptical and circular planforms is part of the project. To ensure safety against the danger of collapse, the study set out to discover relevant ranges of geometric characteristics and areas for concentrated loads. Furthermore, a case study involving the steps of the Convent of San Domingo de Bonaval was conducted using the LASA technique, which was then compared to a rigid block model. In this case, the steps interface at their inner ends, creating a virtual rib that can effectively transfer external loads to the ground.

In 2024, Shan and colleagues presented the results of an experimental investigation that evaluated the flexural behavior of a staircase made of ultra high performance concrete (UHPC). During the course of the parametric investigation, the behavior of a precast staircase composed of NSC was explored. In addition, an experimental investigation was conducted to assess the influence of fiber contents (0.75%, 1.0%, and 1.5%) and the incorporation of steel bars in the UHPC staircase. The results revealed that the crack development and load–deflection curve comparisons demonstrated that the flexural performance of the UHPC staircases exhibited greater resistance to cracking compared to that of the NSC staircase. Moreover, enhancing the fiber content proved advantageous in increasing the crack resistance of the UHPC staircases and reducing the stress concentration at the step roots on the rib slabs, which in turn improved their load-bearing capacity. The lack of rebar did not significantly impact the flexural performance of the UHPC staircases prior to cracking, but it had a detrimental effect on their bending behavior post-cracking. Additionally, a short-term stiffness model for UHPC stairs was developed using the effective moment of inertia method along with a modified steel fiber conversion area parameter, achieving a deviation of less than 6%. In conclusion, a comprehensive parametric study was carried out utilizing a validated finite element (FE) model, leading to valuable recommendations regarding the selection of section

sizes to enhance the flexural performance of the proposed ultra-high-performance concrete (UHPC) staircases. It was observed that the bends in reinforced concrete stair slabs (RCSS) subjected to opening moments can sustain damage due to inadequate detailing of tensile reinforcement or construction errors, which can compromise their structural integrity. Consequently, it is crucial to implement strengthening measures to restore the flexural strength of these damaged bends.

Despite the fact that such interventions are required, there is a significant lack of research that focuss on the behavior of reinforced classroom support systems (RCSS). Recent research conducted by Hamoda and colleagues (2023) has shed light on this matter by presenting both experimental and simulation assessments of reinforced concrete reinforced with steel (RCSS) that has been strengthened by employing steel plates that are externally bonded and steel bars that are near-surface mounted. A comprehensive test program was utilized in their investigation, which consisted of six full-scale strengthened RCSS specimens. These specimens were loaded to the point of failure, which enabled an in-depth analysis of their performance. ABAQUS software was utilized in order to create a finite element model for the purpose of simulating the experimental responses of these further reinforced RCSS. According to the findings, the strengthening strategies that were utilized resulted in significant enhancements to the cracking load, ultimate load capacity, and energy absorption of the composite reinforced concrete structural system (RCSS). A further point to consider is that the strong correlation that exists between the numerical simulations and the experimental data provides evidence that the nonlinear inelastic analysis model has the potential to be applied in a dependable manner for additional parametric research in the future.

In the year 2024, Zhang and colleagues carried out a comprehensive investigation on the ways in which precast reinforced concrete (RC) stairs performed

when they were subjected to earthquake loading. Through their research, they were able to overcome the issues that were brought about by the negative diagonal support effect that is often associated with regular precast RC stairs that have rigid connections (also known as TS). Due to the fact that this issue frequently results in the accumulation of negative tension, the RC flights are susceptible to being damaged. An innovative low-damage stair system was developed by the researchers in order to address these difficulties. This system features a sliding joint at the base of the precast RC steps, which are classified as SS. The purpose of this design is to accomplish both the enhancement of flexibility and the reduction of stress concentration during seismic events. A full evaluation of the seismic reactions of these stair systems was made possible as a result of the study, which comprised both experimental and numerical evaluations of the TS and SS specimens. The results of this study demonstrate that the sliding joint design is an excellent method for reducing the negative impacts that are normally seen in stair systems that are coupled in a rigid manner. The findings indicate that this low-damage technique not only enhances the structural resilience of precast RC stairs when subjected to seismic conditions, but it also provides a potential alternative for the design of future steps. An illustration of the experimental setup and the results may be found in Figure 2-6. This figure offers a visual representation of the comparative performance of the two different stair layouts when subjected to seismic loads. During the course of the testing, it was proved that the SS was capable of successfully removing the negative diagonal support effect that is associated with conventional stair systems as well as the unexpected high stress concentration that was present in the RC components. From the inter-story drift ratio all the way up to the final level of 4.00%, the RC flight and landing beam of the low-damage stair systems that were proposed did not sustain any damage. Through the utilization of the sliding joint, specimen SS exhibits a remarkable capacity for energy dissipation as well as hysteretic behavioral

characteristics. In addition, the results of the parametric analysis demonstrate that the seismic responses of the innovative stairs are significantly influenced by the strength of the concrete, and that the effect of the friction factor of the sliding joint on seismic performance is not uniform under both positive and negative loadings.

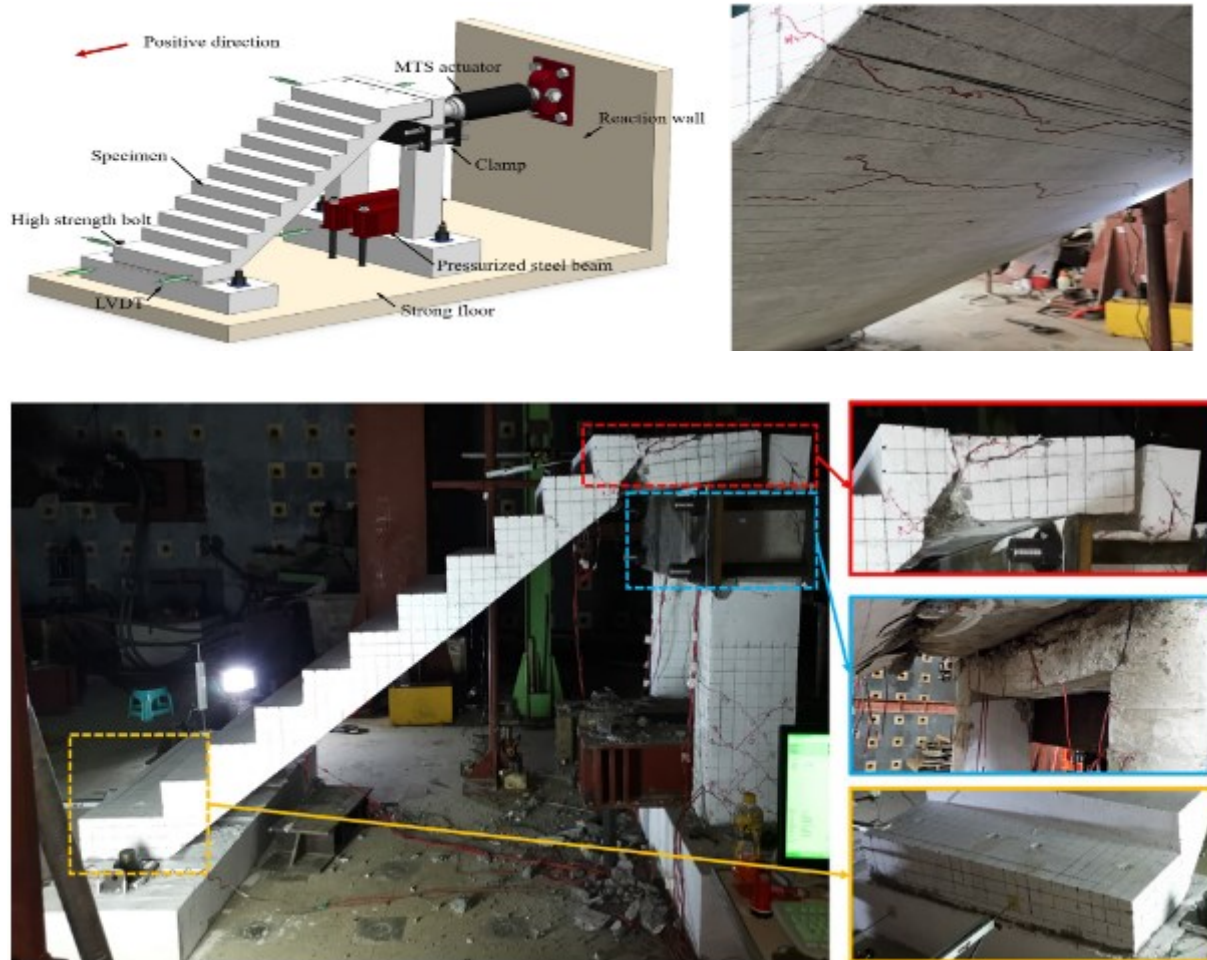


Figure 2-6 Tested staircases presented by Zhang [29]

In the year 2024, Wang et al. [30] conducted an investigation into the efficiency of lightweight prefabricated concrete stairs that had a hollow landing slab that was created in a specially designed manner. This article provides a comprehensive account of the development of a unique lightweight concrete stair structure, as seen

in Figure 2–7. Following the clarification of the particular structural composition, the design approach was provided and validated with an example.

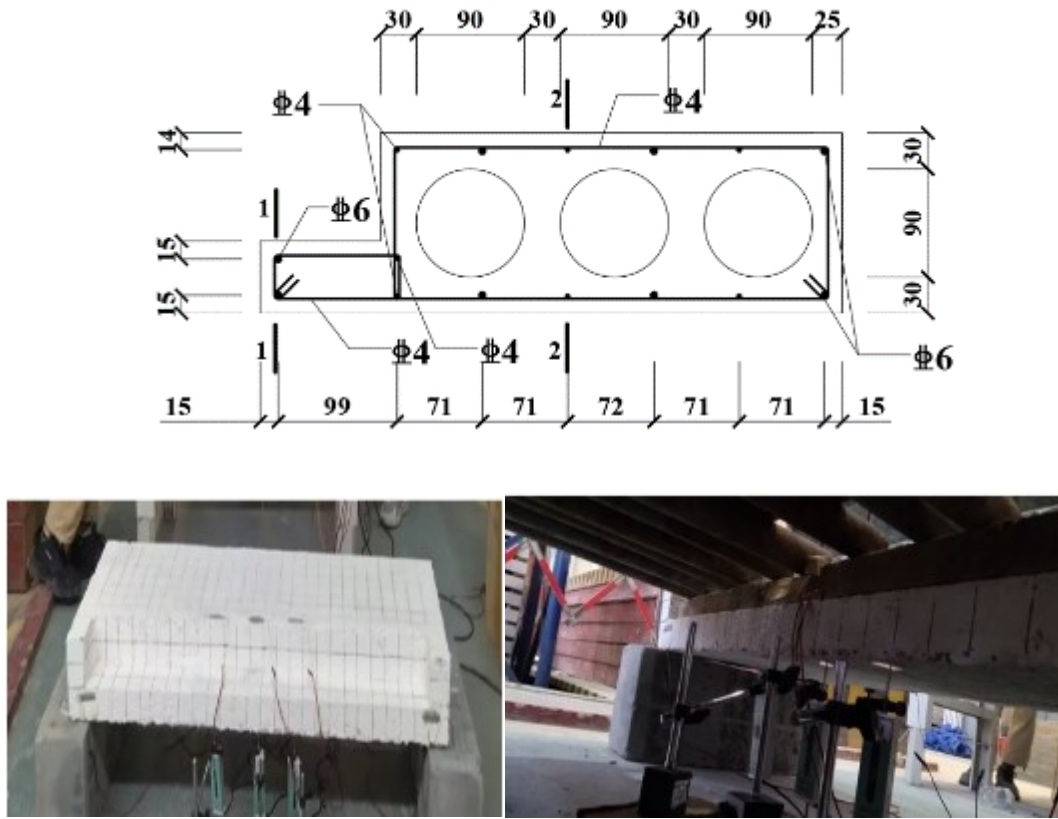


Figure 2-7 staircases tested by Wang. [30].

A more in-depth examination into the influence of the parameters was carried out by employing numerical modeling and conducting experiments. To be more specific, the parameters that were utilized included a stair system that featured a hollow landing slab that was prefabricated in a certain shape, in addition to flight and support beams, which included a platform support beam and a floor beam. It was found that numerical simulation was the most effective method for determining the stress situation of the concrete component under the design load for the special-shaped prefabricated hollow landing slab. This conclusion was reached after taking into account all of the requirements for the construction project. Following that, the design of the reinforcement may be completed. A new type of lightweight stair

system has the potential to be used in a variety of applications in the future because it requires little in the way of transportation, has a low weight and volume, and has a high level of uniformity.

2.3 Summary

According to the researchers' knowledge, there was limited of the previous investigations included a comprehensive parametric study on slabless staircases. Moreover, there appears to be a lack of prior empirical investigations specifically addressing steel reinforcement configurations in slabless stairs within the existing literature. The complex characteristics of concrete—such as nonlinearity, anisotropy, cracking, and elastoplasticity—make it challenging to predict the behavior of reinforced concrete (RC) components without experimental testing. The behavior of slabless stairs is also heavily influenced by the specific reinforcement provided. Local norms and engineering judgment offer various detailing options for these staircases; however, the effectiveness of these reinforcement patterns and their impact on overall structural behavior remain unclear. Consequently, there are instances where slabless RC stairs may experience failure even under conditions that do not exceed design service loads. This gap in understanding the need for further research into the reinforcement strategies for slabless stairs, aiming to clarify their effectiveness and enhance safety and performance in practical applications. A systematic investigation into the behavior of these structures under various loading conditions is essential to develop reliable design guidelines and ensure structural integrity.

CHAPTER THREE: FINITE ELEMENT FORMULATION AND MATHEMATICAL MODELING

3.1 General

To acquire data and solutions to these equations, structural analysts often turn to numerical approaches, as the majority of structural analysis problems are difficult. Analysing various structural parts are possible with the use of the finite element method (FEM), one of the most significant computational approaches for addressing complicated issues. Consequently, approximate solutions to real-world issues are obtained using numerical processes like FEM. FEM is a game-changing technique that engineers may use to solve a wide variety of challenges. This study investigates the behavior of RC stairs that are subjected to a constant load using nonlinear finite element analysis[31].

3.2 Numerical Evaluation of Structures in a Nonlinear System

The field of solid mechanics deals with several nonlinear processes. But there are a number of cases when the engineering solution can be obtained just fine by employing linear formulation. High deflection and post-yielding are two examples of challenges that might necessitate nonlinear property analysis in order to get practical outcomes. Nonlinearity according to materials, nonlinearity according to geometry, and combined nonlinearity of materials and geometry are the three forms of nonlinear problems that can arise from nonlinear causes [31]. In the finite element approach, variables are interpolated among a small set of discrete, non-overlapping parts called "elements" that make up the complex structure. The elements are linked at numerous points along their perimeter, called 'nodes' or 'nodal points,' as shown in Fig.(3-1)[32].

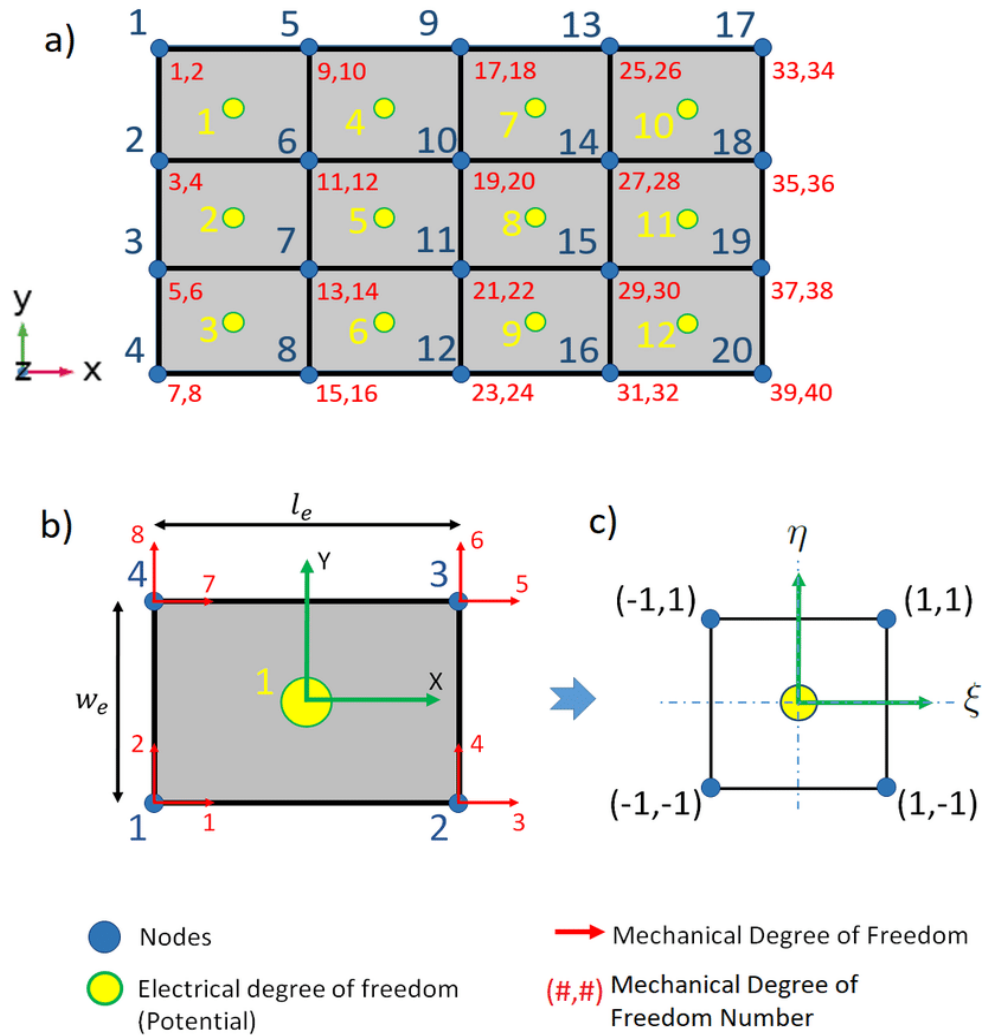


Figure 3-1 Finite element discretization [32].

To get the overall structure's global stiffness matrix and load vector, it is necessary to compute the applied load vector and stiffness matrix for each individual element. Unknown nodal variables, representing displacement components, are solved for pertaining to structural issues through the process of solving the system of simultaneous equations that was produced [32].

3.3 The Fundamentals of the Finite Element Theory

What follows is a rundown of the fundamental procedures for solving any problem using finite element analysis [33]:

- a) Elements undergo all operations during the pre-processing step, including creation, discretisation, matrix generation, and assembly leading to the achieved results. Below is a thorough explanation of each step:

Break down the issue into manageable chunks by creating and discretising the solution domain into a certain number of finite parts. Then, organise these pieces into nodes. It is believed that the physical behavior of an element may be defined by a form function, which in turn can offer the element's solution, and that this shape function is the approximation continuous function.

To demonstrate the entire issue and produce a generic stiffness matrix, you must first design and construct stiffness matrices with respect to inclusion.

Solving the problem by applying loading, starting conditions, and boundary conditions.

- b) As part of the solution phase, the algebraic equations that have been generated are solved in order to get node outcomes, such as displacement at a number of different nodes.
- c) The stage after processing is when further data like stress distribution, strain and stress values, shear force, bending moments, etc. are obtained.

3.4 Material Modeling

3.4.1 Concrete Modeling

A) Plasticity Approach

In order to evaluate how concrete reacts to different types of stress, numerous component models have been created. Models based on plasticity and elasticity are among the primary component models. An elastoplastic reaction to the stressed material is provided by the mathematical expression that is based on plasticity in this study's model. In the compression algorithm, smashing concrete is like applying a plasticity law [34]. The independent yielding criterion determined by the rate of

Von-Mises, representing a uniaxial stress-strain relationship, is also the basis of this method's operation. The direction of plastic strain is determined by the law of flow after the yield point, while the yield term denotes the magnitude of stress that causes the material to yield. As yield varies gradually, the hardening rule specifies how the yield surface changes.

B) Material Nonlinearity

When the stress-strain curve, or substantial material relation stops being linear, we say that the material is nonlinear in solid mechanics. It is no longer reasonable to presume that stress and strain are directly proportional, just as in the classic linear elastic case. The connection is a stress function, either combined or individual. The stress-strain curve is the primary tool for characterising material behavior. The rationale for a nonlinear structural behavior is due to the fact that the material stress-strain curve is nonlinear. The stress-strain properties of a material can be affected by a variety of factors, including the loading circumstances and the type of material being used. Due to the fact that it directly influences the material's resistance to loads and cracks, in addition to its resistance to creep and corrosion, it is essential to take into consideration that the nonlinearity of the material generally has an effect on the structural behavior of the material.

When it comes to the behavior of the element after the yield stage, the nonlinearity of the material varies according to the material. This is because the behavior of the steel material after the yield point is different from that of the concrete material. Because the steel material continues to resist the loads that are imposed with a higher strength than the concrete material, which loses its stiffness more quickly than steel does before it reaches the failure point [35]. This is an illustration of the linearity of the stress-strain curve for concrete, which can be found in Fig.(3-2).

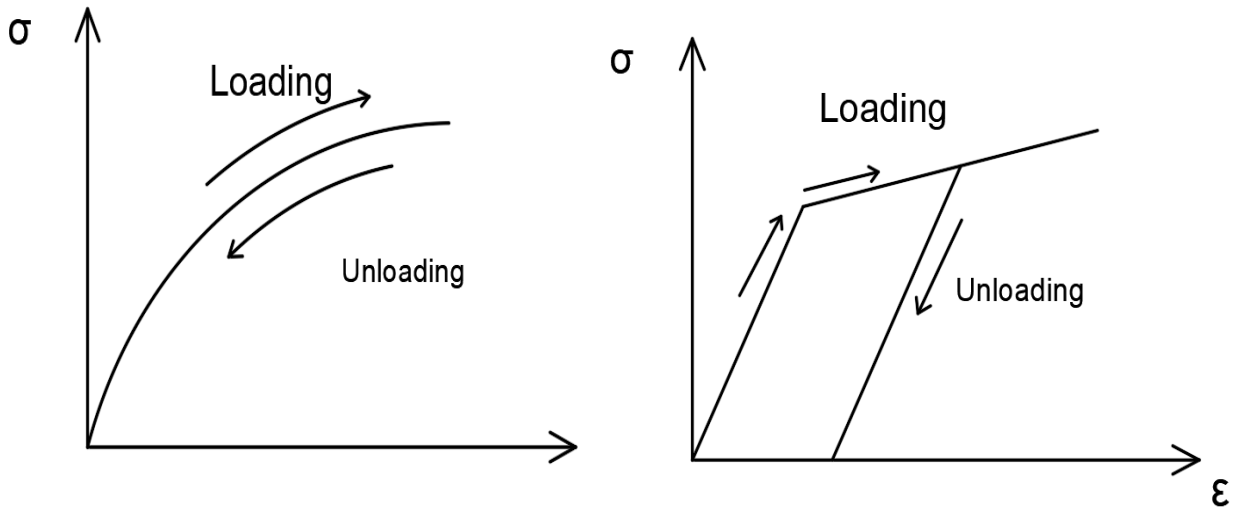


Figure 3-2 a) Nonlinear elastic material response b) Nonlinear plastic material response [35].

C) Multilinear Relationship between Stress and Strain

The usual stress-strain response of concrete when compressed in one direction is seen in Fig. (3-3) . Up to about 30% to 50% of concrete's ultimate strength, the material behaves in a fairly linear fashion [36]. Once the concrete hits its ultimate strain increase of 0.0035, crushing begins and the curve begins to drop until the concrete reaches the rupture point, at which time crushing is complete. Although it is more solid and stiff, high-strength concrete (HSC) is extremely brittle and elastically weak due to its poor ductility. In comparison to regular concrete, the HSC has a higher linear phase. After the curve reaches its maximum, there will be a sharp decline; at this period, the concrete will exhibit very brittle behavior, losing a significant amount of a measure of its rigidity when steel is compressed to the point of ultimate failure [36].

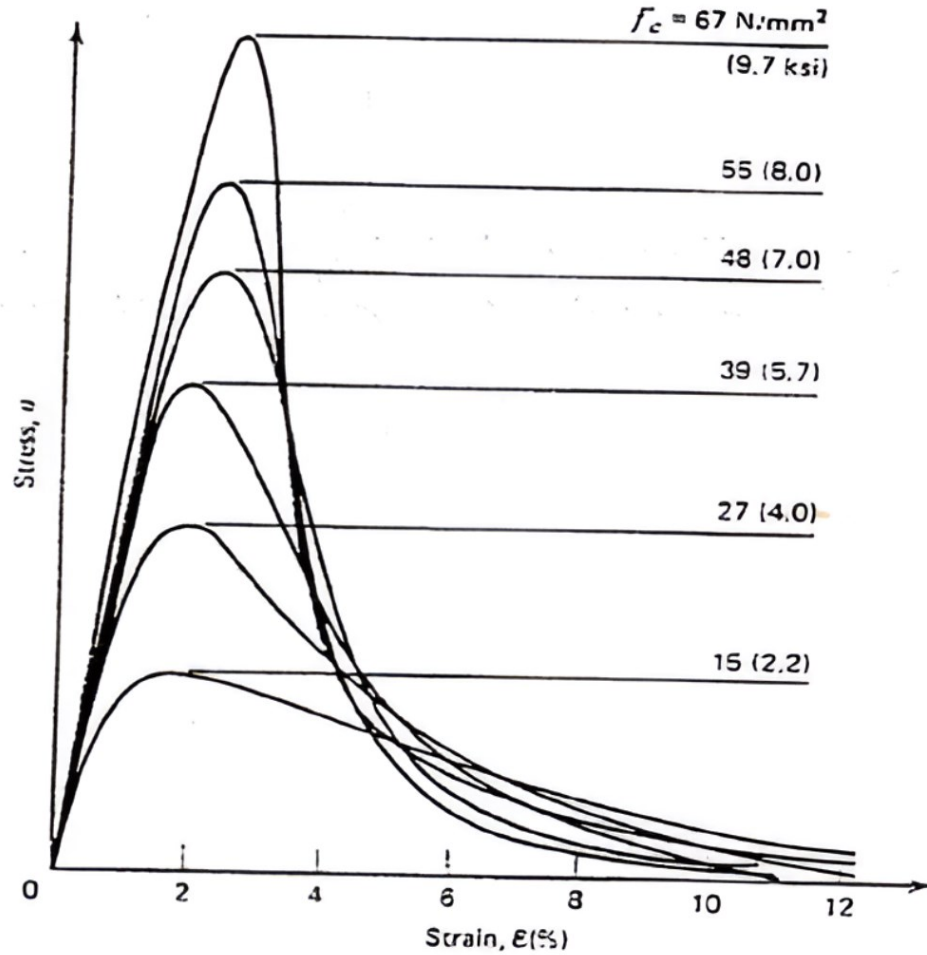


Figure 3-3 Various concrete strengths are represented by a uniaxial compressive strain curve [36].

The Young modulus (E_c), which varies between normal and high strength concrete, is one of the most crucial properties that essential to be defined for the purpose of comprehension the behavior of concrete and is also required for concrete definition in the ABAQUS program. The formula for calculating the Young modulus (E_c) can be found in ACI 318M-19 [37].

$$E_c = 4700\sqrt{f'_c} , \quad (MPa) \quad \dots\dots (3.1)$$

Hsu and Hsu [46] provided values for the elasticity modulus for high strength concrete;

$$E_c = 124.31f'_c + 22653, \quad (MPa) \quad \dots\dots (3.2)$$

The RC stair study makes use of Poisson's ratio, which can take on values between 0.15 and 0.22, although a value of 0.2 is used for this investigation [38]. An origin-towards-increasing Both linear and nonlinear phases are included in the stress-strain curve. Characterises the behavior of concrete under uniaxial compression in ABAQUSO ther parts of the market have steeper slopes than the initial segment, and the slope of the curve is correlated with the modulus of elasticity of the material. It should be mentioned that the ABAQUS program rejects the idea of a stress-strain curve that is falling because it views the numbers that produce such a curve as a numerical mistake. Fig. (3-4) and the following equations [39] show the idealised uniaxial stress-strain diagram for a concrete specimen:

$$f_c = \varepsilon E_c \quad \text{for} \quad 0 \leq \varepsilon \leq \varepsilon_1 \quad \dots\dots (3.3)$$

$$f_c = \frac{\varepsilon E_c}{1 + \left(\frac{\varepsilon}{\varepsilon_o}\right)^2} \quad \text{for} \quad \varepsilon_1 \leq \varepsilon \leq \varepsilon_o \quad \dots\dots (3.4)$$

$$f_c = f'_c \quad \text{for} \quad \varepsilon_o \leq \varepsilon \leq \varepsilon_{cu} \quad \dots\dots(3.5)$$

$$\varepsilon_1 = \frac{0.3f'_c}{E_c} \quad (\text{Hooke's law}) \quad \dots\dots(3.6)$$

$$\varepsilon_o = \frac{2f'_c}{E_c} \quad \dots\dots(3.7)$$

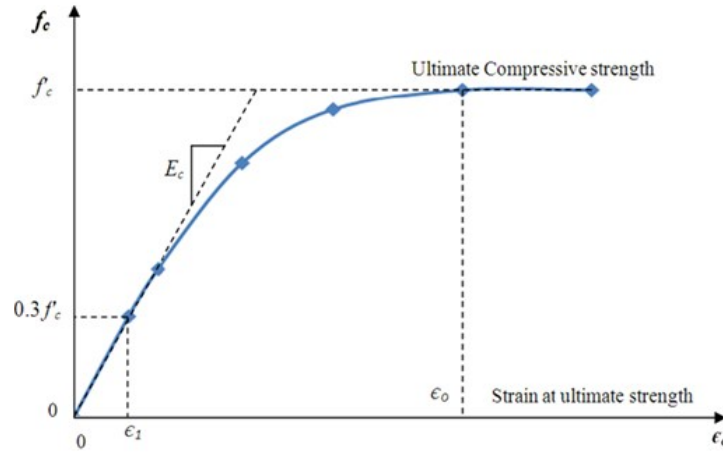


Figure 3-4 Simplified stress-strain for NSC [39].

For HSC, (Hsu and Hsu 1994) [38], stress-strain equation is used

$$f_c = f_c' \frac{n \beta (\varepsilon/\varepsilon_o)}{n \beta - 1 + (\varepsilon/\varepsilon_o)^{n \beta}} \quad \dots\dots (3.8)$$

$$\beta = \left(\frac{f_c'}{65.23} \right)^3 + 2.59 \quad \dots\dots (3.9)$$

$$\varepsilon_o = 1.29 \times 10^{-5} f_c' + 2.114 \times 10^{-3} \quad \dots\dots (3.10)$$

Where, f_c is the stress at any strain ε in (MPa).

f_c' is the ultimate compressive strength at strain ε_o in (MP

n is a parameter that depends on material strength , $n=1$ for $0 < \varepsilon < \varepsilon_o$.

β is a parameter that depends on the shape of the stress-strain curve.

D) Modelling for Cracks

Deflections and the distribution of internal stresses in concrete members are both impacted by cracking. When it comes to FE modelling, this phenomenon can be modelled in three different ways namely, strain, crack displacement, and fracture energy. The first method through defining stress-strain relationship can cause sensitivity in meshing a plain concrete. Because refinement causes narrower fracture bands rather than producing more cracks,

the modelling predictions do not converge to a solution with mesh refinement [40]. Because of this, simulating plain concrete using the strain method is not a good idea. Fig. (3-5) and Equation 3.11 show the tabular data for cracking strain and yield strain, which is the softening data produced in this approach:

$$\epsilon_t^{\sim ck} = \epsilon_t - \epsilon_{0t}^{\sim el} \dots\dots\dots(3.11)$$

Where,

$\epsilon_t^{\sim ck}$: Cracking strain,

ϵ_t : Total strain, and

$\epsilon_{0t}^{\sim el}$: Elastic strain and equals σ_t/E_{cm} where σ_t is the tensile stress

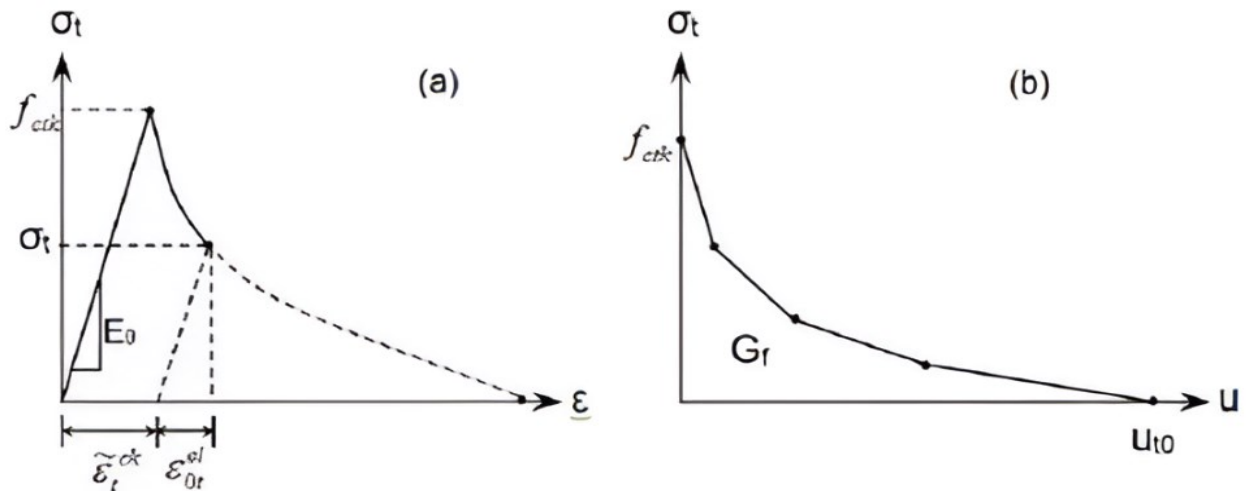


Figure 3-5(a) Stress-strain method; (b) fracture behavior after failure [40].

The tensile behavior of concrete can be described using both the stress displacement and fracture energy approaches at the same time due to the interconnectedness of both methodologies. which are founded on the fracture energy cracking requirements indicated by Hillerborg et al. (1976) [41], alleviate the problem of meshing dependency in the strain method. The methodology is grounded

in the idea of cracks and the brittle behavior of concrete. It defines fracture energy as the amount of energy needed to open a specific area of cracks in a material. At first, the cracked concrete has a little tension along the crack's longitudinal axis as a result the interaction that takes place between the concrete and the steel reinforcement on the concrete. As can be seen in Fig.(3-6), the analysis took the tension stiffening effect into account. We assumed that strains in the concrete would gradually relax as we worked our way ,away from the crack plane. Wang and Hsu (2001) [42] identified an exponential curve, Peterson (1996) [43] found a bilinear curve, and the image depicts a linear curve

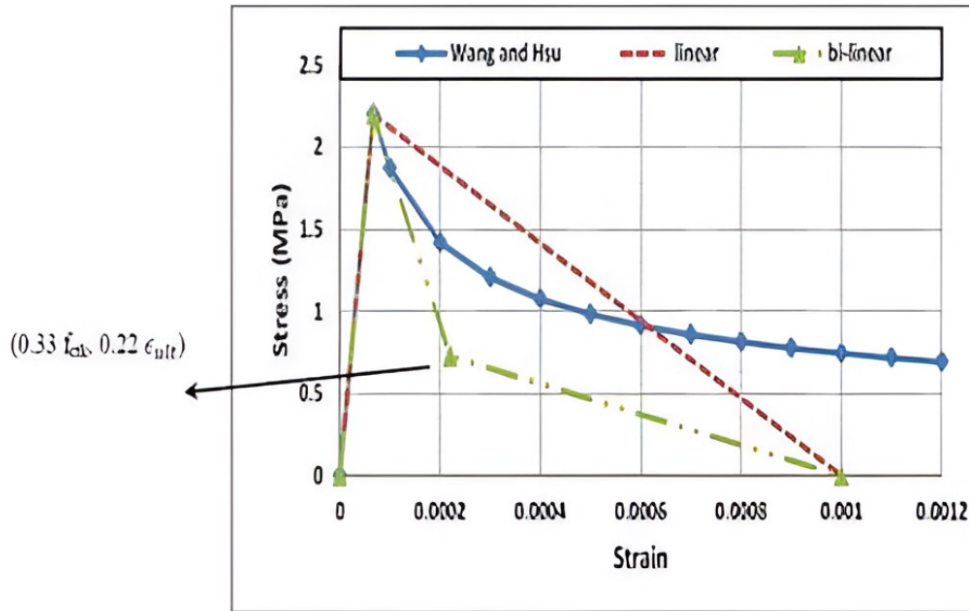


Figure 3-6 The concrete's uniaxial tensile stress-strain behavior [40].

E) Crushing Modeling

When analyzed by finite element, the failure that occurs as a result of axial, biaxial, or triaxial loading is in the form of a fast retrogradation in the value of the stiffness and after reaching the maximum strength of the body, where the decay in the stiffness of the material is linear and rapid [44].

F) Steel Reinforcement Bars

Typically, reinforcement concrete will include a combination of concrete, steel rebar, and other additives. Because the concrete gives the stair its compressive strength and the steel rebar gives it its flexural strength, the stair's behavior is a composite behavior of the sum of the behavior of the components in this compound. Fig. (3.7) shows that steel exhibits nonlinear behavior, which is known as bilinear behavior, and that defining the behavior of these materials is essential in order for the program to indicate the behavior of these elements. The bilinear curve's initial segment depicts the steel rebar's linear phase, with the slope denoted as the modulus of elasticity (E_s). Conforming to the principle of elastic perfect plastic, the second part of the curve in its entirety has no slope. Assuming that the longitudinal bar and stirrups have a yield stress of around the same magnitude, the strain hardening modulus is taken for granted in this study. The convergence was achieved by carefully selecting this number [44]. The steel reinforcement made use of Poisson's ratio $\mu = 0.3$.

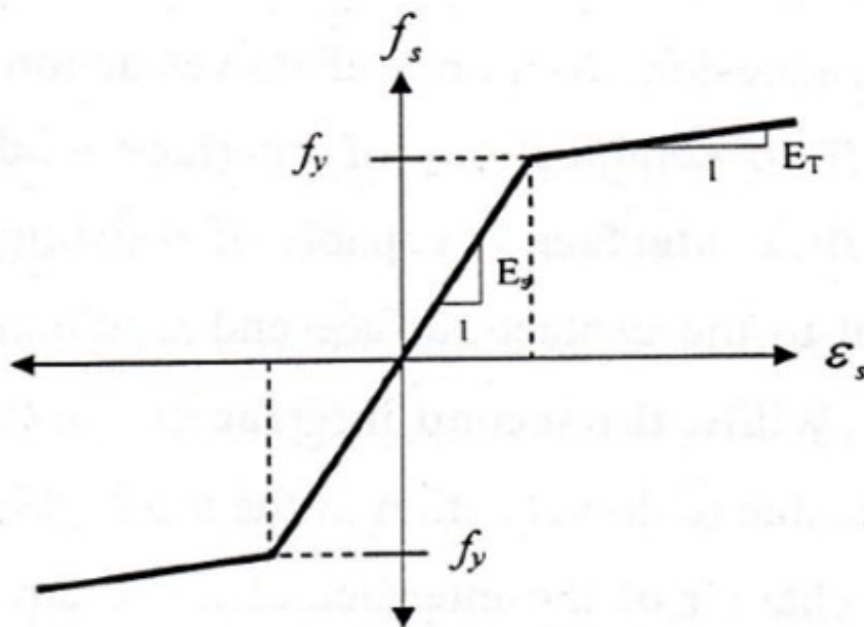


Figure 3-7 Modeling of reinforcing bars [44].

3.5 ABAQUS Computer Program

ABAQUS is an advanced finite element program suite used for engineering simulations.. The program is designed to be simple to use even while dealing with difficult issues., with a broad variety of preprocessing and postprocessing output presentation options, as well as complete data checking capabilities. The range of issues that can be solved using ABAQUS is quite broad, spanning from relatively straightforward linear analysis to the most difficult nonlinear simulations. Therefore, it will be used to execute the numerical analysis of slabless staircases behavior under torsional and flexural combined effect. You may model almost any geometry with the help of ABAQUS's large library of elements. Along with a long list of geotechnical materials like soils and rocks, it also includes a long list of common engineering materials like metals, rubber, polymers, composites, reinforced concrete, crushable foams, and resilient foams. [45]. In order to ensure that problems that include several components are accurately represented, the geometry that describes each component is linked to the appropriate material models, and the interactions between the components are specified.. If you run a nonlinear analysis with ABAQUS, it will pick the right load increments and convergence tolerances and tweak them as you go along to get a good solution quickly. ABAQUS/Standard will be utilised in this thesis because it is a suitable solution technique for static events, which are situations in which extremely precise stress solutions are of crucial importance.

3.5.1 Solution Technique

The solution is unique in linear analysis as for non-linear problems, may not be the best solution. Therefore, the accomplished solution may be not necessarily to be the solution sought [46] · For nonlinear analyses problems, various techniques are presented. Briefly, three methods will be described, namely:

- Incremental or stepwise procedure (Euler-Cauchy method).
- Iterative procedure (Newton-Raphson method).
- Combined methods.

The combined solution procedure is adopted in this thesis instead of these methods. The prescribed solution procedure combined of full or Newton-Raphson iterations method coupled with incremental load[46].

3.5.2 The Riks Method

The problems of nonlinear geometry sometimes involve buckling collapse demeanor or unstable post-buckling response where a negative stiffness matrix has been developed in the load-deflection behavior, in which some strain energy must be release to stay in equilibrium [46] . For the static analysis procedures, an automated version adaptive in ABAQUS/Standard software. Modified Riks method was adopted during the unstable response of the structure Fig. (3-8) in static equilibrium situation. Otherwise the method is employed to solve the status where the loading is proportional [46]

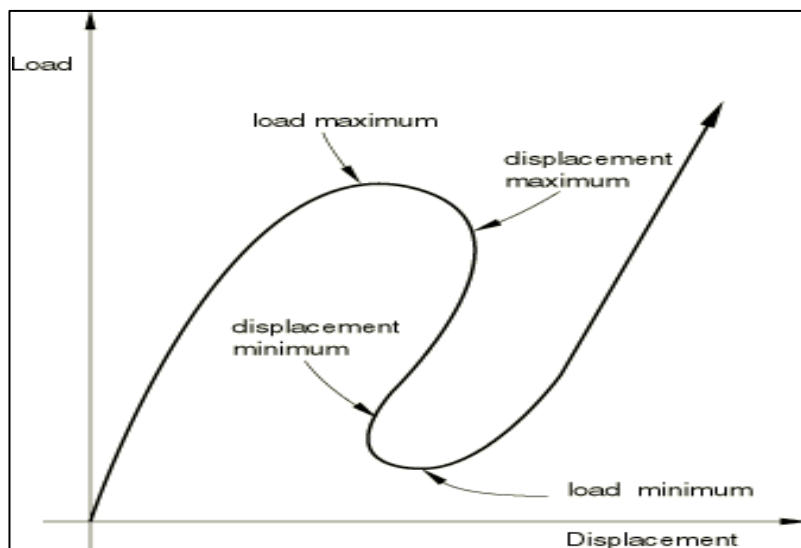


Figure 3-8 Typical unstable static response [46].

ABAQUS employed the standard Newton-Raphson method and the modified Riks method to solve the load versus vertical deflection nonlinear trace and nonlinear problems. For nonlinear equation, the standard Newton- Raphson method used iteratively and incrementally possesses the tangent stiffness matrix. This method solved simultaneously for displacement approached using the load as an unknown extension in the unloading response for structural buckling behavior. In the load-displacement approached, the arc length method (l) is adopted to accomplished this approached in static equilibrium method Fig. (3.9) Moreover, if the convergence issue fails in the finite element analysis, the initial increments must be modified, Finally, the load computed automatically after every increments. The end result will be the maximum value for displacement or load [46].

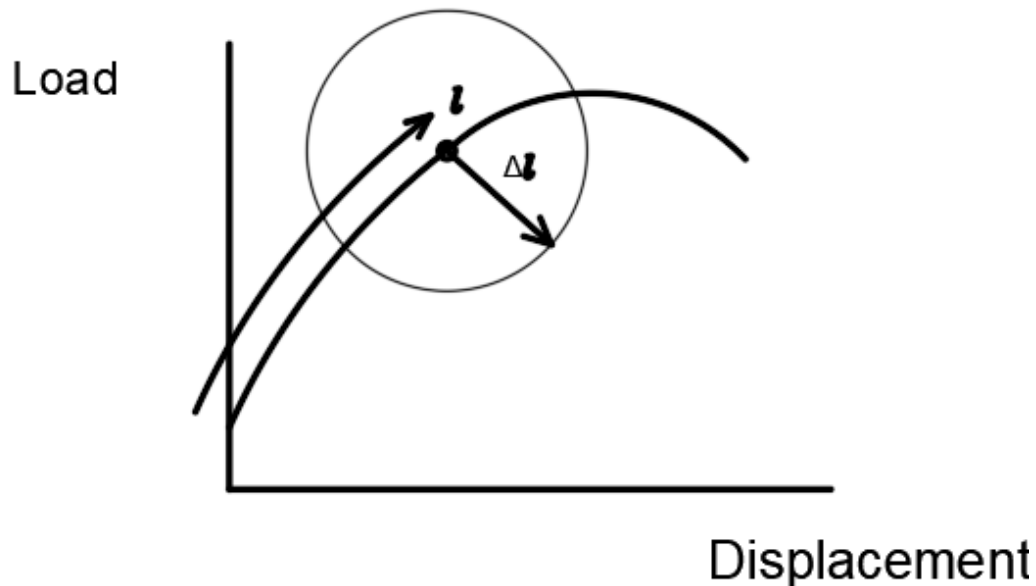
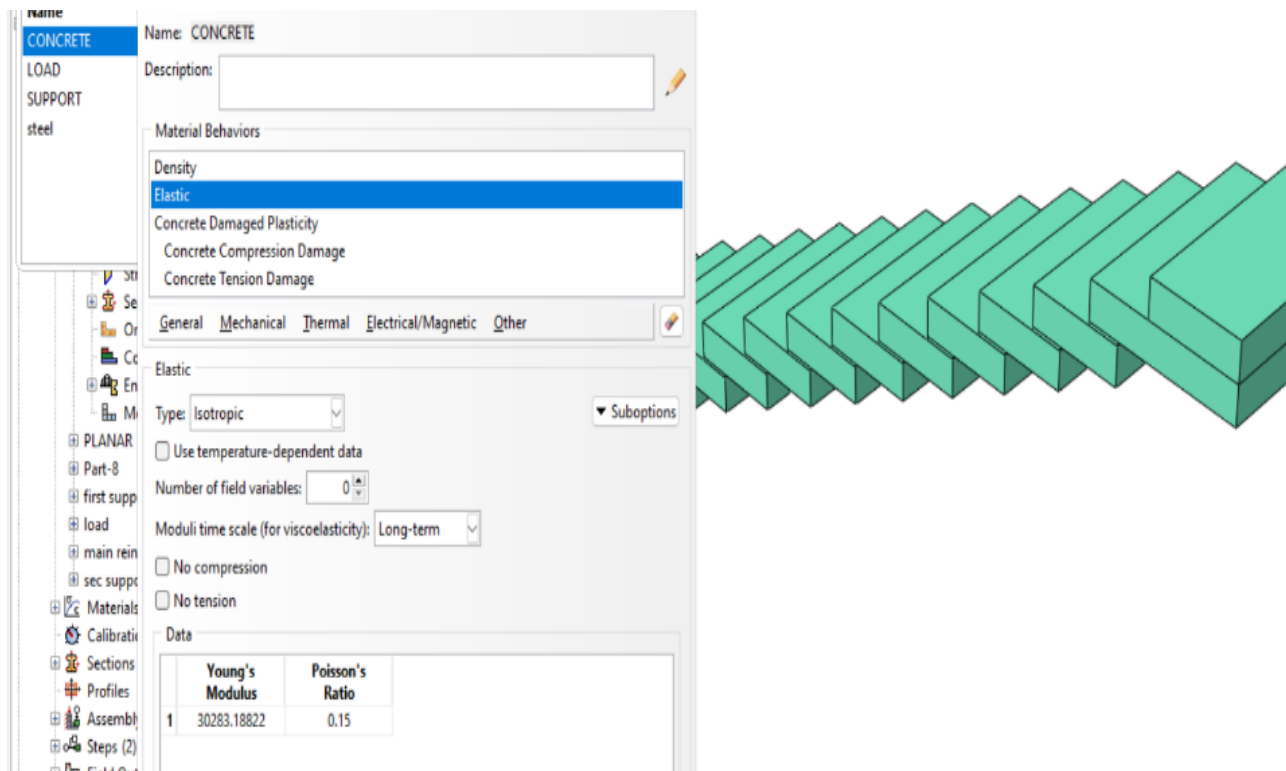


Figure 3-9 Arc length and arc length increment[46] .

3.6 ABAQUS Finite Element Model

3.6.1 Define Material Properties

In this step, specify the material properties for both concrete and reinforcement in Abaqus. For concrete, define the following: Young's Modulus (E) to determine stiffness, Poisson's Ratio (ν) as the ratio of transverse strain to axial strain, Compressive Strength (f'_c) as the characteristic compressive strength, density for concrete load calculations, and Tension Behavior to define cracking properties if necessary as seen in Fig .(3.10) . For reinforcement (rebars), include Yield Strength (f_y) for the bars, Young's Modulus for the stiffness of the steel, Poisson's Ratio for the reinforcement material, and density for the steel as seen in Fig .(3.11). Additionally, define interaction properties if using embedded or tied regions for reinforcement. This sets the foundation for the subsequent steps in modeling the staircase.



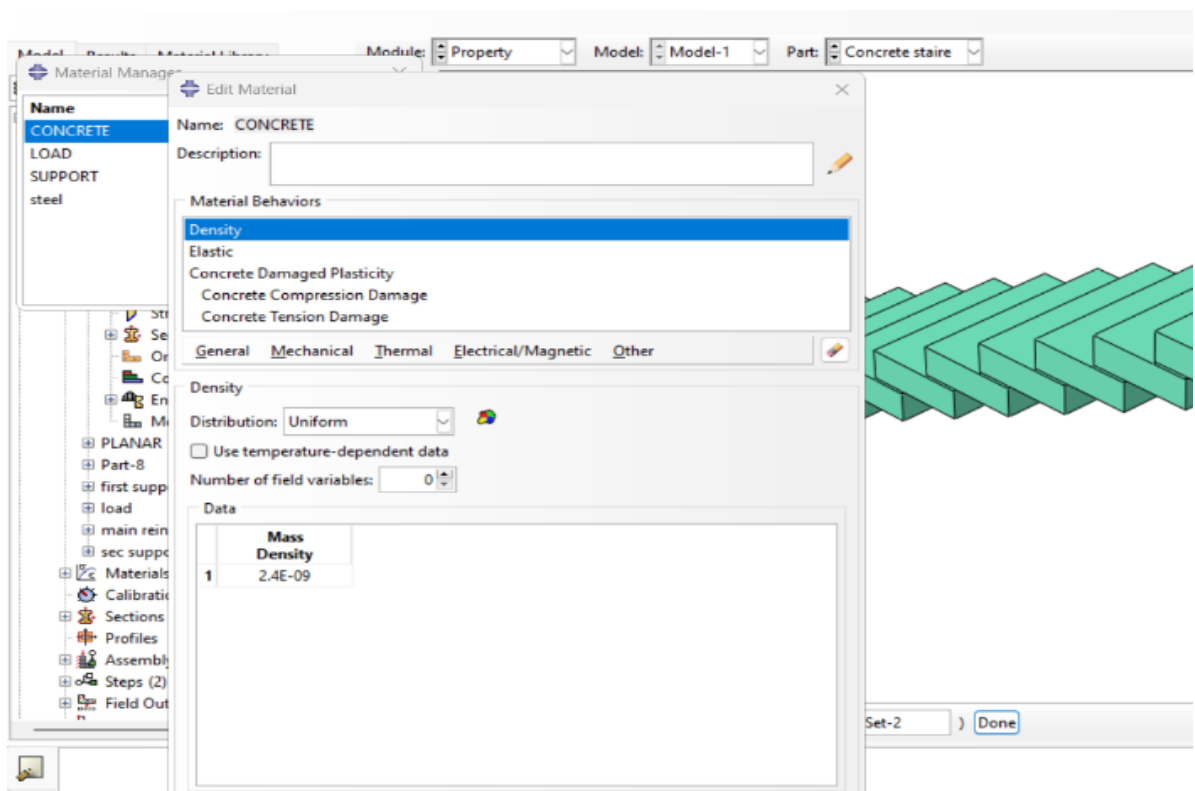
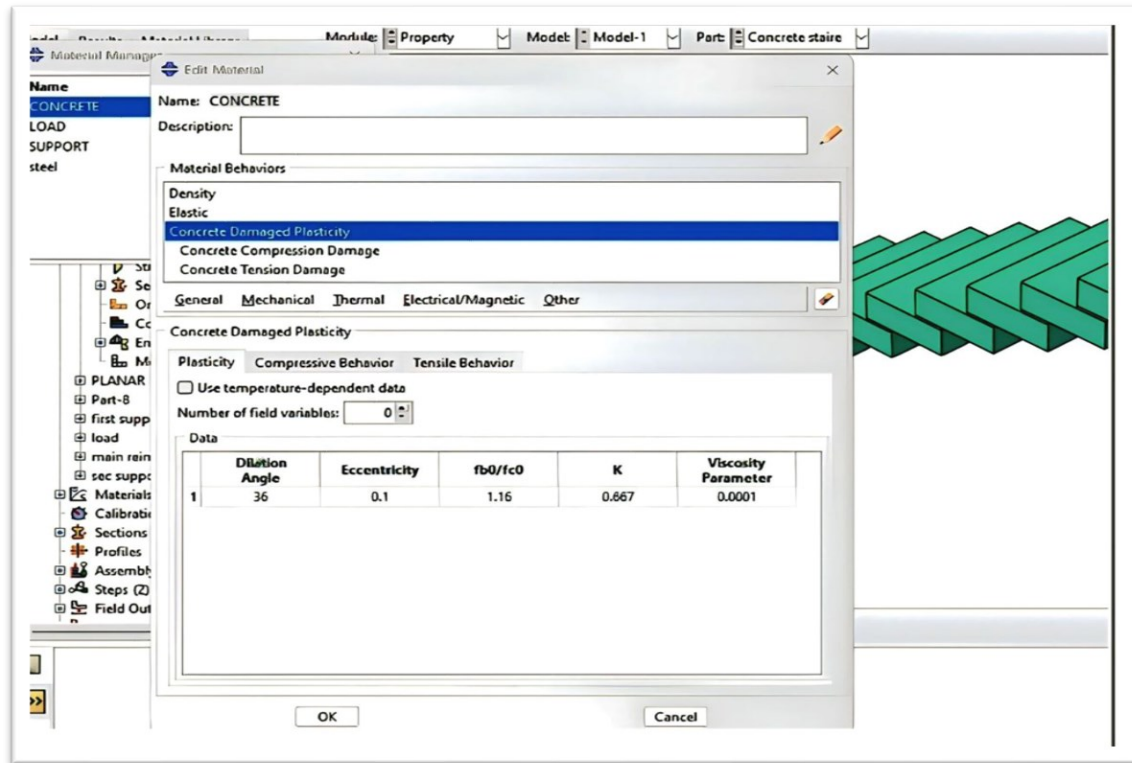


Figure 3-10 Properties of concrete in Abaqus

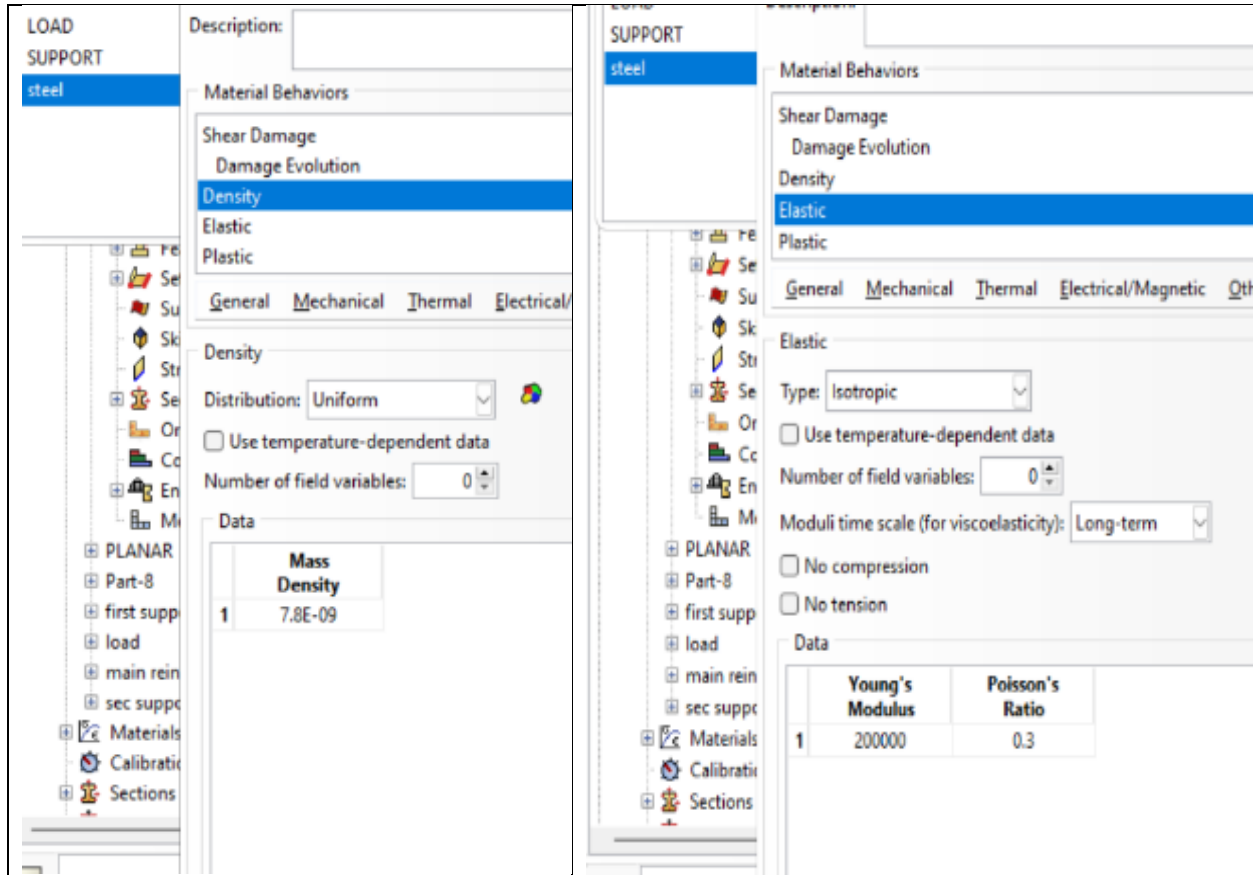


Figure 3-11 Properties of reinforcement in Abaqus.

3.6.2 Create Geometry

In this step, model the geometry of the slabless staircase in Abaqus. Begin by defining the overall dimensions, including the width, depth, and height of the staircase. It creates the individual flights and landings, ensuring that the configuration reflects the intended design. Use appropriate tools to model the flights, specifying angles and lengths according to architectural plans, and design the horizontal sections at the top and bottom of the flights. Ensure that the geometry is clear and properly defined, as this will be crucial for accurate meshing and analysis in subsequent steps. Once the geometry is complete, you can proceed to assign sections.

3.6.3 Element Mesh and Type

A) Solid element description

Elements with a three-dimensional solid structure can be made of a single, uniform material or a combination of materials in multiple layers. for large deformations, plasticity and contact behavior during linear and nonlinear analyses. A three-dimensional eight-node element (C3D8R) was utilised for the concrete slab and reinforcement. This element, as illustrated in Fig. (3.12), has eight nodes, three degrees of freedom for translation reduction in the integration with the hourglass control apparatus, and uses a linear approximation of displacement. At each integration node and stress can be supplied at different places across the element's thickness. Hexahedral and other first-order interpolation elements may be stiff and have although they have a poor convergence rate, they are able to avoid mesh locking in reduced integration analysis. procedures and provide better accuracy in second-order components [47]. Nevertheless, in order to avoid compact contact conditions and ensure correct modelling of contact surfaces, first-order elements were employed.

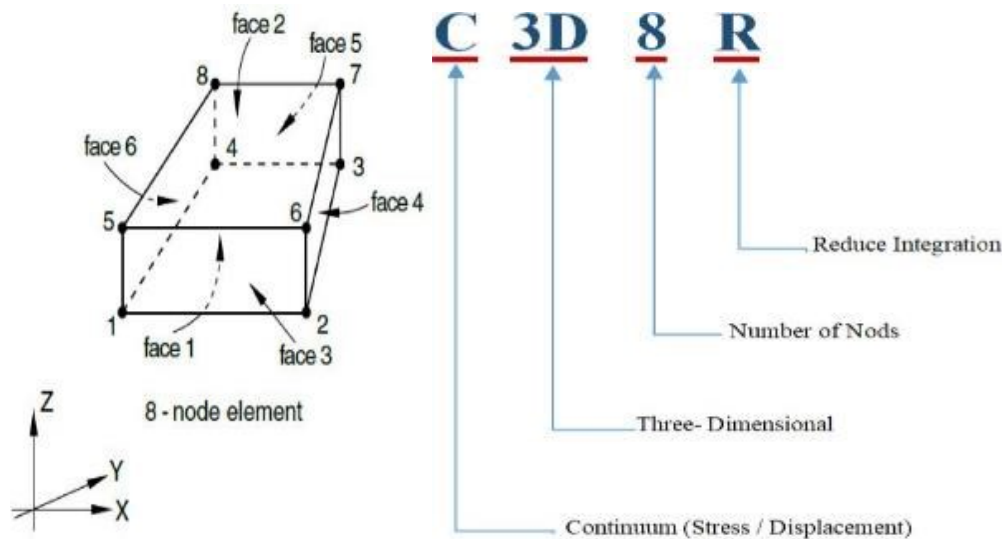


Figure 3-12 Solid element conditions [47].

B) Truss element description

When modelling slender, line-like structures that can only support loading along the axis or the centerline of the element, truss elements are utilised in both two-dimensional and three-dimensional modelling. There are no moments or forces that are supported that are perpendicular to the centerline. There is a straight truss element with two nodes are available in ABAQUS/Standard. This element employs linear interpolation for position and displacement, and it has a constant stress. In addition, a 3-dimension straight truss element which uses quadratic interpolation for position and displacement so that the strain varies linearly along the element is available in ABAQUS/Standard too [47] . The three-dimensional two-node truss element (TSD2) with linear approximation of displacement was utilised for the reinforcing steel. This element consisted of two nodes and three translational degrees of freedom for each node, as demonstrated in the given diagram. Fig.(3-13). Figure (3-14) shows mesh sizes the kinds of components that were utilised presented in the finite element model for slabless staircases.

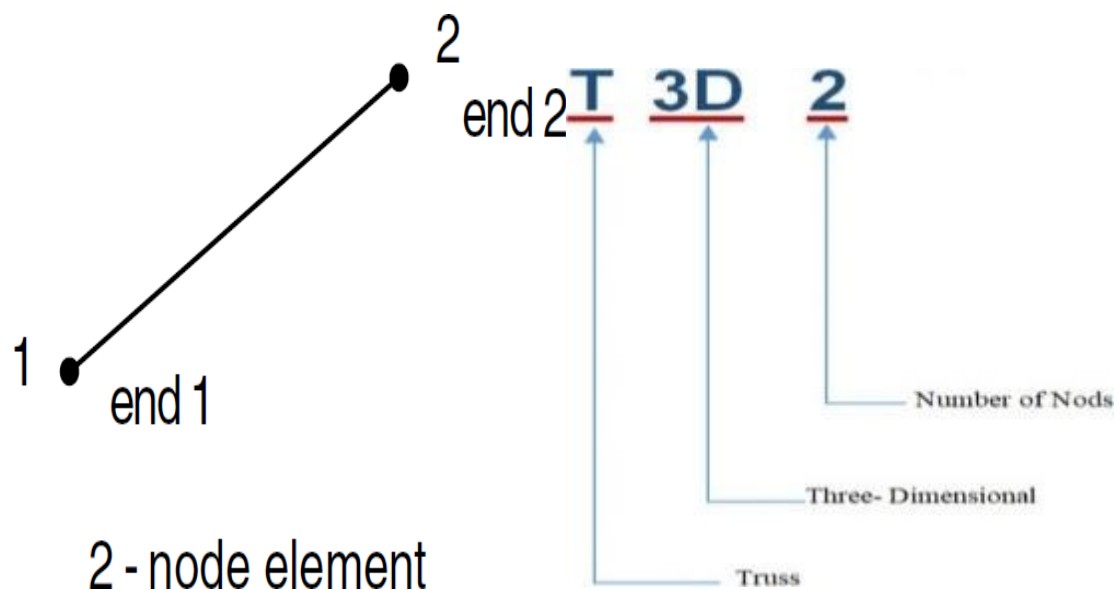


Figure 3-13 T3D2 element description [47]

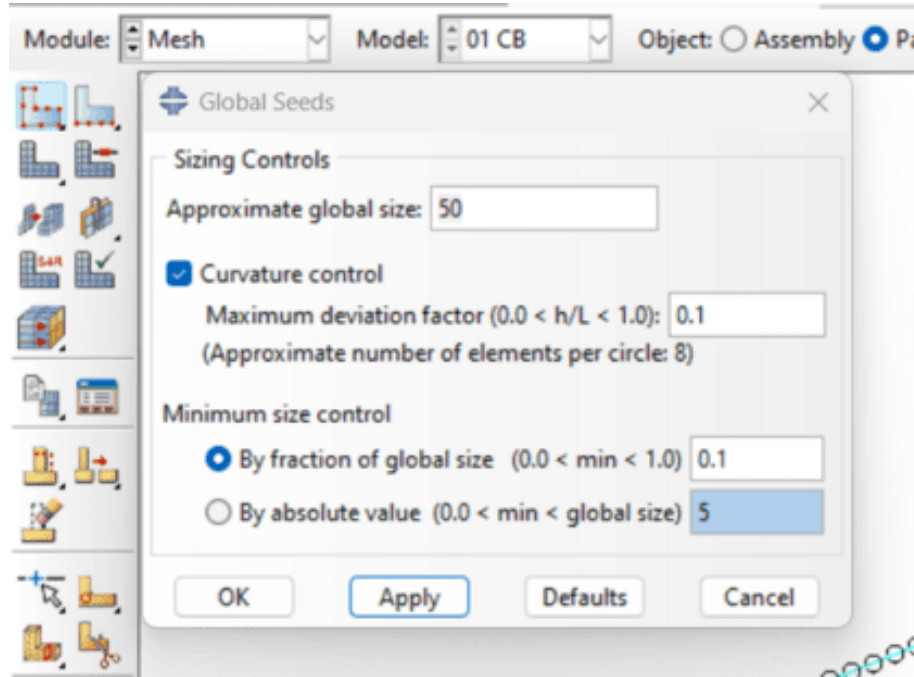


Figure 3-14 Mesh size of slabless staircases.

After everything is in its rightful place, the interaction between components can be described using a suitable constraint. Contact interactions play a significant role in FEM. When doing numerical simulations, it is crucial to account for physical processes in boundary conditions and surface interactions. Given the inclusion of multiple components in the simulation, including steel rebar and concrete, an incorrect specification could potentially impact the simulation overhead in the current thesis. Multiple methods for compressing general contacts, contact pairings, and contact elements are available in ABAQUS/Standard for defining contacts [48]. Interface contact surfaces, such as those between reinforcement and concrete stairs, can be subject to finite or tiny sliding in both two- and three-dimensional constructions. In addition to surface-based ties and coupling constraints, contact interactions can also represent kinematic constraints. Because they specify the structure's support or the fixed displacements at node sites In the field of stress analysis, boundary conditions can be thought of as a form of kinematic constraint.

3.6.4 Contact Interaction and Boundary Conditions

After everything is in its rightful place, the interaction between components may be described using the correct constraint. Contact interactions play a significant role in FEM. When doing numerical simulations, it is crucial to account for physical processes in boundary conditions and surface interactions. Given the inclusion of multiple components in the simulation, including the steel beam, concrete slab, shear connection, and rebars, an incorrect specification could potentially impact the simulation overhead in the current thesis. Contact pairs, generic contacts, and contact elements can be defined in ABAQUS/Standard using one of several methods [48].

3.6.4.1 Defining Contact Pairs and Properties of Contact

For contact pair definition, the interacted surfaces pairs must be indicated or which surfaces must interact with themselves. All regions in the contact surfaces must be included far enough through an analysis. The nodes on the two contact surfaces by contact pair are not allowed to involve, but the master and slaves' surfaces must be choosing [89]. When performing a contact simulation, the contact bodies interacting with one another is defined by assigning property of contact to a contact interaction. Hard contact model utilized by ABAQUS is the default pressure-overclosure contact relationship, which has been adopted in this work. Surface-based communication that is accessible in ABAQUS and is utilised for interface communication between the concrete stair and the reinforcement. The concrete surface has been chosen to be the master surface whilst the reinforcement to be a slave surface as seen in Fig.(3.15) .

Small-sliding formulation was used, in which the load was transfers to the master nodes according to the slave node of current position for geometric nonlinear analyses, the prescribed formulation presumes an arbitrarily large rotations but the

slave node and the master surface will interact with the same local area throughout the analysis. This type can be used instead of Tie constraint to improve the model robustness. In the normal direction in order to lessen the amount of slave node penetration and to stop the tensile stress from travelling via the interface, a hard contact connection was utilised. as seen in Fig.(3-15).

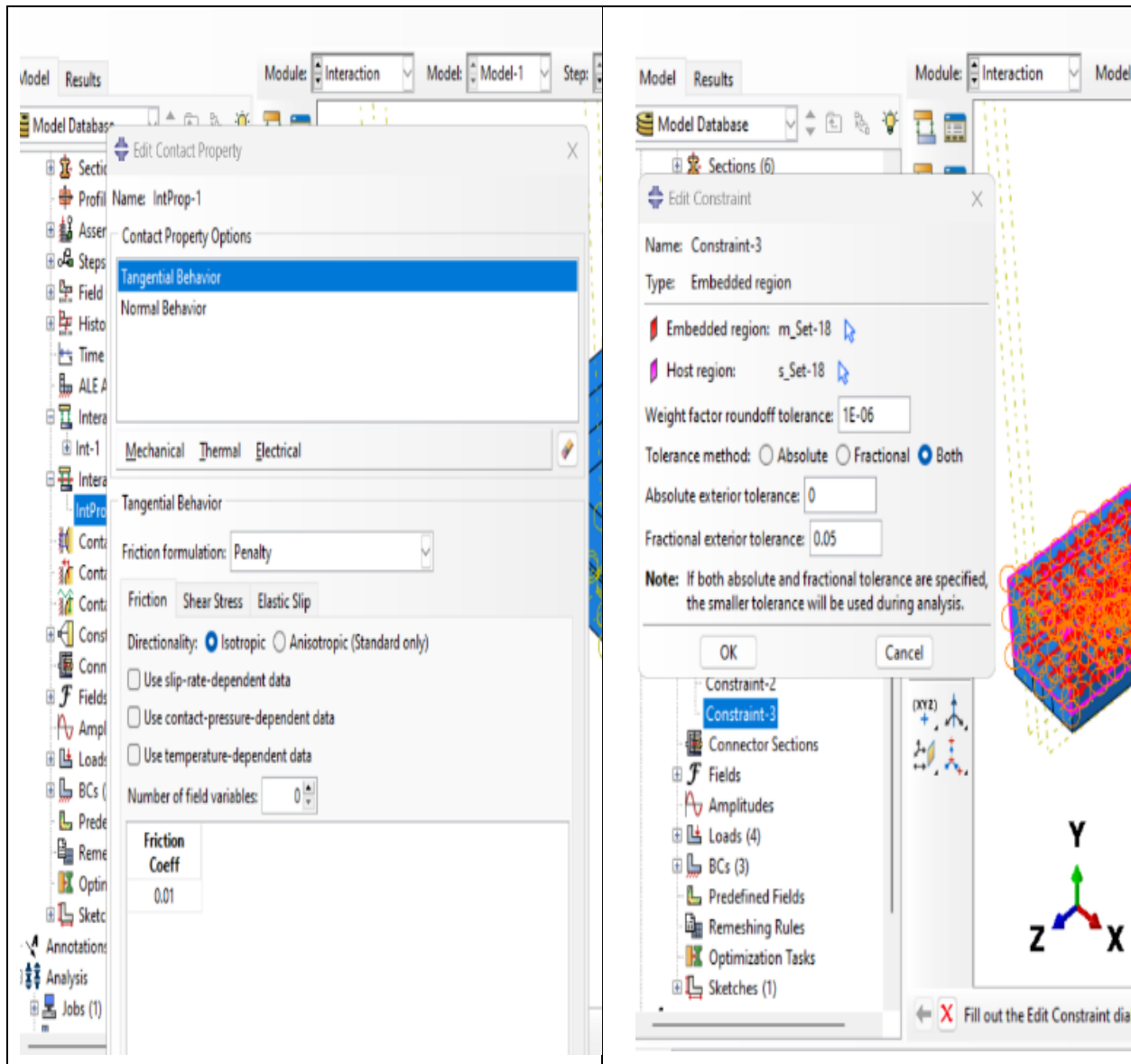


Figure 3-15 Properties of contact between concrete and reinforcement .

3.6.4.2 Boundary Conditions

In this step, set up the boundary conditions for the slabless staircase model in Abaqus. Boundary conditions are essential for accurately simulating real-case constraints and loading conditions. Begin by defining the support conditions at the base of the staircase, choosing options such as pinned supports and roller supports based on design requirements. Apply any necessary constraints to prevent unwanted movements, ensuring that certain degrees of freedom are fixed to simulate interactions with adjacent structures. If the staircase design is symmetrical, consider applying symmetry boundary conditions to reduce model size and computational effort. Additionally, ensure that the boundary conditions do not interfere with the points where loads will be applied later, particularly at the stair flights and landings. Once the boundary conditions are established, you can proceed to apply loads to the model.

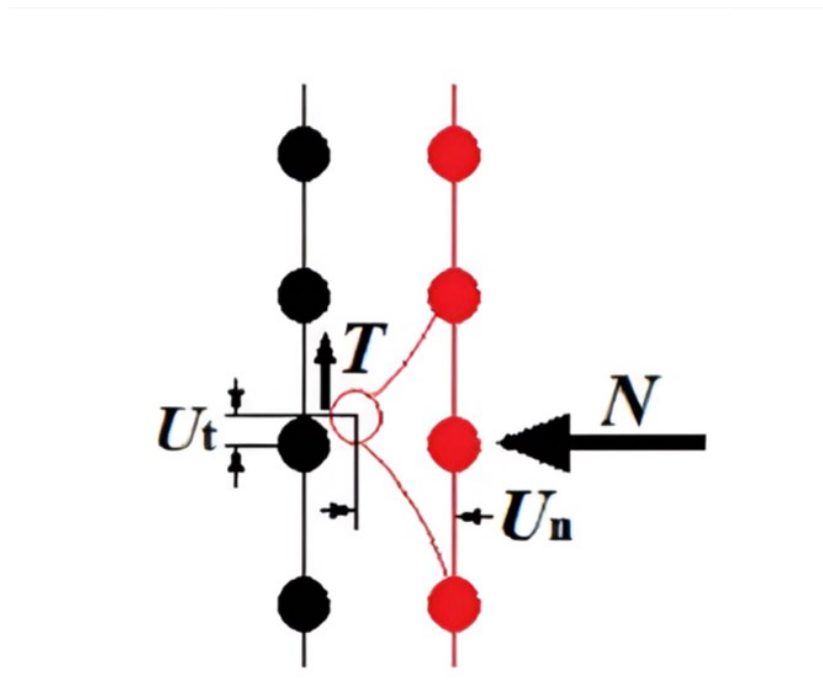


Figure 3-16 Variables of Contact

The contact between elements is based on the Kinematic approach in which the contact without friction or penetration at the nodes are Kinematically described. These are presented by forces and displacement as shown in Fig(3-16), where U_n and N represent normal displacement and corresponding normal force, respectively while U_t and T are tangential displacement and corresponding tangential force, respectively. Practically, for two materials there should be two lines as close to each other as possible for making the contact between the nearby front-nodes. This provides adequate interactive and convergence processs.

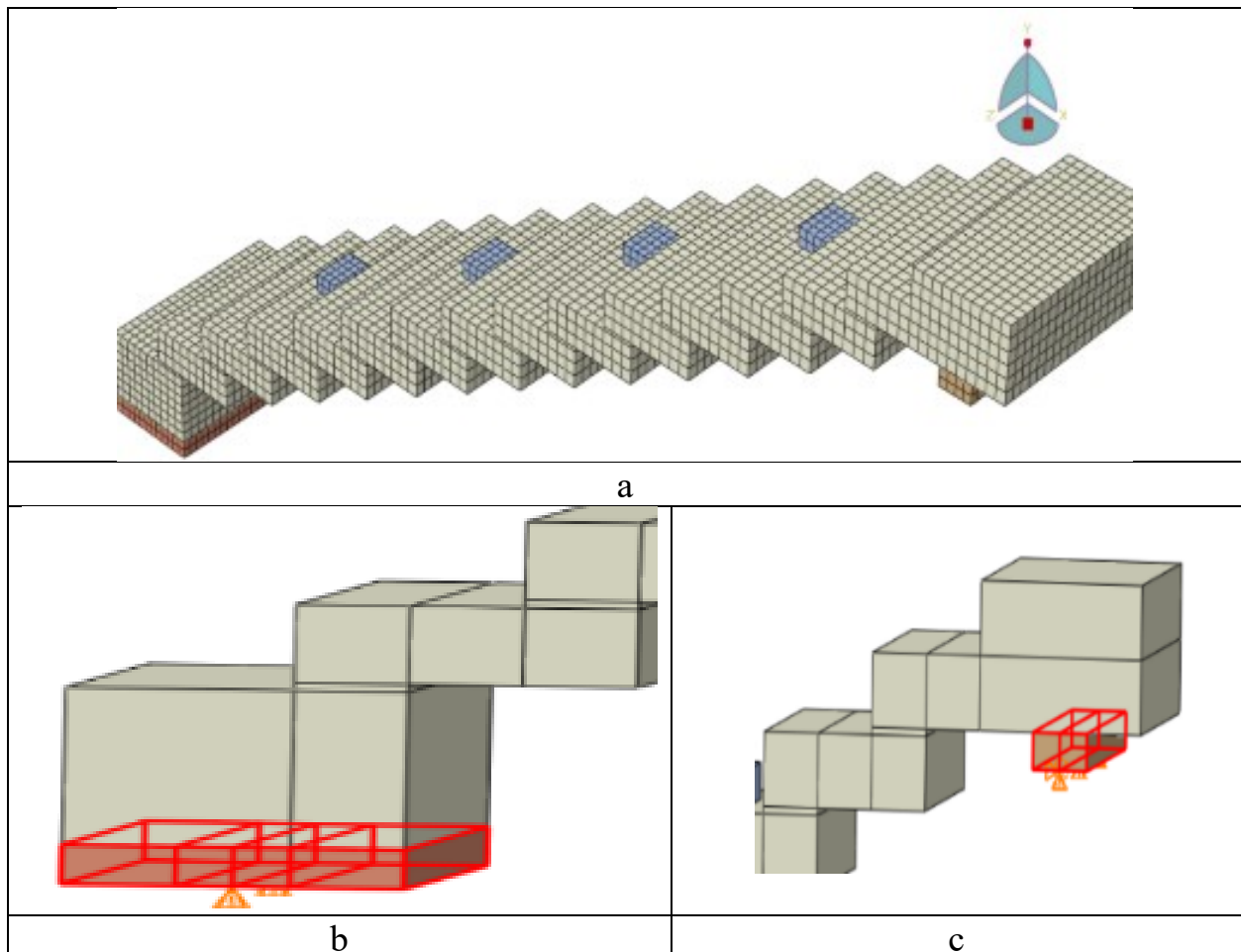


Figure 3-17 a) Boundary conditions and applied loading conditions were considered. b) The bottom support c) The top support

For slabless stair , two supports were used for the stair. Surface to surface interaction was used for modelling the contacts between the stair and the supports, with normal and tangential behavior. The bottom of the first support was restricted in Y directions. for the second support was restricted in X, Y and Z. The load control was applied to the model at two positions by the use of rectangular steel parts. The boundary conditions for stair model are shown in Fig. (3-17).

To simulate the boundary conditions as experimental work, translational D.O.F in x and y directions are restrained at both ends of the concrete stairs[49]. As a means of controlling displacement, loading was utilised. where the displacement applied as a downward pressure forces in order to prevent the concrete from experiencing a large concentration of stress treads.

3.6.5 Analysis Steps

In this step, specify the analysis steps for the slabless staircase model in Abaqus to simulate the staircase's behavior under various loading conditions. Start by choosing the appropriate analysis type, typically, a static analysis for assessing load-bearing capacity as seen in Fig (3-18). If the staircase is expected to experience dynamic loads (e.g., from foot traffic), consider a dynamic analysis as well. For example, if varying loads are anticipated, a dynamic analysis may be warranted.

Define the analysis steps clearly: begin with an initial step to apply the dead loads, which includes the self-weight of the staircase. For instance, if the staircase has a total concrete volume of 10 m^3 and a concrete density of 25 kN/m^3 , the total dead load would be approximately 250 kN . This step can have a duration of 1 second. Next, create a load step to apply live loads, which could be a uniform load of 4 kN/m^2 , a common design value for residential staircases. If the staircase has a surface area of 20 m^2 , the total live load applied would be 80 kN .

This step can be defined with a duration of 1 second. Set the total time for each static step to 1 second, with a time increment of 0.1 seconds, allowing the solver to capture the structure's response effectively. If performing a dynamic analysis, consider a total time of 5 seconds with smaller increments (e.g., 0.01 seconds) for accurate dynamic response. Finally, specify output requests to capture essential results, including nodal displacements at key points to evaluate deflection, stress results in the concrete and reinforcement to ensure they meet design limits, and reaction forces at support locations to verify that they are within acceptable limits. Once these analysis steps and parameters are defined, you can create and submit the analysis job for execution, allowing for an evaluation of the staircase's performance under the specified loading conditions.

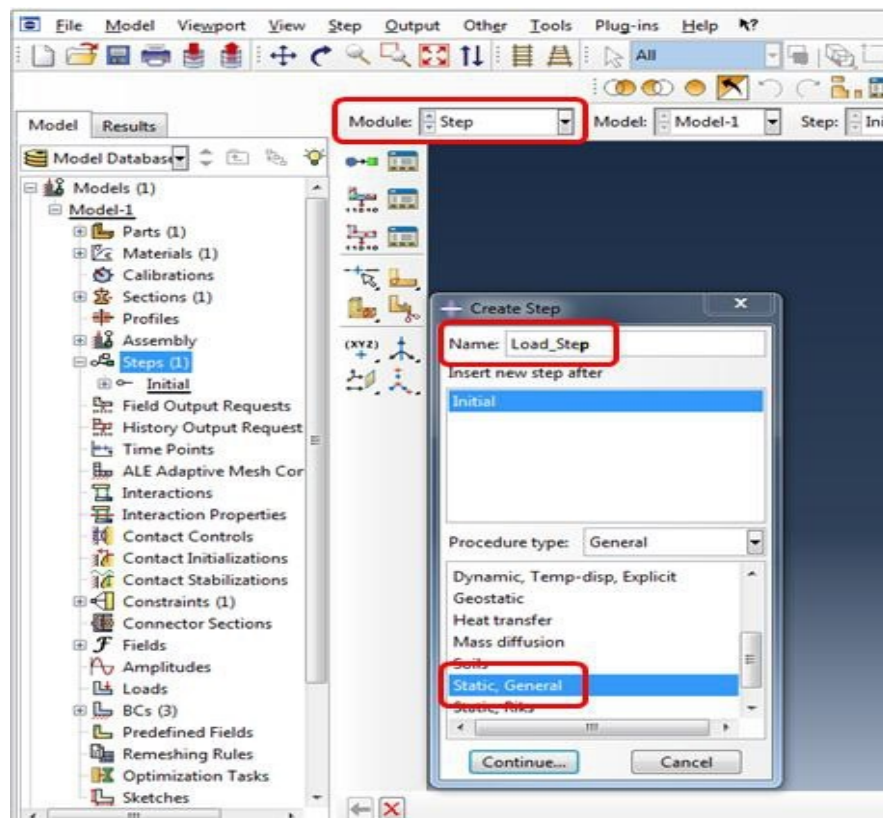


Figure 3-18 Appropriate analysis type in abaqus.

CHAPTER FOUR: RESULTS AND DISCUSSION

4.1 General

Slabless staircases are analyzed using three-dimensional FEM utilizing ABAQUS program. The present investigation delves into eight numerical examples supplied by earlier experimental efforts. In order to ensure that the FE technique is accurate and reliable, it is verified with experimental results. Experimental and FEM findings are contrasted with respect to load-deflection curves and crack patterns. The maximum deflection and ultimate loads are also calculated during this research. In addition, look at how several criteria that are thought to influence the behavior of slabless staircases really play out. The following factors are:

- 1) Steel reinforcement configuration.
- 2) f_c' of concrete.
- 3) Usage of CFRP bars to strengthening slabless staircases.
- 4) Usage of CFRP sheets to strengthening slabless staircases.

4.2 Procedure of the Study

Using existing experimental data, this study simulates the structural behavior of slabless staircases with simply supported rectangular cross-sections. Three groups of slabless staircases are analyzed. The first group, as presented by Özbek et al. [25], consists of eight specimens featuring a new configuration of steel reinforcement. The remaining groups are geometrically derived from Özbek et al. [25] and incorporate various parameters. This series explores the modification of conventional steel reinforcement by employing triangular shapes in multiple configurations. The second group comprises 14 slabless staircases utilizing CFRP bars, following the same configuration as the first series. This group investigates the strengthening of slabless staircases through both external and internal applications

of CFRP sheets, alongside variations in f_c' . The third series focuses on the investigation of geometric configurations, including the addition of landings and variations in f_c' , to assess their effects on structural performance.

4.3 Verification Process

The experimental data presented by Özbek et al. [25] was adopted to verify the present FE model. The model used in this analysis are identical in terms of size, material characteristics, and boundary conditions. The verification revealed that there was an extraordinarily high level of agreement between the findings obtained from the experiments and the numerical calculations about the load deflection, and test outcomes. The agreement of validation was very good; however, it is important to note that certain curves of the numerical analysis reached the maximum load and then stopped. The numerical model yields findings that demonstrate a reasonable concurrence in terms of load and mid-span deflection. On the other hand, ABAQUS models exhibit a higher degree of stiffness in the elastic zone of the load-deflection curve. This is especially noticeable in the figures for the T and C groups (C, t, and T series refers to the steel reinforcement configuration in validated study [25]. Table (4-1) and Fig. (4-1) provide a comprehensive analysis of the comparison between the ABAQUS model and the experimental specimens. Thoroughly analyses the quantitative results obtained from analyzing the suggested ABAQUS model, it is essential to take carefully analyses the inherent discretization errors that occur in finite element analysis. Based on the findings of the comparison investigation detailed in this study , the ABAQUS model provided for the prototype analysis is deemed to be accurate and dependable. This result is reached by considering the variables discussed earlier. For the mismatch agreement values especially for concrete models, these errors arise from translating a mathematical model into a finite-element one, where the number of degrees of freedom is finite. The finite

element analysis solution is impacted by various factors such as the number of elements, nodes per element, element shape functions, integration rules, and formulation details of specific elements.

Table 4-1 The results of the validated comparison between the numerical study and the experimental study.

SPi.	Experimental				Abaqus				$V_{ABAQUS}/V_{Exp. \%}$			
	Uy (mm)	Py (kN)	Uf(mm)	Pf(kN)	Uy(mm)	Py(kN)	Uf(mm)	Pf(kN)	Uy(%)	Py(%)	Uf(%)	Pf(%)
t100/100	52.0	22.00	121.0	21.3	51.58	21.8	130.7	25.17	1	1	-8	-18
t100/80	53.9	22.47	120.0	20.3	62.00	23.0	125.0	24.00	-15	-2	-4	-18
t80/100	61.0	16.00	120.0	18.0	68.00	18.0	131.7	22.00	-11	-13	-10	-22
T100/100	62.8	31.00	144.7	32.0	52.77	34.8	148.3	38.61	16	-12	-3	-21
T100/80	65.4	27.90	127.3	32.6	51.50	31.6	138.1	34.72	21	-13	-8	-7
T80/100	69.0	25.00	142.0	26.6	48.00	23.0	155.0	30.00	30	8	-9	-13
C100/100	69.0	29.00	111.6	34.0	49.47	32.5	126.7	36.60	28	-12	-13	-8
C100/80	64.4	30.00	120.0	33.0	53.00	33.0	129.0	37.00	18	-10	-8	-12

Uy: yield displacement

Py: yield load

Uf: failure displacement

Pf: failure load

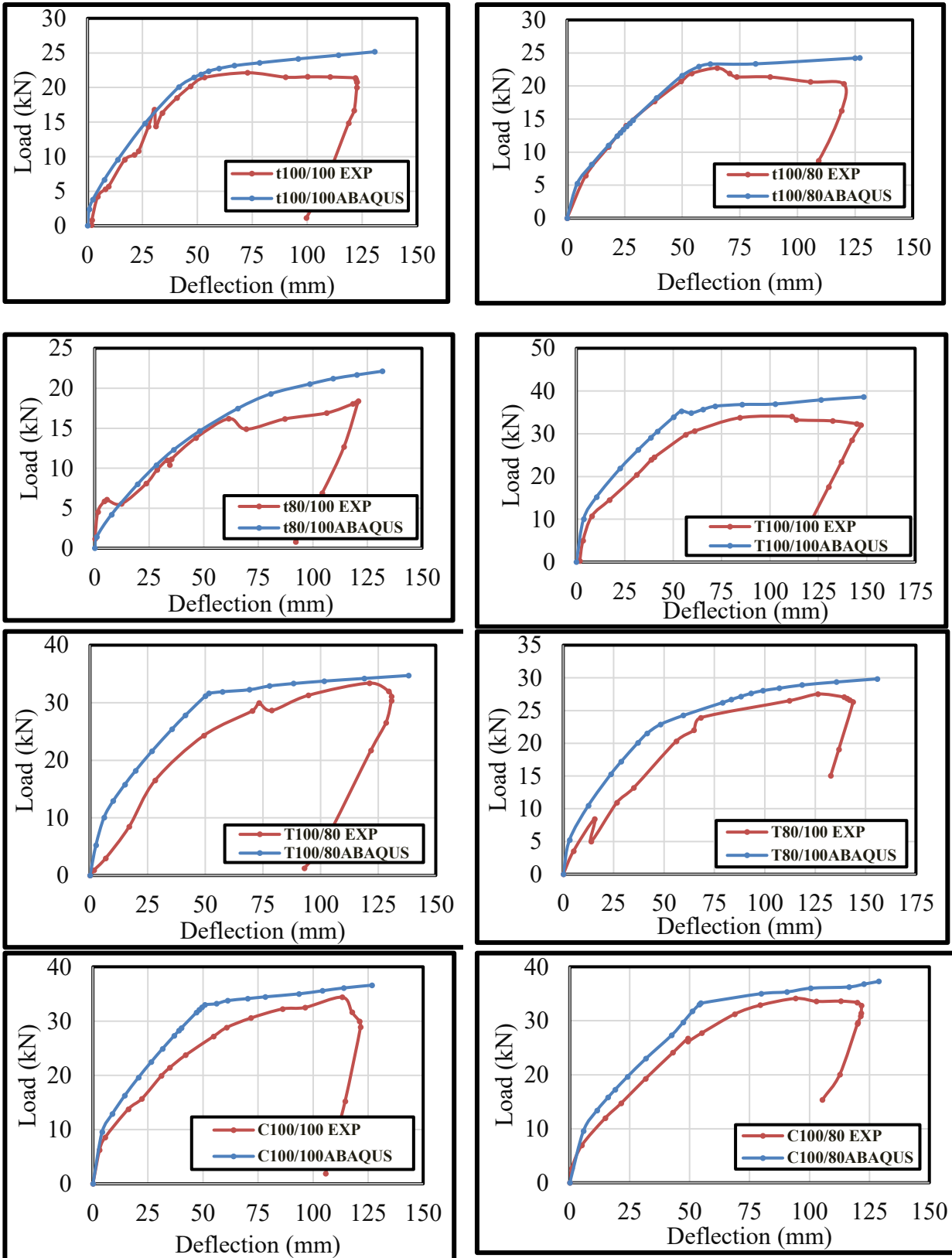


Figure 4-1 Load-deflection curve of experimental vs. numerical data:-

4.4 Finite Element Analysis of Slabless Staircases

Within this section, apply the finite element method (FEM) that was covered in the chapter that came before this one to the slabless staircases. For the purpose of determining the efficacy of these slabless staircases, examine the load-deflection curves, cracking load, ultimate load, maximum deflection, crack pattern, failure mechanism, and shear stress distribution. A total of three different sets of study have been conducted to demonstrate how different parameters influence the behavior of slabless staircases.

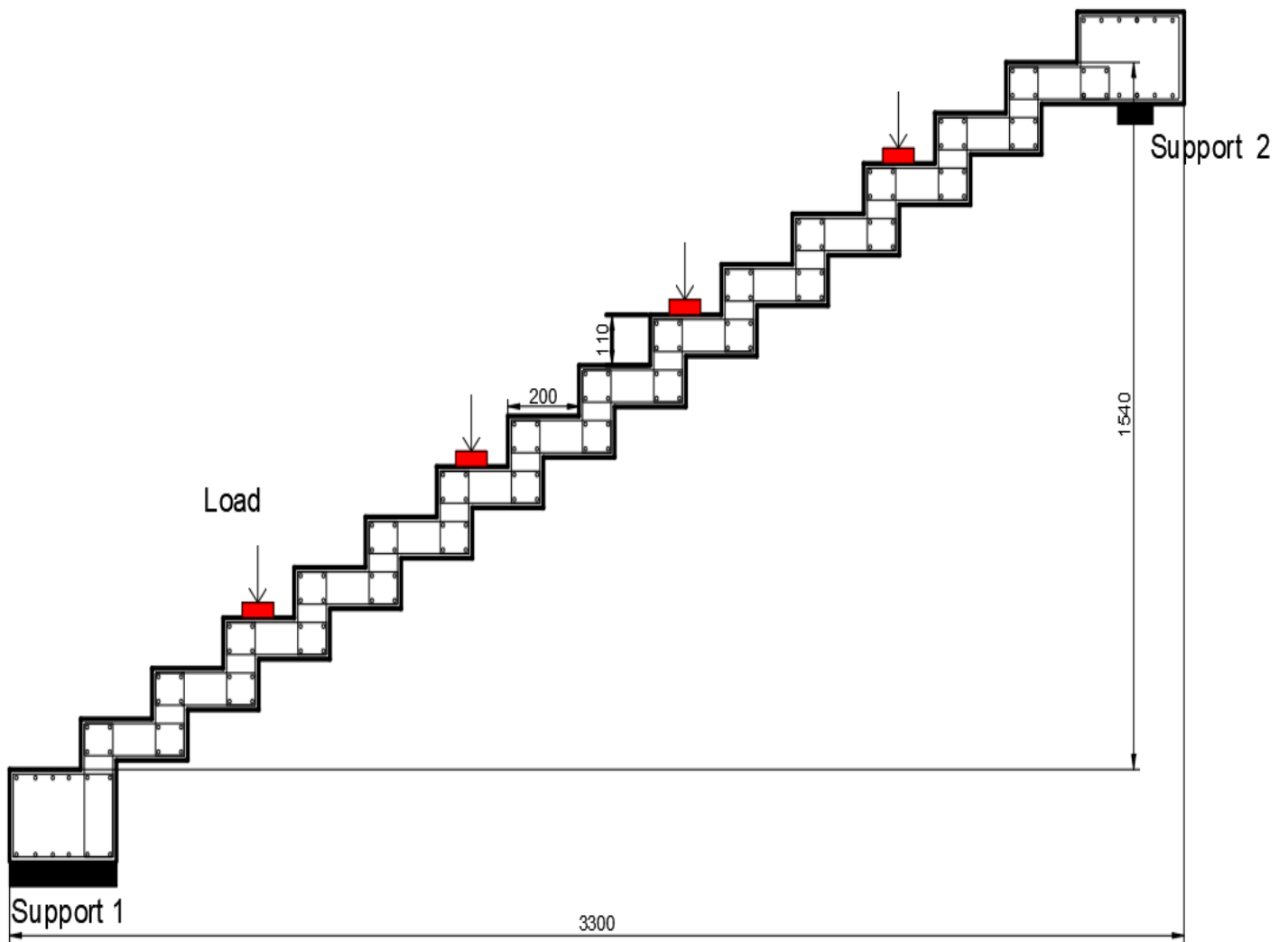
4.4.1 Effect of Steel Reinforcement Configuration (Series One)

The verified FE model was used to extend the parametric study required for the response of slabless staircase. Staircases made of reinforced concrete were built and discussed. In order to generate the specimens, conventional dimensions that are typically utilized in practical applications were utilized, and the limits of the testing instruments were also taken into consideration. There were fourteen steps on the stairs, and they were positioned between two beams. At both ends, the beams had a cross section that measured 200 x 300 mm in width and depth respectively. Based on the information shown in Fig. (4-2), the dimensions of the stairs are as follows: the width of the stairs (b_w) is 600 mm, the width of the treads (t) is 200 mm, and the height of the risers (r) is 110 mm. When it comes to slabless stairs, the tread thickness (t_h) and the riser thickness (t_v) can be created in such a way that they are either identical to one another or different from one another due to. The test parameters of t_h and t_v were taken into consideration and evaluated because of the impact that was anticipated to be exerted on both strength and behavior. However, this curiosity is reduced when the thicknesses are substantial. As a result, it was determined that the thicknesses to be examined are either 100 mm. The slabless stairs were modelled as part of the parametric study, which also included the introduction of several

properties such as the specimens' compressive strength and steel arrangement. Many distinct values for the compressive strength of concrete were contained within the range of that variable. This group contained values between 50 and 70 MPa. The staircases were fortified with steel bars arranged in a triangle pattern, with each tread beginning, middle, and ending with a triangle. The strut and tie method were the foundation of this steel reinforcement configuration method, as seen in Fig.(4-2) and Table(4-2).

Table 4-2 Description of Specimens

Var.	SPI.	f_c' (MPa)	Variable Details
Steel bars configuration	ST	50	-
	ST-M	50	Configuring the steel bars in triangular with crown at middle
	ST-L	50	Configuring the steel bars in triangular from the left
	ST-R	50	Configuring the steel bars in triangular from the right
	ST-L-R-1	50	Configuring the steel bars in triangular from the right and left one by one
	ST-L-R-4	50	Configuring the steel bars in triangular from the right and left four by four
	ST-M-WoP	50	Configuring the steel bars in triangular with crown at middle without planer bars
	ST-L-WoP	50	Configuring the steel bars in triangular from the left without planer bars
	ST-R-WoP	50	Configuring the steel bars in triangular from the right and left without planer bars
Compressive Strength	ST-M -70	70	Change the compressive strength to 70 MPa
	ST-L-70	70	Change the compressive strength to 70 MPa
	ST-R-70	70	Change the compressive strength to 70 MPa



(a)

Figure 4-2 Demonstrations of geometry tests

- (a) Slabless Staircases Model (ST) (b)) S-Zones distribution (c) ST-M
 (d) ST-L (e) ST-R (f) ST-L-R-1 (g) ST-L-R-4 (h) ST-M-WoP
 (i) ST-L-WoP (j) ST-R-WoP

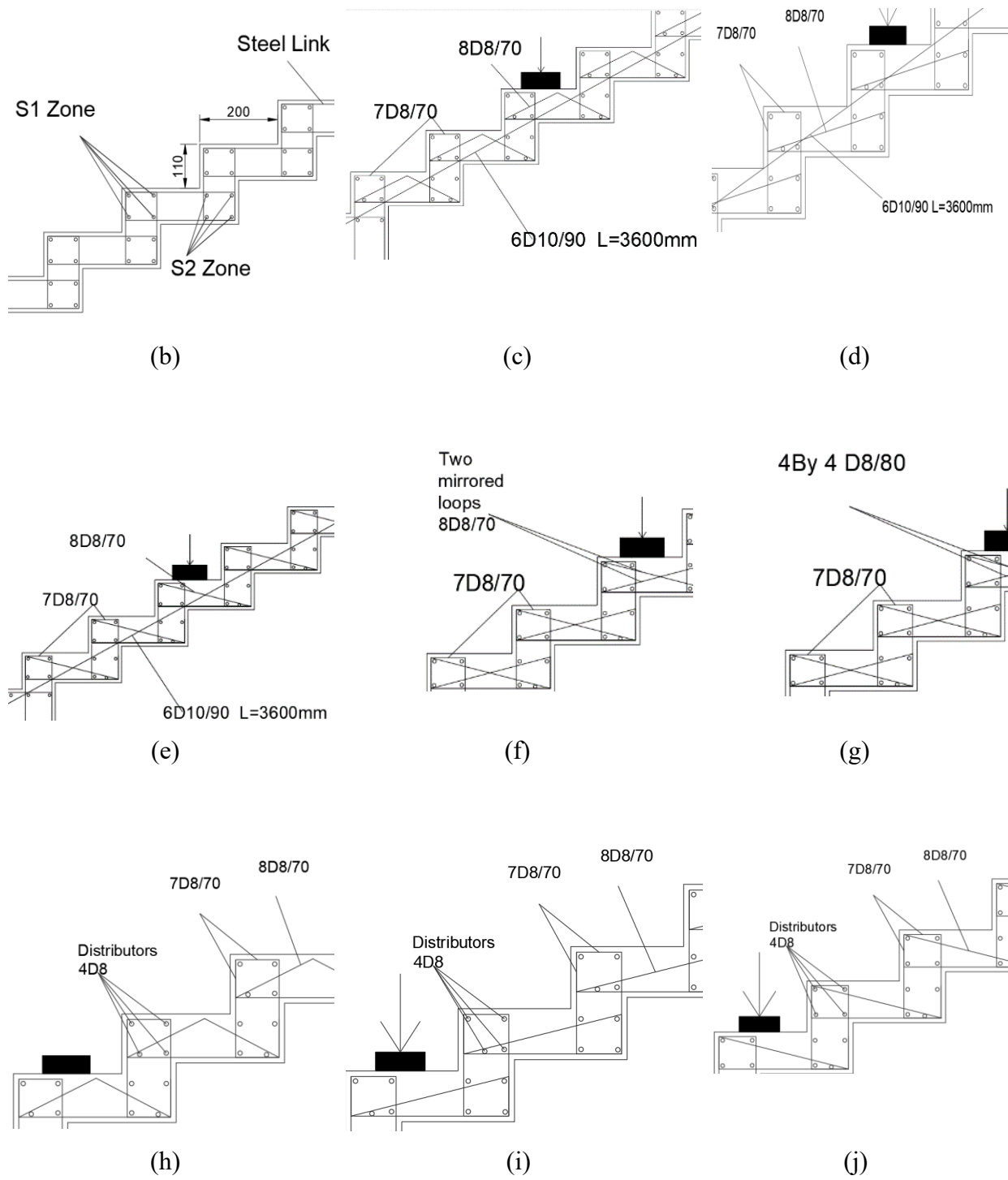


Figure 4-2 Continued.

4.4.1.1 Results and Discussion Series One

A) Effect of Bar Configuration

Partially replacing the steel reinforcement with the new configuration bars based on the strut and tie analysis helped alleviate the effects of steel rebar on the flexural behavior of slabless staircases. The specimen models have two regions which called S1 and S2 as revealed in Fig. 4-2. These regions were reinforced with steel and CFRP bars to investigate their effect on the general behavior. The steel bars were installed at S1, S2, and the S1-S2 zones to replace the steel reinforcement. The behavior was better in comparison to the traditional models when the steel reinforcement configuration specimens were modified as revealed in Table below.

Table 4-3 Test result of Speciment Tested.

ID	Per kN	Δy mm	Pu (kN)	Δu (mm)	Initial Stiffness (kN/mm)	Ductility Index
ST	10.48	28.68	38.61	148.33	1.10	5.17
ST-M	13.12	30.93	40.47	161.84	1.27	5.12
ST-L	11.64	51.12	41.36	174.24	0.68	3.41
ST-R	13.54	48.52	45.56	165.37	0.84	3.41
ST-L-R-1	15.00	25.42	44.19	175.78	1.70	8.02
ST-L-R-4	12.15	27.40	43.59	174.44	1.36	7.45
ST-M-WoP	9.18	41.76	38.24	171.52	1.14	4.85
ST-L-WoP	10.68	48.10	40.50	177.70	0.64	3.14
ST-R-WoP	9.09	76.34	44.39	171.87	0.78	3.25
ST-M -70	16.59	25.12	63.26	111.18	1.98	4.43
ST-L-70	15.03	34.61	69.19	100.71	1.30	2.91
ST-R-70	18.75	35.08	80.90	104.68	1.60	2.98

A cracking load of 10.48 kN is displayed by the model (ST). But when the steel reinforcement was rearranged into a triangle with the head positioned in the middle of the tread span, the cracking load rose to 13.12 kN, a 25.2% increase from the model (ST). It was also determined that the cracking resistance increased less when the steel reinforcing bar in the S1 zone (ST-L) was replaced compared to the S1-S2 zone (ST-M) as seen in Fig.(4-3). The reason behind this is that one area experiences more stress compared to another. Fig. (4-3)(a) shows that placing the triangle shape of the steel bars in the starting zone (S1 zone) increased the cracking load by 11.1%, whereas placing the same shape at the end of the treads in the S2 zone increased the cracking load by 29.2%.

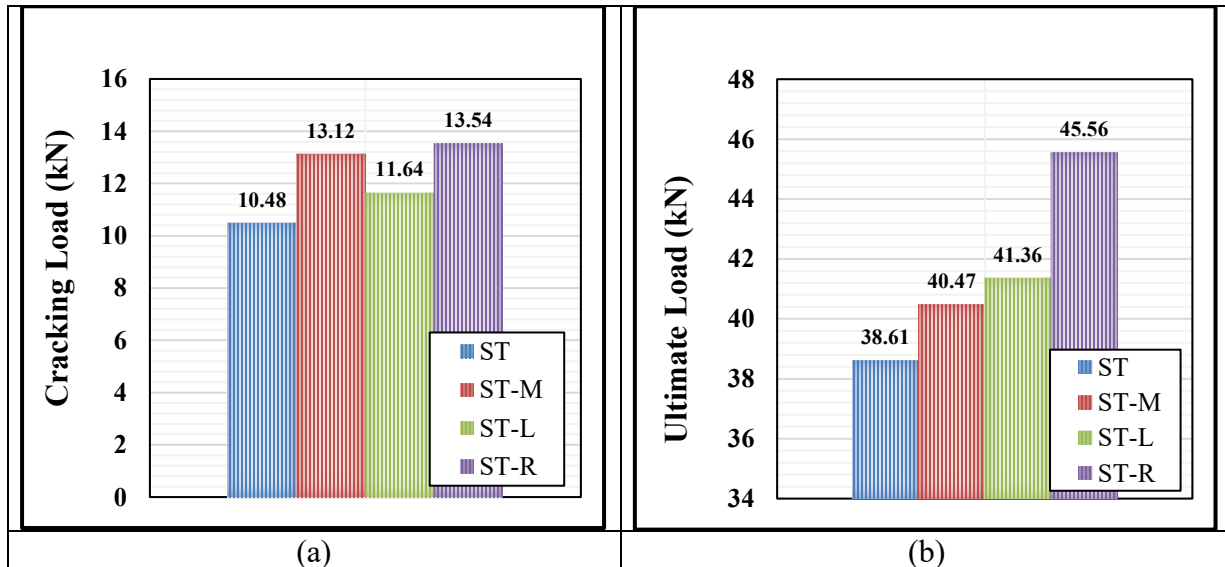


Figure 4-3 Cracking and ultimate load results for first group.

(a) Cracking load of ST, ST-M, ST-L, ST-R (b) Ultimate load of ST, ST-M, ST-L, ST-R

For the models with triangular staggered bars (ST-L-R-1 and ST-L-R-4), the results revealed that cracking load changed by +43.2% and +15.9% for model with triangular staggered bars (ST-L-R-1 and ST-L-R-4) respectively as seen in Fig. (4-4) (a). The ultimate load, as shown by the model (ST), is 38.61 kN. The ultimate load (model ST-M) slightly increased to 40.47 kN, or 4.8% more than the model (ST), when the steel reinforcement was rearranged to a triangle shape with the head

positioned in the middle of the tread span. It was also determined that the ultimate resistance increased less when the steel reinforcing bar in the S1 zone (ST-L) was replaced compared to the S1-S2 zone (ST-M). Fig.(4-3)(b) illustrates that positioning the triangular configuration of steel bars in the starting zone (S1) resulted in a 7.1% increase in ultimate load, whereas mirroring the triangular configuration to the S2 zone (at the end of the treads) yielded a greater increase of 18% in ultimate load. For the models with triangular staggered bars (ST-L-R-1 and ST-L-R-4), the results revealed that ultimate load changed by +14.5% and +12.9% for model with triangular staggered bars (ST-L-R-1 and ST-L-R-4), respectively as seen in Fig. (4-4) (b). The model (ST) demonstrates a deflection of 9.56 mm. Upon altering the configuration of the steel reinforcement to a triangle shape with the apex positioned at the mid-span of the tread, the deflection (model ST-M) escalated to 10.31 mm, representing a 7.8% increase relative to the model (ST). Furthermore, it was determined that substituting the steel reinforcing bar in the S1 zone (ST-L) led to a deflection increase that was inferior to that observed in the S1-S2 zone (ST-M). This is because this region experiences greater stressors than another region.

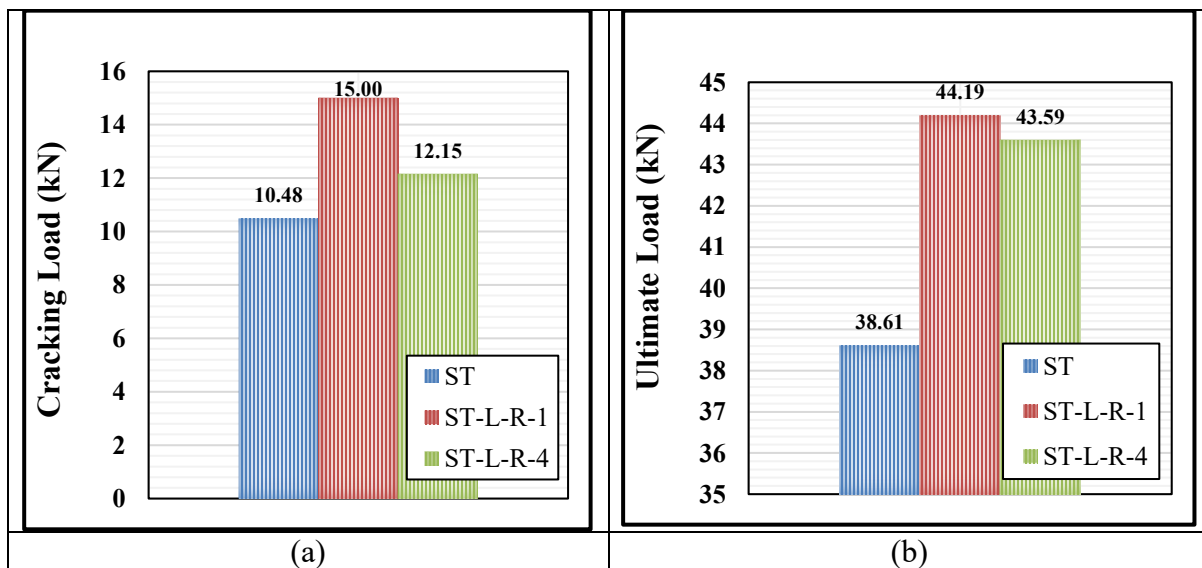


Figure 4-4 Cracking and ultimate load results.

(a) Cracking load of ST-L-R-1, ST-L-R-4 (b) Ultimate load of ST-L-R-1, ST-L-R-4

Fig. (4-5) illustrates that positioning the triangular configuration of steel bars in the starting zone (S1) resulted in a deflection increase of 78.2%, whereas mirroring the triangular configuration to the S2 zone (at the end of the treads) led to a deflection increase of 69.2%. For the models with triangular staggered bars (ST-L-R-1 & ST-L-R-4), the load deflection curve revealed that maximum deflection changed by +18.5% and +17.5% for model with triangular staggered bars (ST-L-R-1 and ST-L-R-4) respectively as seen in Fig.(4-6).

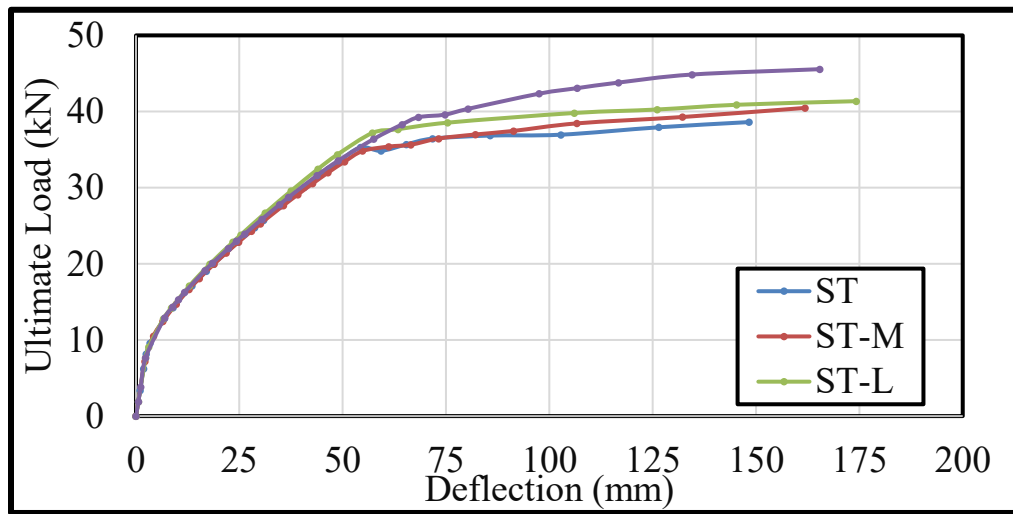


Figure 4-5 Load deflection relationship of ST-M, ST-L and ST-R slabless staircases models.

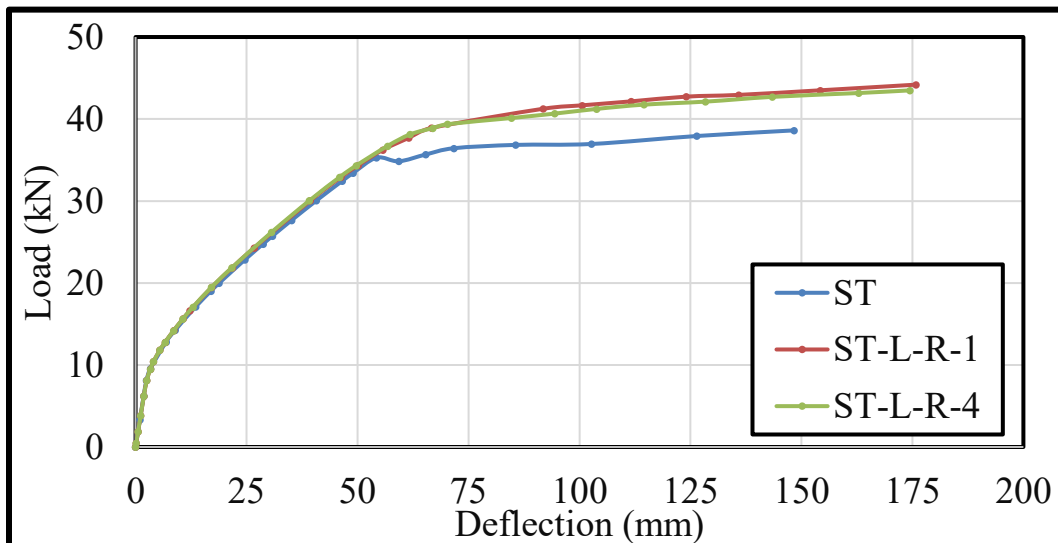


Figure 4-6 Load deflection relationship of ST-L-R-1 and ST-L-R-4 slabless staircases models

B) Effect of Planner Steel Bars

When comparing between the specimens have planner reinforcement along the stairs with the corresponding models without planner reinforcement revealed an effect on the structural behavior. The cracking load of the model (ST-M-WoP) decreased with 30.1% when the planner removed from model with triangular form of steel reinforcement with middle head position when compared with the model (ST-M). For the models with triangular form at the left and right (ST-L-WoP and ST-R-WoP), the cracking load changed by -19.2% and -30.9% respectively when compared with the models (ST-L and ST-R) as revealed in Fig. (4-7) (a). While the ultimate load showed distinct outcomes which the ultimate load of the model (ST-M-WoP) changed with -5.5% when the planner removed from model with triangular form of steel reinforcement with middle head position when compared with the model (ST-M).

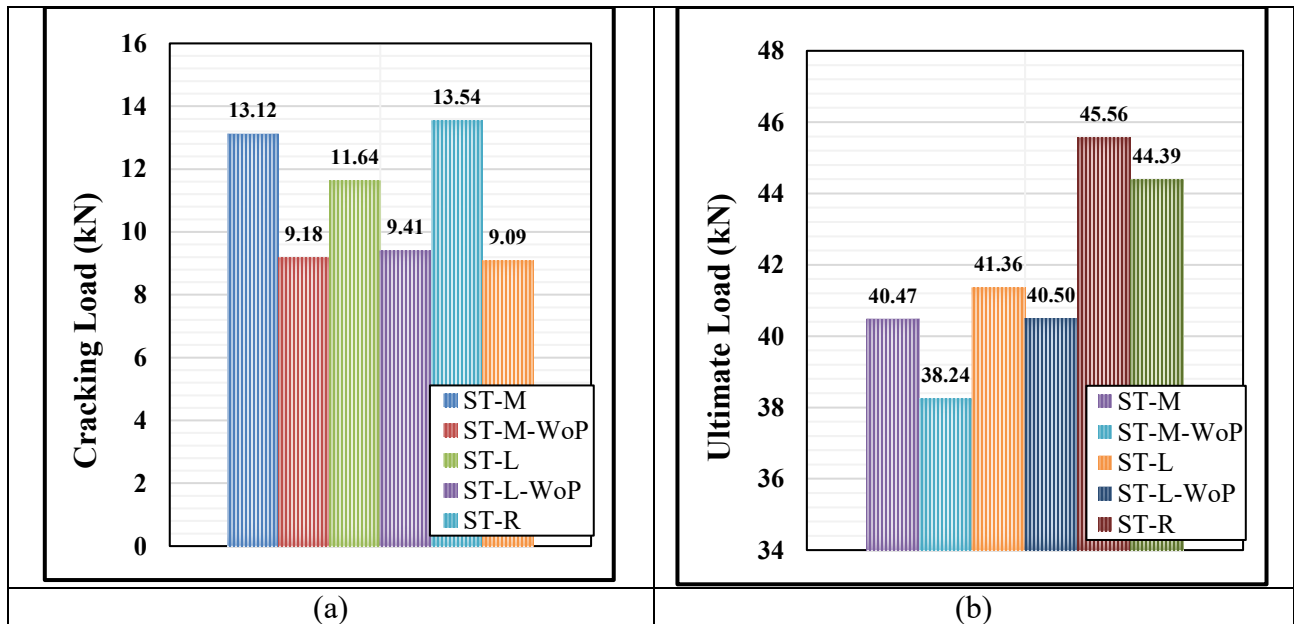


Figure 4-7 Cracking and ultimate load results.

- (a) Cracking load of ST-M, ST-M-WoP, ST-L, ST-L-WoP, ST-R, ST-R-WoP.
 (b) Ultimate load of ST-M, ST-M-WoP, ST-L, ST-L-WoP, ST-R, ST-R-WoP.

For the models with triangular form at the left and right (ST-L-WoP and ST-R-WoP), the ultimate load changed by -2.1% and -2.5% respectively when compared with the models (ST-L and ST-R) as revealed in Fig. (4-7) (b). The deflection increased significantly with 10.9%, 8.9%, and 14.2% for the specimens (ST-M-WoP, ST-L-WoP and ST-R-WoP) when compared with the corresponding models (ST-M, ST-L and ST-R) respectively as revealed in Fig. (4-8), (4-9) and (4-10).

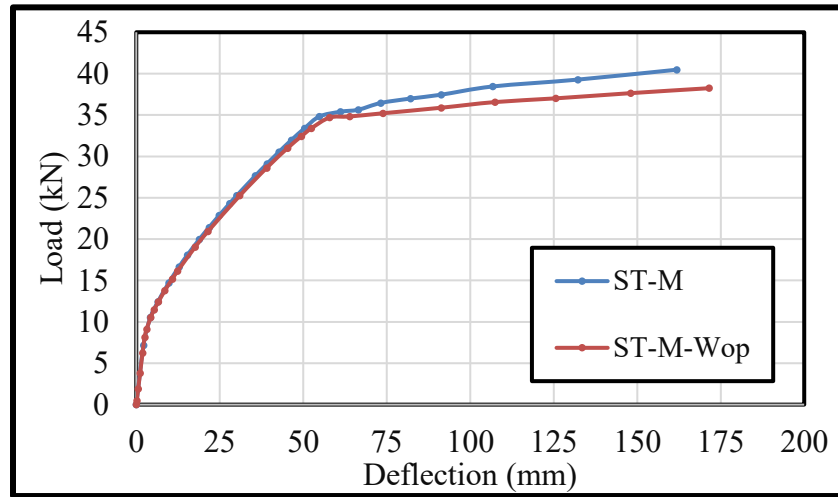


Figure 4-8 Load deflection relationship of ST-M and ST-M-Wop slabless staircases models

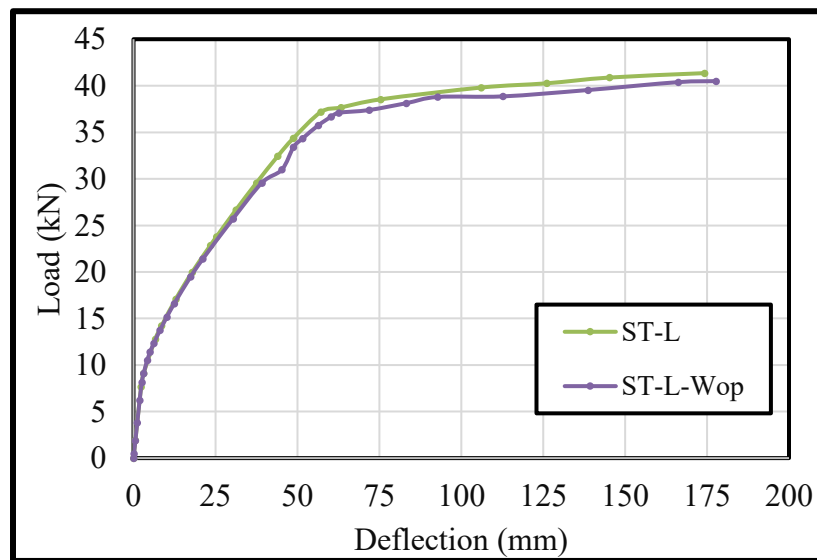


Figure 4-9 Load deflection relationship of ST-L and ST-L-Wop slabless staircases models

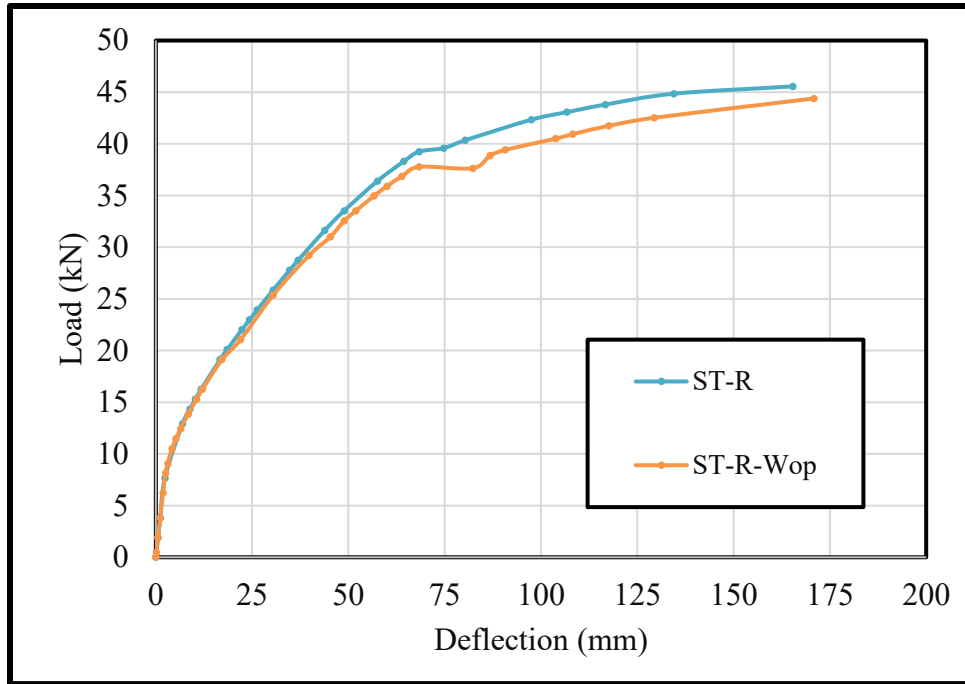


Figure 4-10 Load deflection relationship of ST-R and ST-R-Wop slabless staircases models

C) Effect of Compressive Strength

The results of the testing of RC staircases that were subjected to flexural stresses are detailed in Table (4-2). Substantial variations were identified among the concrete slabless stairs. The difference was attributed to the substantial impact of concrete strength on the staircase response. In order to examine the influence of the compressive strength of concrete on the flexural behavior of staircases, the compressive strength values used were 50 and 70 MPa. The specimen (ST-M-70) exhibited a higher cracking load resistance of 16.59 kN when contrasted with the corresponding model of conventional concrete (ST-M). The compressive strength of the concrete was directly proportional to the fracture load. According to Fig. (4-11), the fracture strength of models (ST-M-70, ST-L-70, and ST-R-70) increased by approximately 58.3%, 43.4%, and 78.9%, respectively, as the compressive strength increased from 50 to 70 MPa. The maximum load values in Fig. (4-11) were significantly improved by approximately 63.8%, 79.2%, and 109.5%, respectively,

as a result of the increase in concrete compressive strength from 50 to 70 MPa. The deflection behavior was dissimilar to that of fracture and ultimate load, as the deflection decreased as the compressive strength increased, as illustrated in Figs. (4-12), (4-13) and (4-14) .

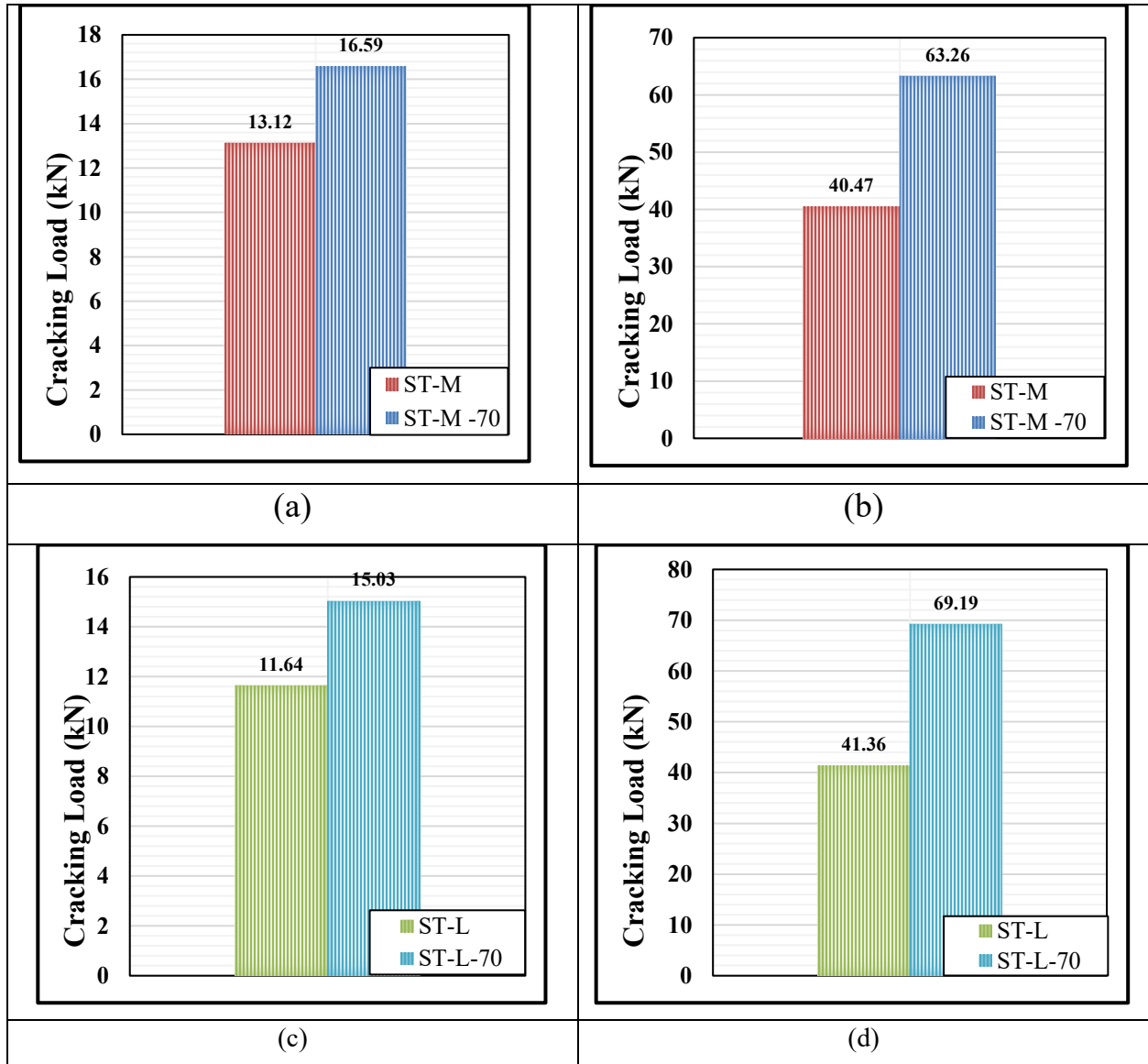


Figure 4-11 Ultimate load and Cracking results.

- (a) Cracking load of ST-M and ST-M-70 (b) Ultimate load of ST-M and ST-M-70
(c) Cracking load of ST-L and ST-L-70 (d) Ultimate load of ST-L and ST-L-70
(e) Cracking load of ST-R and ST-R-70 (f) Ultimate load of ST-L and ST-L-70

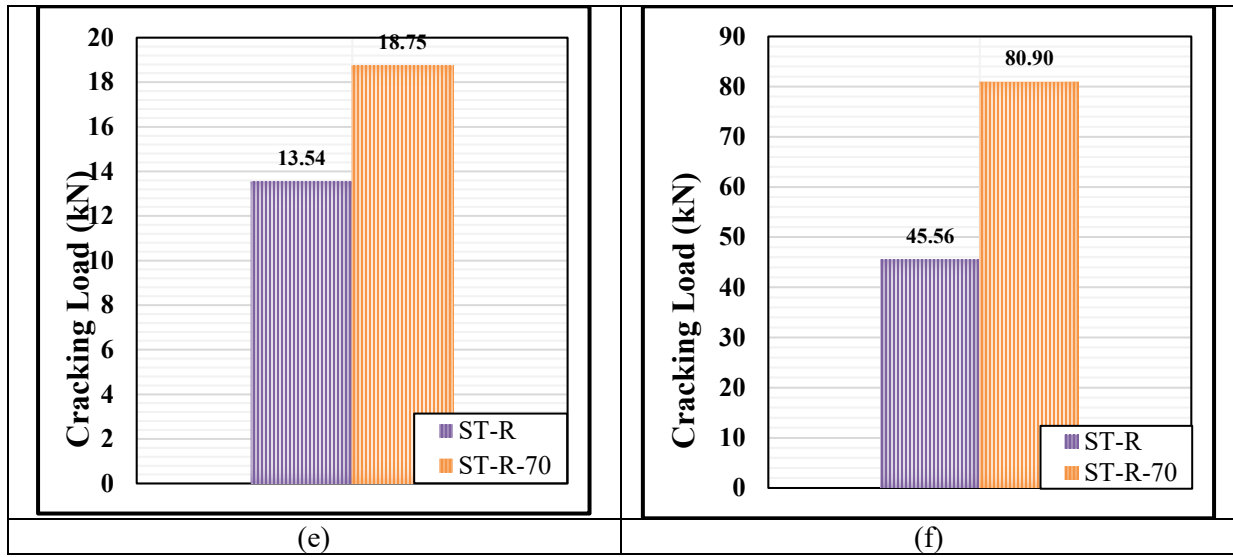


Figure 4-11 Continued.

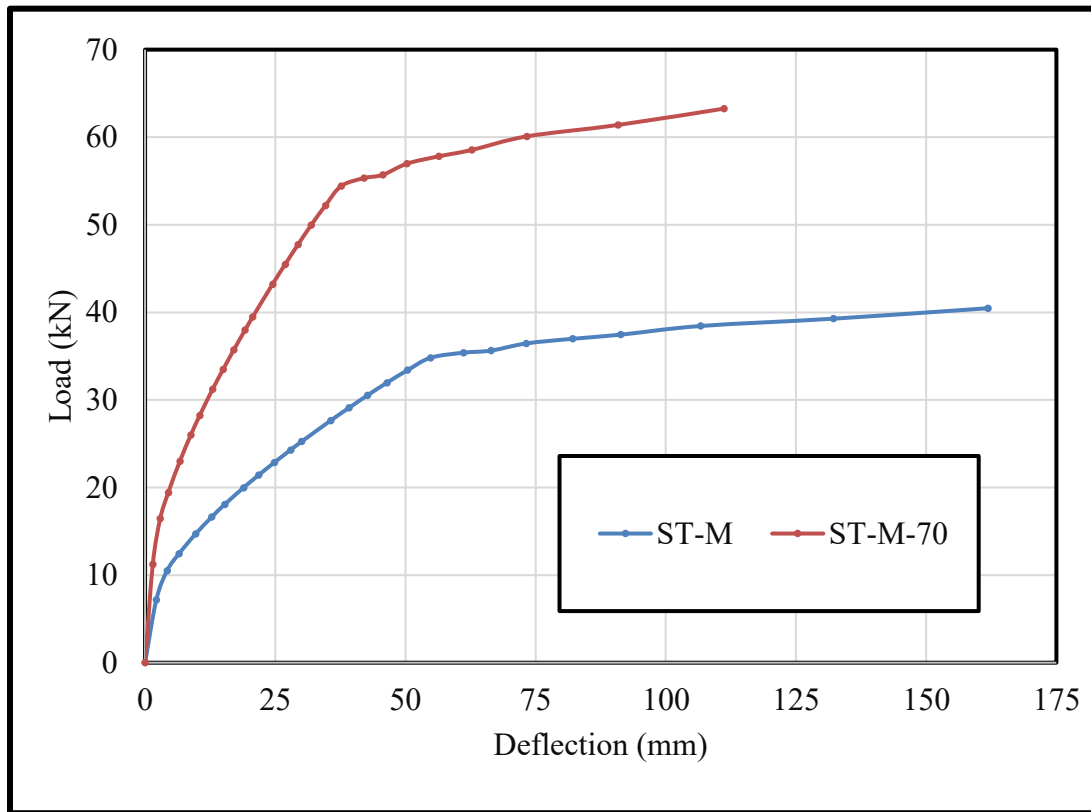


Figure 4-12 Load deflection relationship of ST-M and ST-M-70 slabless staircases models

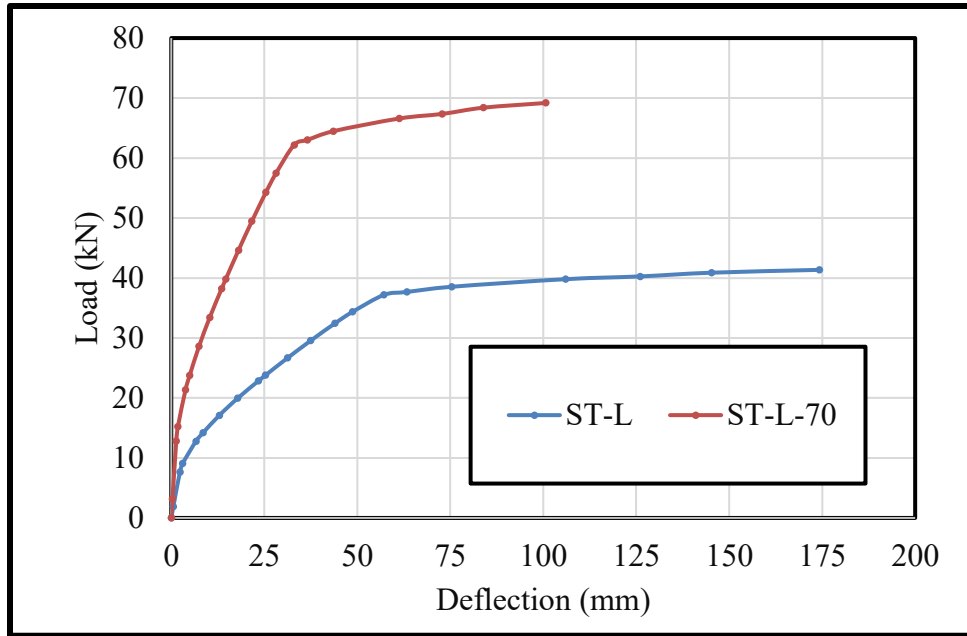


Figure 4-13 Load deflection relationship of ST-L and ST-L-70 slabless staircases models

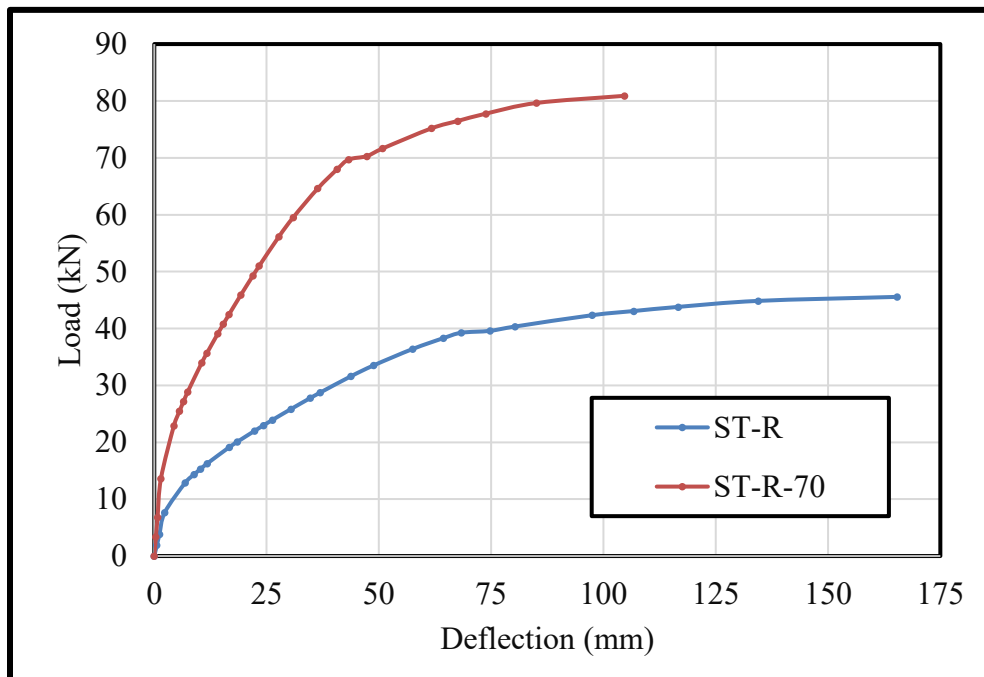


Figure 4-14 Load deflection ST-R and ST-R-70 slabless staircases models.

D) Ductility Index

The material's ability to endure substantial deformation without experiencing abrupt failure is denoted by the term "ductility index". Constructions composed of ductile concrete may exhibit visible deformations, including cracking and bending, when subjected to static stresses. Internal reinforcement is one of the factors that can alter the ductility of concrete, as it can considerably enhance the material's ductility. This contributes to the management and distribution of cracking, as well as the reduction of abrupt failure and the provision of additional strength. By computing the ratio of the ultimate deflection (Δ_u) to the yield deflection (Δ_y), the ductility can be determined [50]. The material's ductility is determined by this ratio. Slabless staircases' ductility index results are illustrated in Table (4-3), respectively. The specimen with the highest ductility index was the ST, which measured 5.17. The ductility decreased to 5.12 when the steel reinforcement was reconfigured in a triangular shape with the head located in the mid-span of the tread, which is equivalent to a 1% decrease in comparison to the ST model. This is in reference to the impact of the steel configuration. In addition, it was determined that the ductility was diminished as a consequence of replacing the steel reinforcing bar in the S1 zone (ST-L). The reason for this is that this region is subjected to greater stresses than another region. Fig. (4-15) and (4-16) illustrates that the ductility decreased by 34% when the triangular steel bars were inserted into the start zone (S1 zone). Conversely, the ductility decreased by 34.1% when the steel triangular configuration was mirrored in the S2 zone (at the end of the treads). As the compressive strength of the concrete increased, the ductility index decreased. For models with compressive strengths of 70 MPa, the ductility index decreased by 14.4%, 44%, and 42.3%, respectively, as the compressive strength of the material was increased from 50 to 70 MPa.

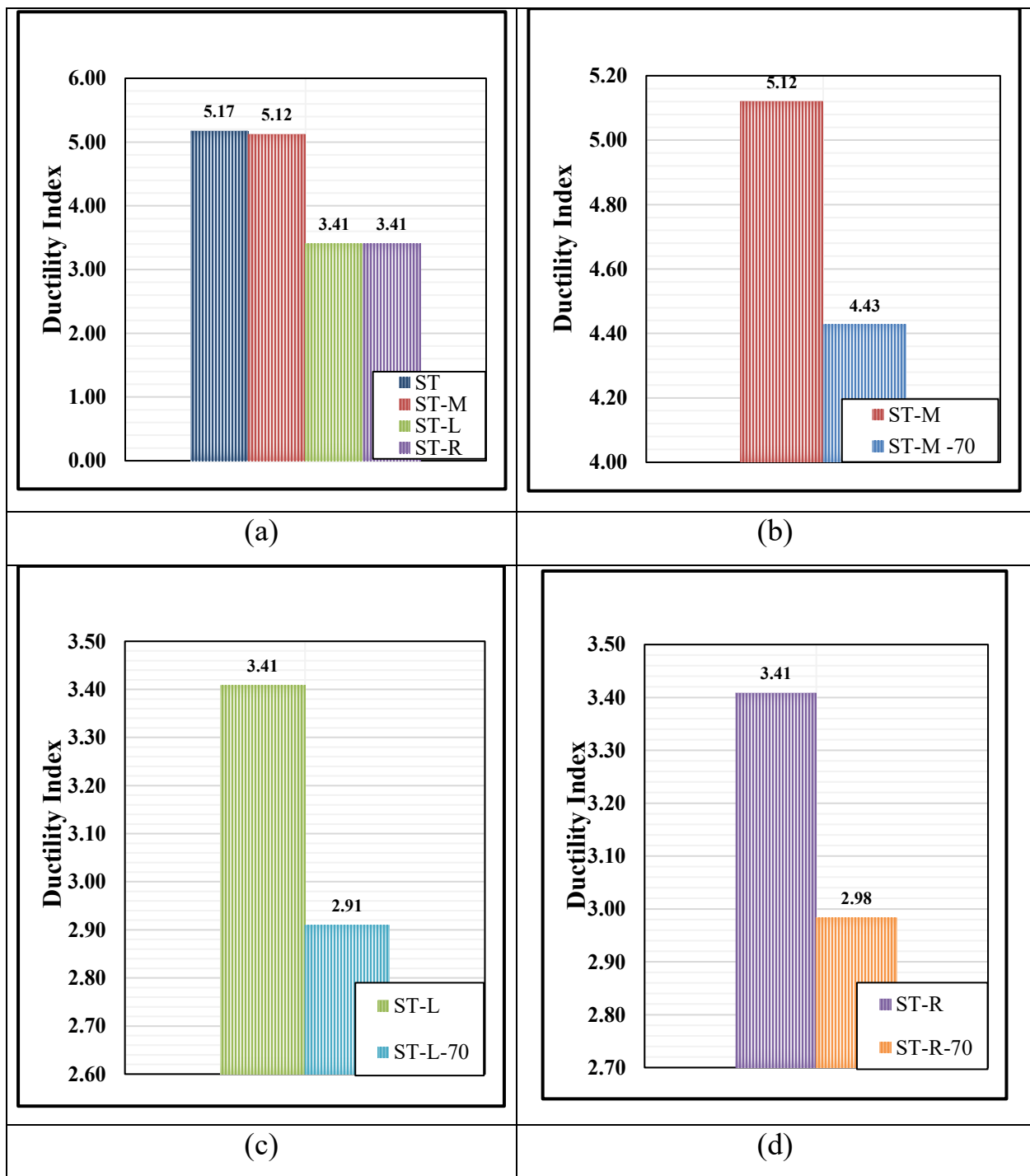


Figure 4-15 Ductility Index.

(a) Ductility results for ST, ST-M, ST-L and ST-R
(c) Ductility results for ST-L and ST-L-70

(b) Ductility results for ST-M and ST-M-70
(d) Ductility results for ST-R and ST-R-70

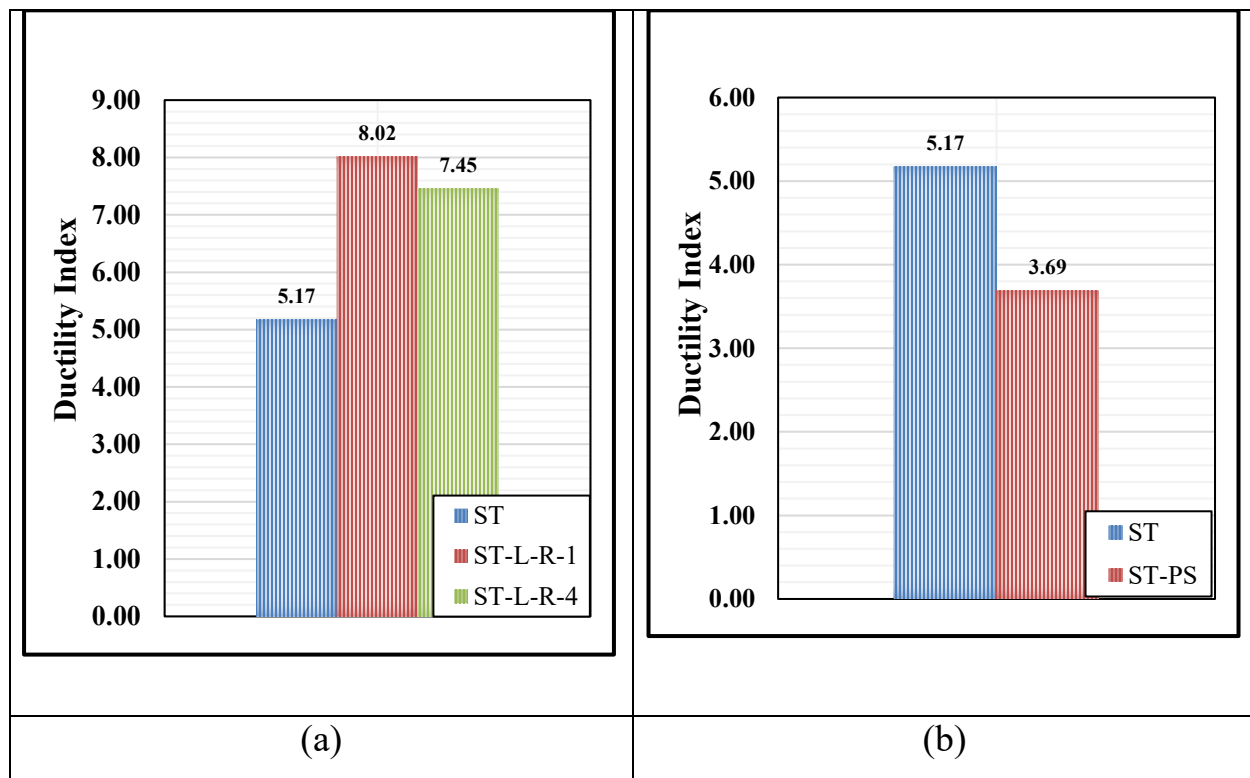


Figure 4-16 Ductility Index.

(a) Ductility results for ST, ST-L-R-1 and ST-L-R-4

(b) Ductility results for ST and ST-PS

E) Initial Stiffness

Initial stiffness refers to the slope of the load-deflection curve at the origin, indicating how much a beam will deform when subjected to an applied load. The calculation method including Examine the load-deflection curve and identify the linear portion at the first stages of loading. The initial stiffness (IS) is defined as the slope of this linear portion: The initial stiffness of the reinforced concrete staircases was varied due to the changing of bar configurations. The first series included ST control mode which revealed 1.1 kN/mm which increased to 1.27 kN/mm for the model ST-M and decreased to the lower stiffness for the models (ST-L and ST-R). presence of the triangular configuration in middle of the tread enhanced the stiffness which balanced the stresses along the member which the left and right triangular configuration concentrated the stresses at specific regions decreased the stiffness

against the loads. The increase of the compressive strength enhanced the initial stiffness as revealed in Fig. 4-17.

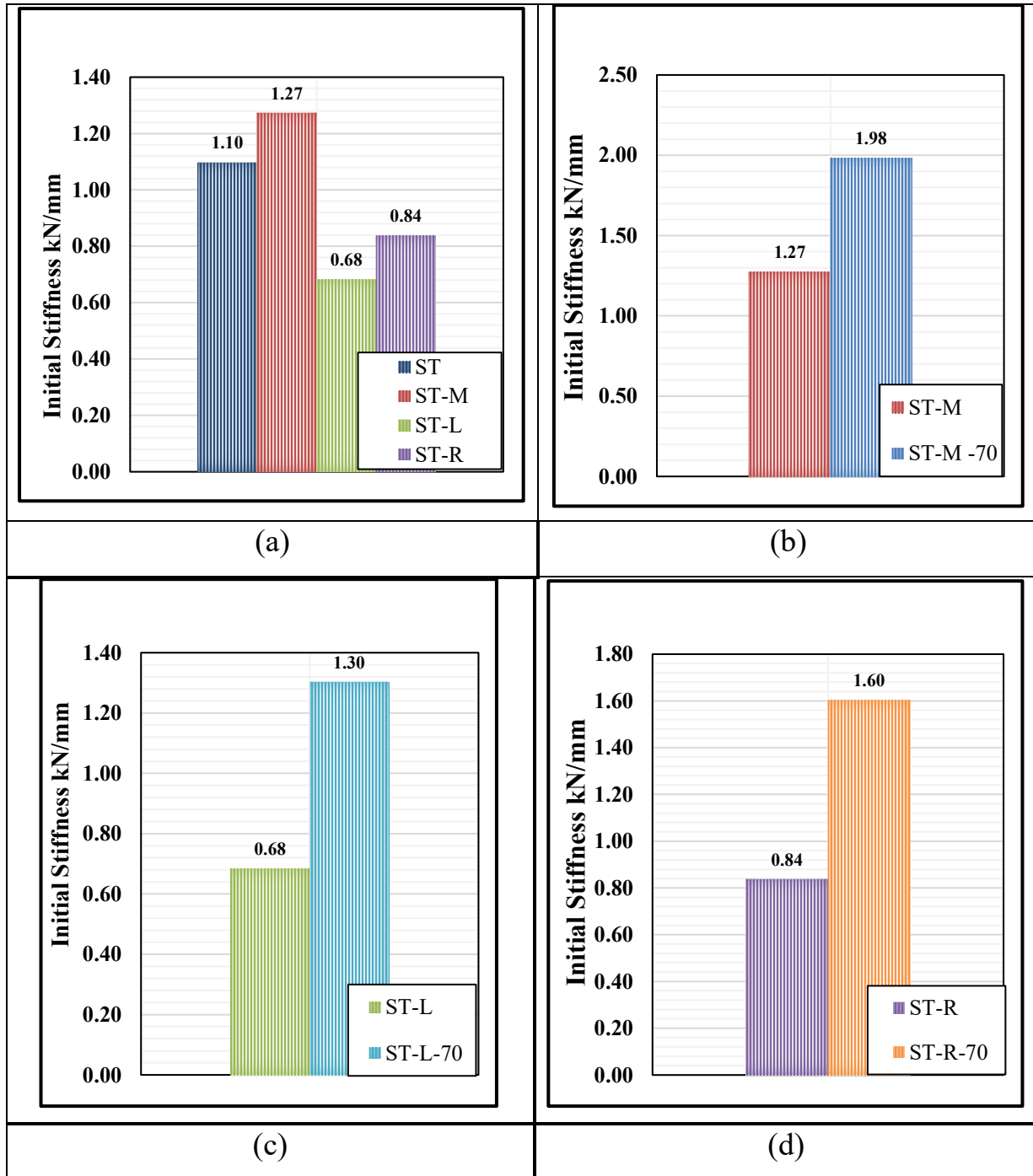


Figure 4-17 Initial stiffness of the slabless staircases .
 (a) for ST,ST-M, ST-L and ST-R (b) for ST-M and ST-M-70
 (c) for ST-L and ST-L-70 (d) for ST-R and ST-R-70

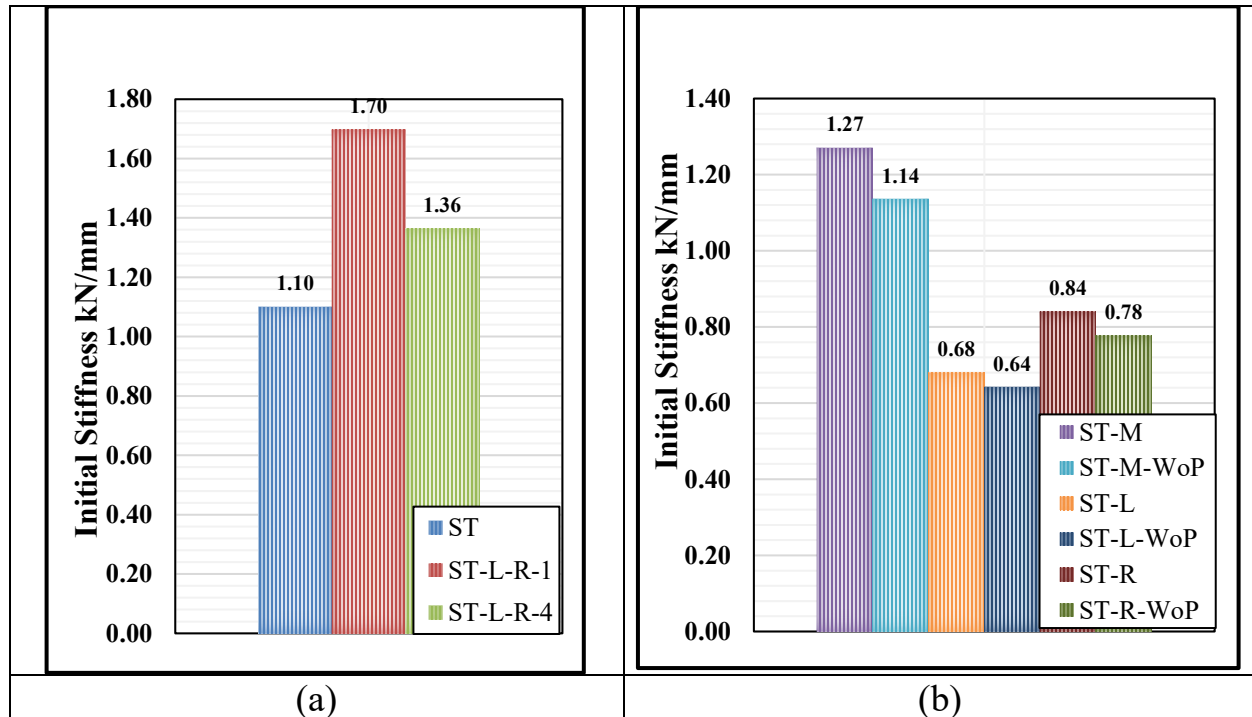
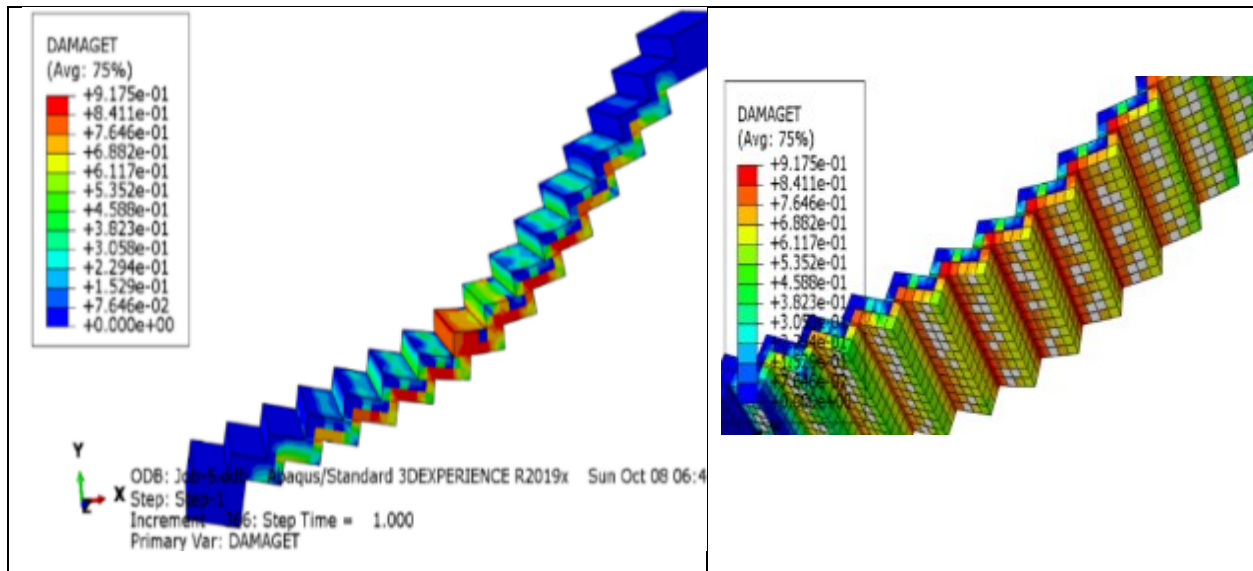


Figure 4-18 Initial stiffness of the slabless staircases .

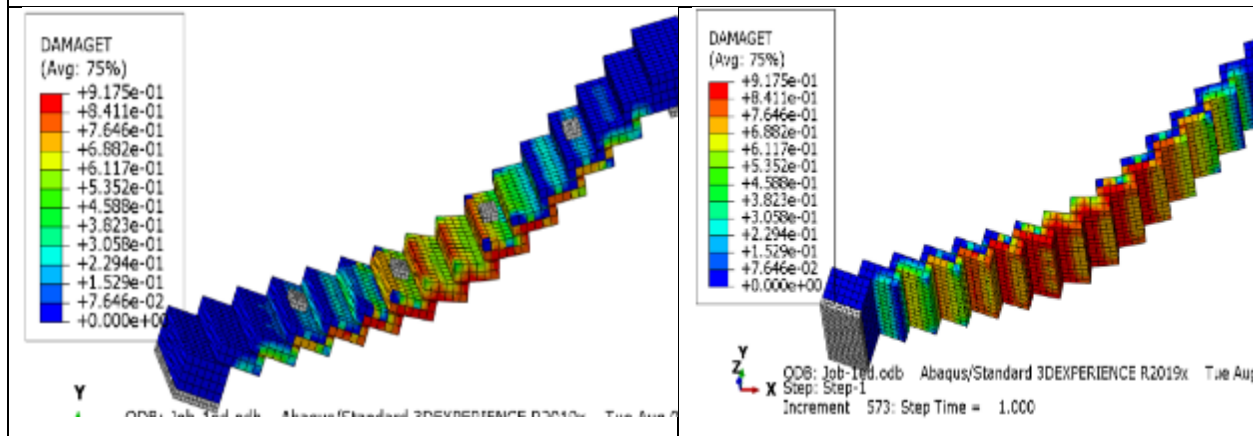
(a) for ST,ST-L-R-1 and ST-L-R-4 (b) for ST-M,ST-M-Wop, ST-L,ST-L-Wop, ST-R and ST-R-Wop

F) Cracking and Failure Mode

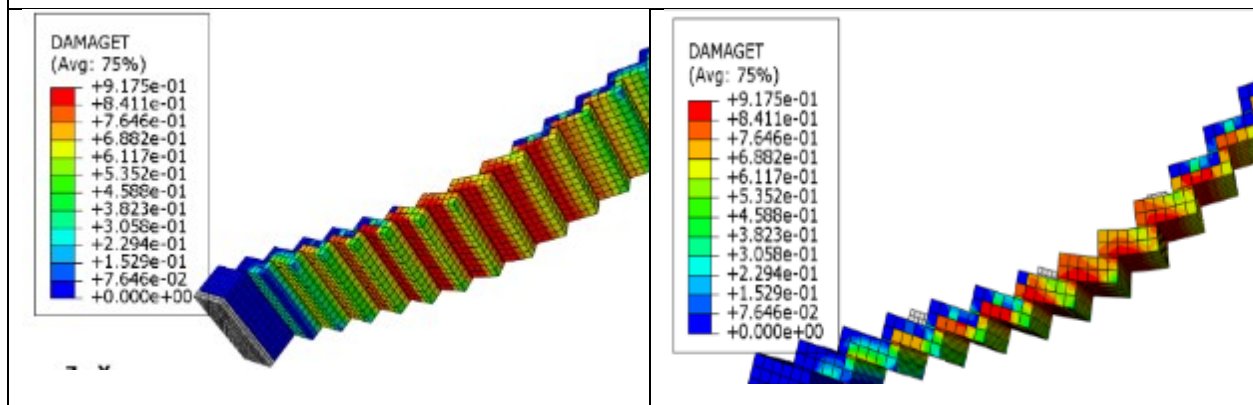
In models (ST-M-70) to (ST-R-70), which included simulating slabless stairs with varied compressive strengths, it was demonstrated in Fig. (4-19), (4-20) and (4-21). That the distribution of stresses did not change as the compressive strength increased. This was the case in all of the models included in the study. In the process of implementing a new configuration of steel reinforcement, the stress distribution was influenced by the utilisation of steel rebar. The results showed that the stresses were concentrated most intensely in the S1 zones when steel rebar was replaced with triangular rebar. Other areas of the structure had lower concentrations of stresses than the S1 zones. Following the replacement of the steel rebar in the S2 zone, the concentration was found to be higher in comparison to the experimental model as shown in Figs. (4-19),(4-20) and (4-21).



(a) ST

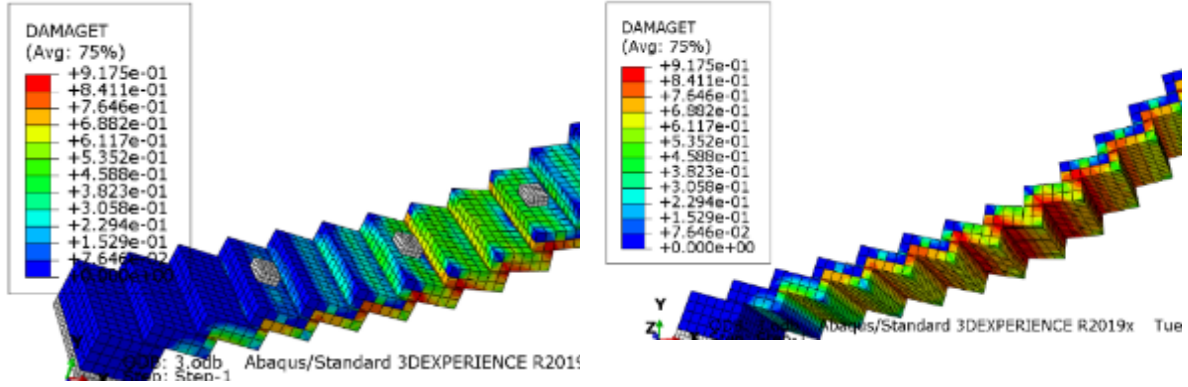


(b) ST-M



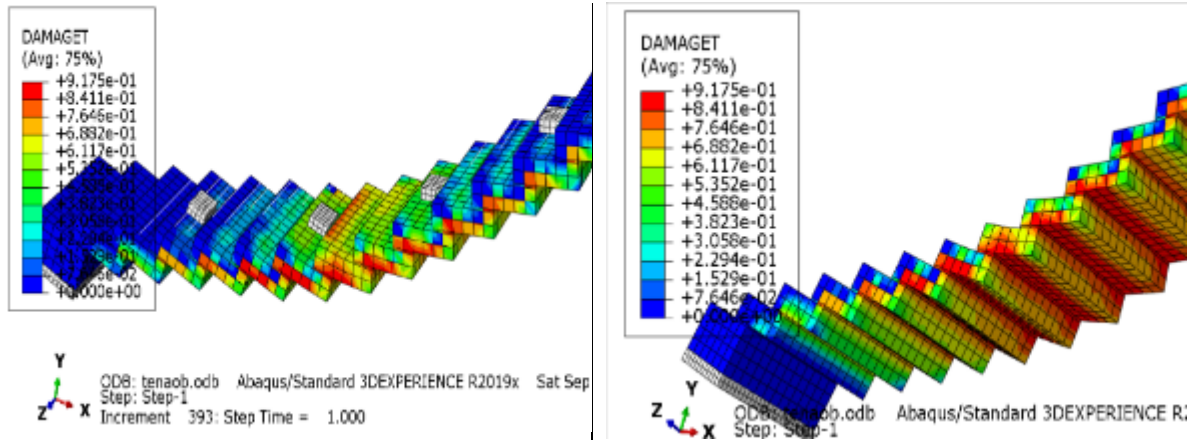
(c) ST-L

Figure 4-18 Cracks pattern for slabless staircases of ST ,ST-M , ST-L and ST-R.

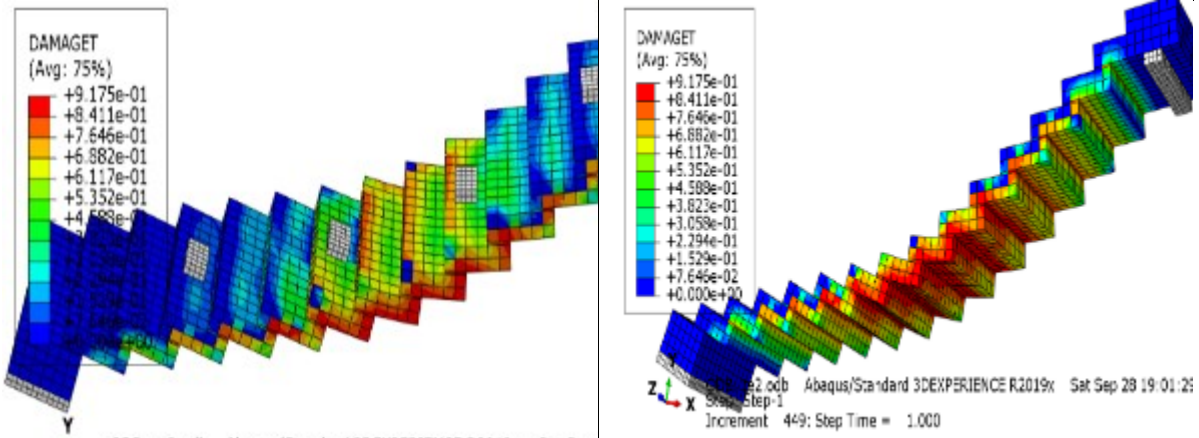


(d) ST-R

Figure 4-19 Continued.



(a) ST-L-R-1



(b) ST-L-R-4

Figure 4-20 Cracks pattern for slabless staircases of ST-L-R-1 ,ST-L-R-4 and ST-PS.

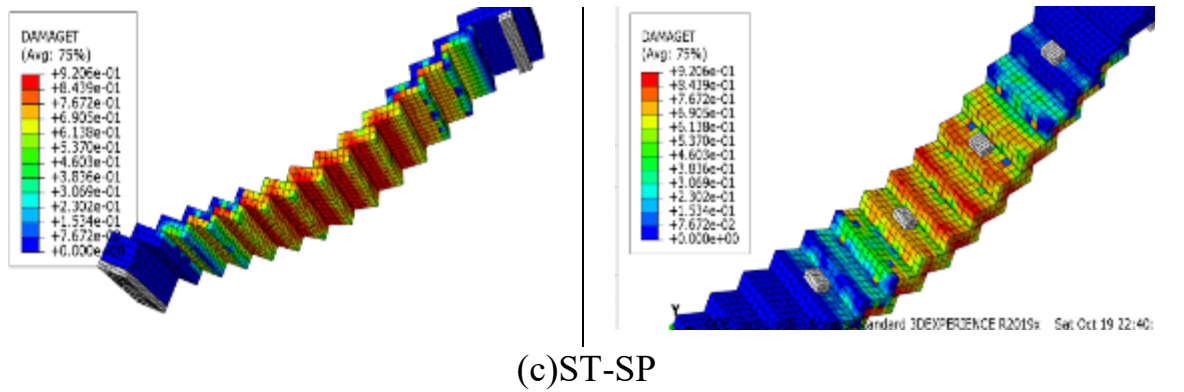


Figure 4-20 Continued.

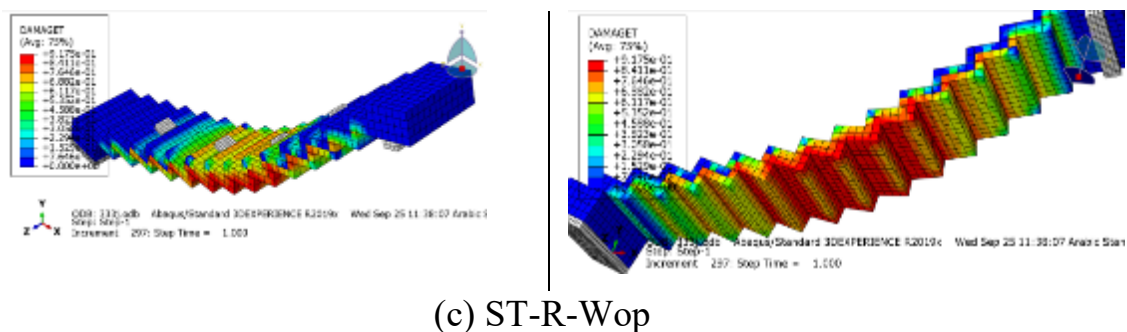
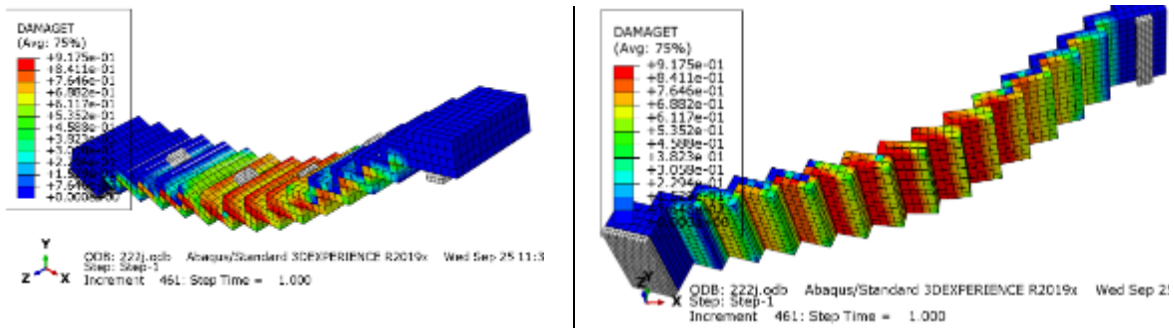
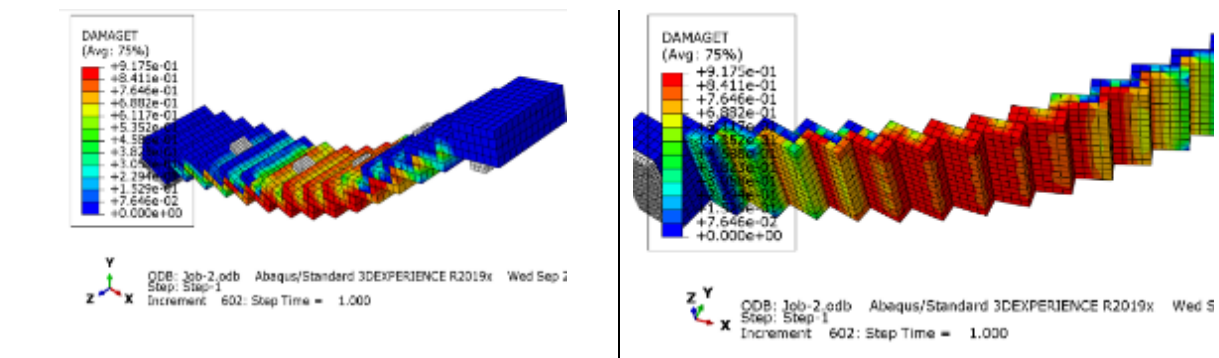


Figure 4-21 Cracks pattern for slabless staircases of ST-M-Wop, ST-L-Wop, and ST-R-Wop

4.4.2 Effect of CFRP Material (Series)Two

The verified FE model was used to extend the parametric study required for the response of slabless staircase. Fourteen staircases made of reinforced concrete were built and discussed. In order to generate the specimens, conventional dimensions that are typically utilized in practical applications were utilized, and the limits of the testing instruments were also taken into consideration. There were fourteen steps of the stair, and they were positioned between two beams. At both ends, the beams had a cross section that measured 200 x 300 mm. Based on the information shown in Fig.(4-22), the dimensions of the stairs are as follows: the width of the stairs (b_w) is 600 mm, the width of the treads (t) is 200 mm, and the height of the risers (r) is 110 mm. When it comes to slabless stairs, the tread thickness (t_h) and the riser thickness (t_v) can be created in such a way that they are either identical to one another or different from one another. The test parameters of t_h and t_v were taken into consideration and evaluated because of the impact that was anticipated to be exerted on both strength and behavior. However, this curiosity is reduced when the thicknesses are substantial. As a result, it was determined that the thicknesses to be examined are 100 mm. A number of parameters, such as the compressive strength and the retrofitting of the specimens with CFRP bar and sheet, were incorporated into the modeling of the slabless staircases that were conducted as part of the parametric study. A variety of concrete compressive strength values were included in the range of the compressive strength variable. These values were 20, 30, 40, 50, 60, and 70 MPa. In addition to the link rebar that connected the two reinforcing zones, the staircases themselves were outfitted with carbon fiber reinforced plastic (CFRP) bars in the S1 and S2 zones. Carbon fiber reinforced plastic sheets were used to cover the lower surface of the staircases. Using both the strips and complete wrapping methods, the slabless staircases were built according to the specifications. Following the application of the CFRP sheets, which were 50, 100, and 150 mm in

width and thickness of 0.5 mm, the tread's bottom surface was covered. Concerning the reinforcement rebar, steel reinforcement ($\phi 8$ mm) and CFRP bar ($\phi 5$ mm) were utilized for the reinforcing and retrofitting as demonstrated in Fig. (4-22) and Table (4-4). For the load and boundary conditions, the simply supported conditions was performed with concentrated loads applied at third, sixth, and ninth treads as demonstrated in Fig. (4-22).

Table 4-4 Description of Specimens

Var.	Spi.	f_c' (MPa)	Variable Details
Compressive Strength	ST-20	20	Compressive strength to 20 MPa
	ST-30	30	Compressive strength to 30 MPa
	ST-40	40	Compressive strength to 40 MPa
	ST-50	50	Compressive strength to 50 MPa
	ST-60	60	Compressive strength to 60 MPa
CFRP Bar	ST-CRS ₁	50	CFRP rebar at S1 reinforcement zone
	ST-CRS ₂	50	CFRP rebar at S2 reinforcement zone
	ST-CRS ₁₋₂	50	CFRP rebar at S1 and S2 reinforcement zone
	ST-CR	50	Fully CFRP rebar except stirrups
	ST-CRL	50	Addition of CFRP as link between S1 and S2 zones
CFRP sheet	ST-CS-5	50	Wrapping the tread bottom surface with CFRP sheet (100mm width)
	ST-CS-10	50	Wrapping the tread bottom surface with CFRP sheet (200mm width)
	ST-CS-15	50	Wrapping the tread bottom surface with CFRP sheet (300mm width)
	ST-CS-F	50	Full Wrapping for the slabless staircases

ST-20: ST; refers to the stairs name and 20 refers to the compressive strength value.

ST-CRS1: CR; refers to the CFRP bar and S1; refers to the use of CFRP bar in S1 zone.

ST-CS-5: CS; refers to the CFRP sheet and 5 refers to the sheet width

ST-CS-F: F: refers to the full wrapping configuration of sheet.

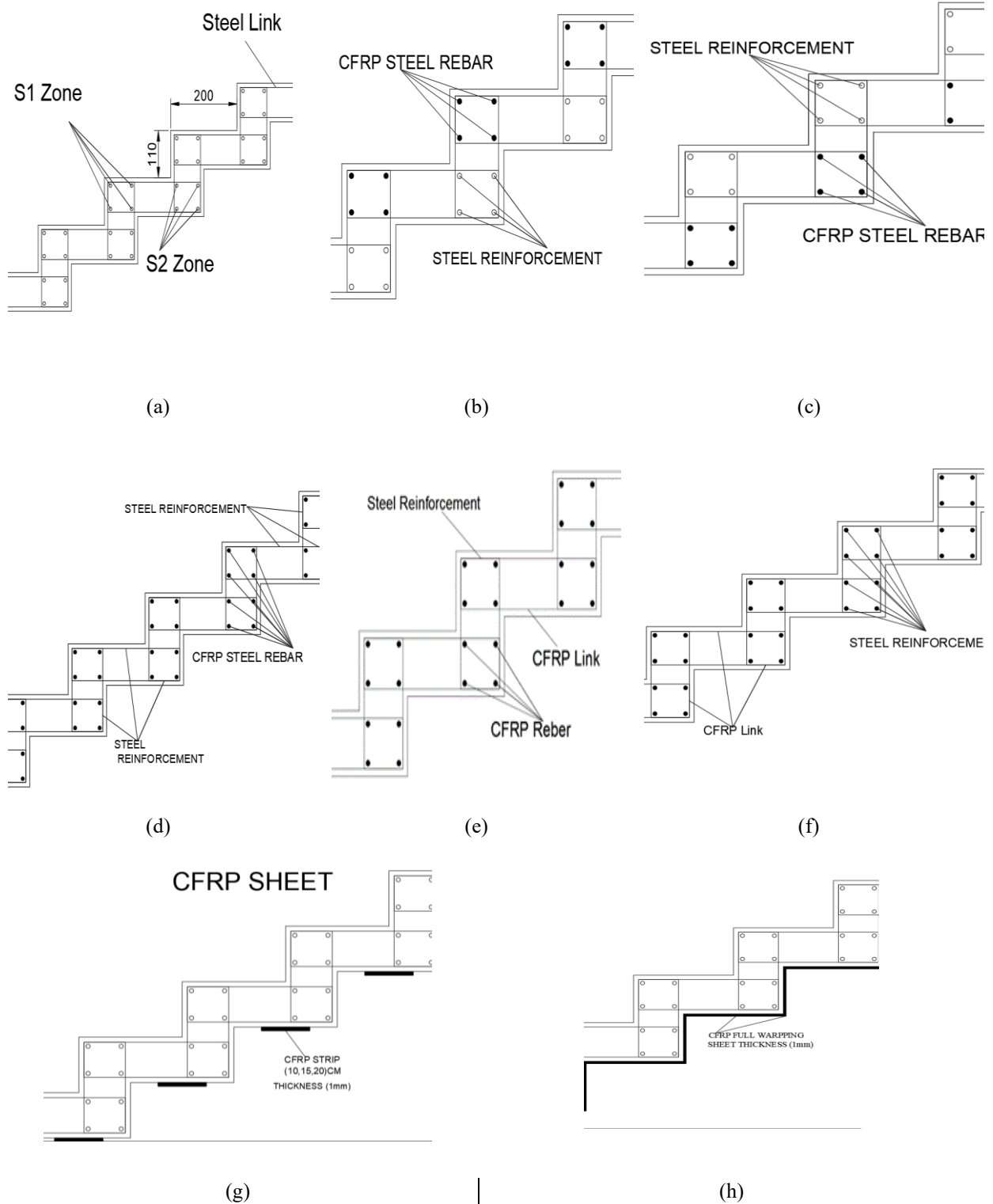


Figure 4-19 Demonstrations of geometry tests

(a) S-Zones distribution (b) ST-CRS₁
(c) ST-CRS₂ (d) ST-CRS₁₋₂ (e) ST-CR (f) ST-CRL (g) ST-CS-5, ST-CS-10, and ST-CS-15 (h) ST-CS-F

4.4.2.1 Results and Discussion

In this section, the results of the specimens are illustrated and summarized in Table (4-5). with relation to the cracking load, ultimate load, load-deflection curves, ductility index, stiffness, energy absorption, and failure mode.

Table 4-5 Test result of Load Deflection Curve

Beam	Py (kN)	Δy (mm)	Pu (kN)	Δu (mm)	Initial Stiffness (kN/mm)	Ductility Index
ST-20	2.38	28.20	8.05	95.38	8.44	3.38
ST-30	4.51	32.19	13.84	98.75	14.02	3.07
ST-40	7.30	38.08	19.88	103.75	19.16	2.72
ST-50	7.62	37.30	25.04	122.50	20.44	3.28
ST-60	8.76	27.74	31.96	101.25	31.57	3.65
ST-70	10.85	15.34	48.00	67.88	70.72	4.42
ST-CRS ₁	10.11	43.38	30.72	139.90	23.31	3.22
ST-CRS ₂	14.13	32.69	40.62	96.95	43.23	2.97
ST-CRS ₁₋₂	15.52	26.62	36.00	75.01	58.32	2.82
ST-CR	16.29	20.63	43.16	57.43	78.94	2.78
ST-CRL	8.15	37.75	27.26	120.58	21.59	3.19
ST-CS-5	9.82	34.84	29.47	94.99	28.19	2.73
ST-CS-10	10.05	34.60	31.72	92.90	29.04	2.69
ST-CS-15	11.01	32.55	33.40	83.05	33.83	2.55
ST-CS-F	13.51	27.48	42.01	62.70	49.19	2.28

A) Effect of Compressive Strength

If the joints (point of connection between the treads and risers) are stiff enough, there are two possible locations for the plastic hinges that are located in the middle of the stairs. Plastic hinges can form on either the tread or the riser. Table (4-5) and Fig. (4-22) explains the results that were obtained from the examing of RC staircases that were subjected to flexural loads. Significant variances were found between the various concrete slabless stairs. The difference was attributed to the significant effect

of concrete strength on the staircase response. The compressive strength values studied was varied from 20, 30, 40, 50, 60, and 70 MPa to investigate the effect of the concrete compressive strength on the flexural behavior of staircases. The specimen (ST-20) showed the lowest cracking load resistance which was (2.74 kN). The increase in compressive strength from 20 MPa to 30, 40, 50 MPa showed an enhancement in the cracking strength by about 89.5%, 206.4%, 220.2%, 267.8%, and 355.6% respectively as revealed in Fig. (4-23). The increase in concrete compressive strength from 20 MPa to 30, 40, 50 MPa showed a significant enhancement in the maximum load values by about 71.9%, 147%, 211%, 297%, and 596.3% respectively as revealed in Fig. (4-23). The deflection behavior was dissimilar of cracking and ultimate load which the variation was little between the specimens with varied compressive strength which the increase of the compressive strength led to decrease in the maximum deflection as seen in Fig. (4-24).

B) Effect of CFRP bar

Regarding the impact of carbon fiber reinforced plastic (CFRP) rebar has on the flexural behavior of slabless staircases, the steel reinforcement was partially replaced with the CFRP bars. The replacement consisted of placing the CFRP bars in place of the steel reinforcement in the S1 and S2 zones, both separately and together, as well as in the link between two reinforcing regions. The conventional specimens reinforced by rebar have the highest ductility, although they have a lower flexural strength than the reinforced specimens bt CFRP bar. The model (ST-CRS1) exhibits a cracking load of 10.11 kN. However, when the configuration of the steel reinforcement was changed, the steel reinforcement in the S1 (ST-CRS2) zone was discovered that the cracking load increased to 14.13 kN, which is equivalent to 32.7% and 85.5% when compared with the model (ST-50). It was concluded that replacing the steel reinforcing bar in the S2 zone (ST-CRS2) resulte in an increase in the cracking resistance that was larger than those of the S1 zone. This is due to

the fact that this region is subjected to higher stresses than another region. As shown in Fig. (4-23), the complete substitution of carbon fiber reinforced plastic (CFRP) for steel reinforcement in both zones, while maintaining the stirrups and steel links as steel rebar, resulted in a greater flexural strength of 15.52 against cracking, which is equivalent to 103.7% when compared to the model (ST-50). Taking into consideration the model (ST-CR), which comprised the substitution of carbon fiber reinforced plastic (CFRP) bar for steel rebar while maintaining the steel stirrups, it was discovered that the reinforced slabless staircases had the highest cracking load, which saw a significant improvement of 113.7%. The previous configuration parameter involved replacing the steel links between the S1 and S2 zones with CFRP sheet. This change resulted in a cracking load that was 8.15 kN higher than the model (ST-50) with only a 7% difference, as illustrated in Figure 26. To examine the effect of carbon fibre reinforced plastic (CFRP) reinforcing bars on the maximum bending strength of stairs without a solid base, a portion of the steel reinforcement was substituted with CFRP bars. Compared to the reinforced specimens, the conventional specimens with steel reinforcement exhibit superior ductility, but lower ultimate strength. The model (ST-CRS1) demonstrates a cracking load of 30.72 kN, which is higher than the cracking load of the model (ST-50). However, when the configuration of the steel reinforcement was modified by replacing the steel reinforcement in the S1 (ST-CRS2) area, it was found that the maximum load increased to 40.62 kN, which corresponds to an increase of 22.7% and 62.2%. The substitution of the steel reinforcing bar at the S2 zone (ST-CRS2) led to a higher increase in the flexural resistance compared to the S1 zone. This is due to the fact that the S2 zone is more susceptible to the flexural stresses. The full replacement of steel reinforcement with carbon fiber reinforced plastic (CFRP) in both zones, while maintaining the stirrups and steel links as steel rebar, demonstrated a greater flexural strength of 36 kN, which is equivalent to 43.77% when compared with the model

(ST-50), as shown in Fig.(4-23). In reference to the model (ST-CR), which comprised the substitution of carbon fiber reinforced plastic (CFRP) bar for steel rebar while maintaining the steel stirrups, it was discovered that the ultimate load was greatest among the reinforced slabless stairs, which improved by 72.36 percent. whereas the final configuration parameter, which consisted of replacing the steel linkages between the S1 and S2 zones with CFRP bar, displayed an ultimate load that was 27.26 kN higher than the model (ST-50) with only 8.9%, as shown in Fig.(4-23).

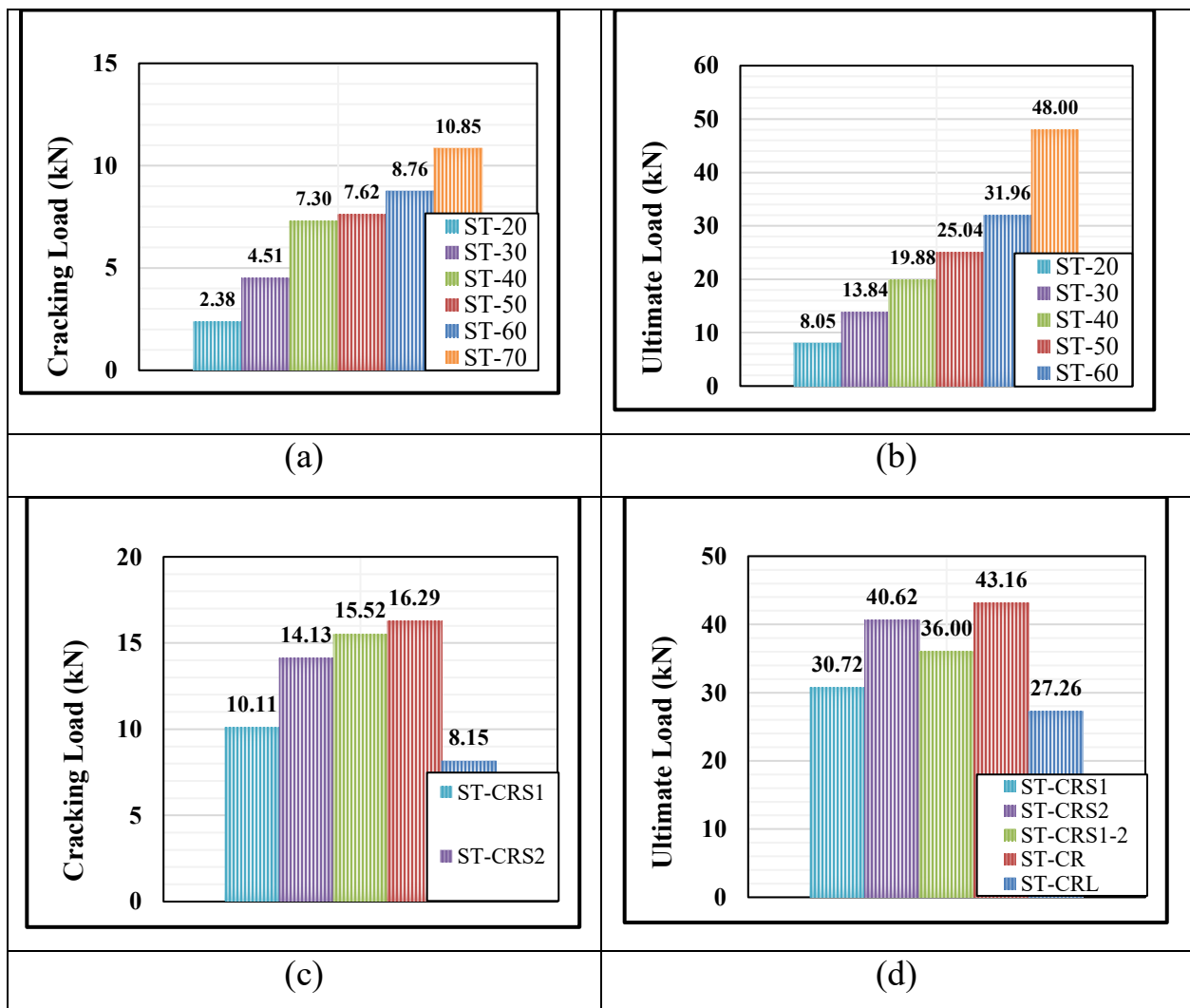


Figure 4-23 Cracking and ultimate load results.

(a) Cracking load of ST-series (b) Ultimate load of ST-series (c) Cracking load of ST-CRS series (d) Ultimate load of ST-CRS series

C) Effect of CFRP Sheet

By wrapping the slabless staircases with CFRP sheet under the tread zone in multiple configurations. From the results of this variable, it is clearly shown that significant improvements were made to the cracking resistance and maximum load capacity of the stairs case. After strengthening the specimens with CFRP strips of 50 mm, 100 mm and 150 mm width, it was concluded that the cracking load was increased in comparison to the control beam (ST-50). As can be seen in Fig. (4-24), the retrofitting with CFRP strips resulted in an increase of 28.9%, 31.84%, and 44.5% in the cracking load of the models ST-CS-5, ST-CS-10, and ST-CS-15, respectively. These improvements were due to the tension resistance of the CFRP sheet placed under the treads which increase the width of the sheet led to more flexural strength. When the ultimate load was compared to the cracking load resistance, it was found that the wrapping by strips for the same models caused the ultimate flexural strength to increase by 17.6%, 26.7%, and 33.4% respectively, as shown in Fig. (4-24). The ultimate load indicated a lower level of enhancement due to the brittleness of the concrete after the yield point. As a result of the linearity of the CFRP sheets, the ability of the stairs to deflect was significantly decreased. The wrapping done by these sheets demonstrated that the deflection was reduced by a percentage that reached the half value. The deflection varied greatly. As can be seen in Fig. (4-25), the model ST-CS-5 demonstrated that the deflection decreased by 22.5%, which resulted in an increase in the width of the strips to 20 and 30 centimeters, respectively, revealing a decrease of 24.2% and 32.3%. When it comes to the full wrapping with CFRP sheets, the behavior was quite different, with more improvements in the cracking and ultimate load, in addition to a significant reduction in the deflection. The cracking load of the model (ST-CS-F) indicated a value of 13.51 kN, which was greater than the control model by 77.35%. This was owing to the fact that the CFRP had the ability to provide additional confinement to the

flexural stresses along the bottom fiber of the staircases. As can be seen in Fig (4-24), the ultimate load showed a greater degree of improvement among the specimens that had been retrofitted with CFRP sheets. This resulted in an increase in the ultimate flexural analysis from 25.04 kN to 42.01 kN, which is equivalent to 67.8%. As can be observed in Fig. (4-25), the deflection experienced a significant reduction, going from 122.5 millimeters to 62.7 millimeters, which is equivalent to 48.2%.

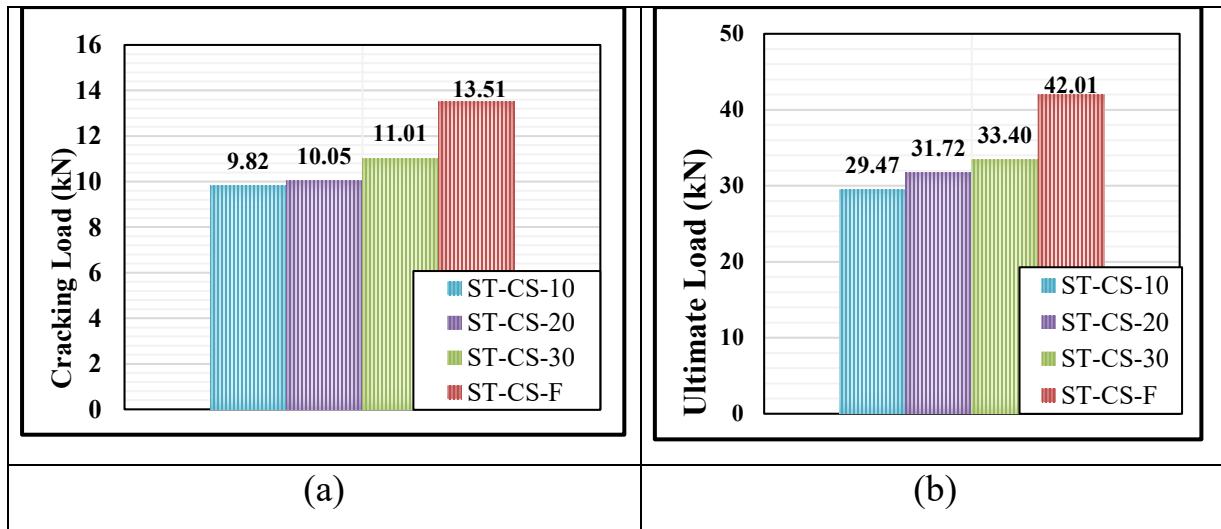


Figure 4-20 Cracking and ultimate load results.

(a) Cracking load of ST-CS series (b) Ultimate load of ST-CS series

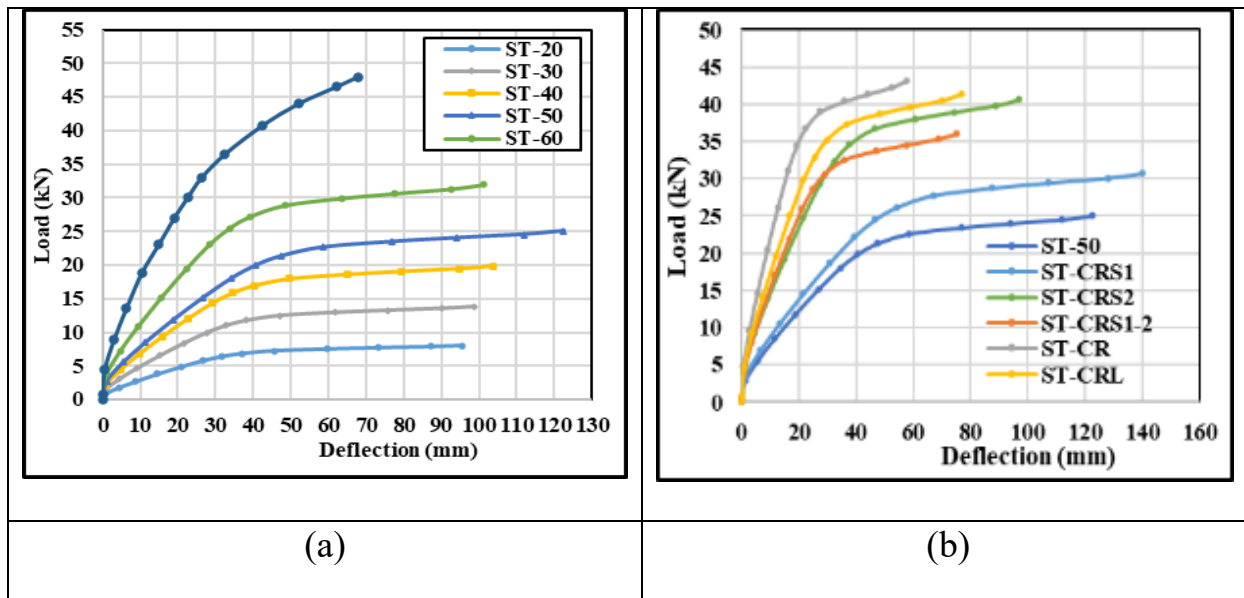


Figure 4-21 Load-deflection curve of slabless staircases.

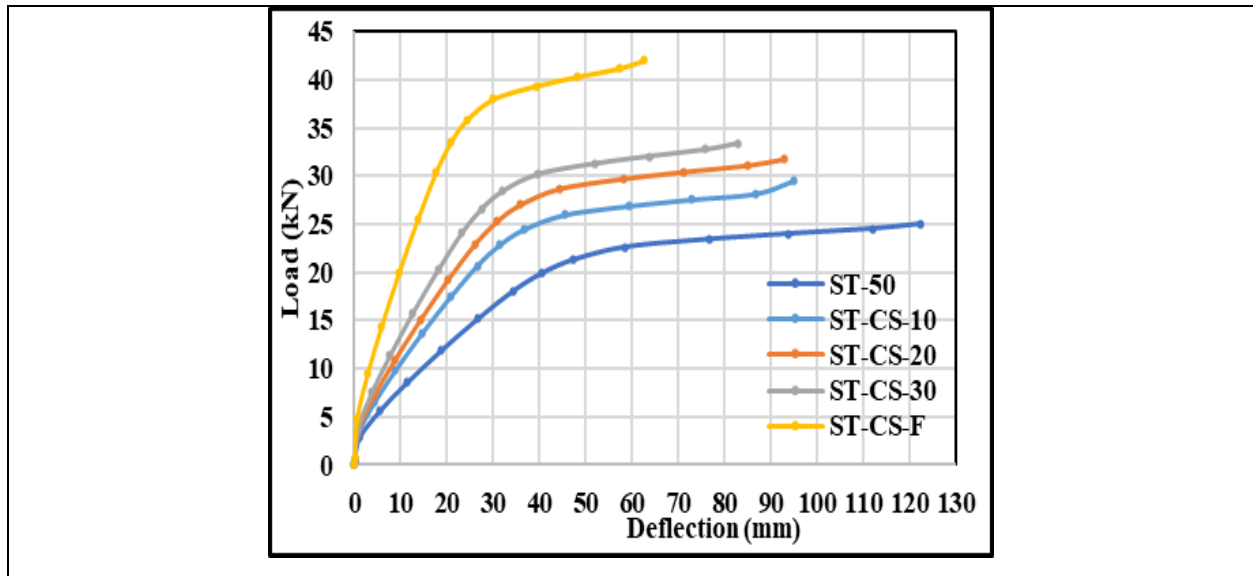


Figure 4-25 Continued.

D) Ductility Index

The results of the ductility index for slabless staircases are displayed in Table (4-5) and Fig.(4- 26), respectively. A ductility index of 3.38 was found to be the greatest among the specimens, which was the ST-20. When the compressive strength of the concrete increased, the ductility index reduced. When the compressive strength of the material was increased from 20 MPa to 30, 40, and 50 MPa, the ductility index increased by 9.3%, 19.4%, and 3% respectively for models with compressive strengths of 30, 40, and 50 MPa. As can be seen in Fig. (4-26), the increase in the ductility index was 8% for models with a f_c of 60 MPa and 30.9% for models with a f_c of 70 MPa. The control specimens with steel reinforcement have the highest ductility among the reinforced specimens, but they have a lower flexural strength. This is the case with retrofitting specimens that contain CFRP bars. The model (ST-CRS1) displays a ductility index of 3.22 which modify the configuration of steel reinforcement by substituting the steel reinforcement in the S1 (ST-CRS2) zone revealed that the ductility index fell to 2.97 which equivalent to 1.7% and 9.6% when compared with the model (ST-50). Due to the fact that this region is more susceptible

to resist flexural loads, the replacement of the steel reinforcing bar at the S2 zone (ST-CRS2) revealed a decrease in the ductility index that was larger than those of the S1 zone. With the stirrups and steel links remaining as steel rebar, the full replacement of steel reinforcement with carbon fiber reinforced plastic (CFRP) in both zones exhibited a lower ductility index of 2.82, which is equivalent to 14.1% when compared with the model (ST-50), as shown in Fig. (4-26). Regarding the model (ST-CR), which comprised the substitution of CFRP bar for steel rebar while maintaining the steel stirrups, it was discovered that the ductility index was the lowest among the reinforced slabless staircases, which experienced a reduction of 15.1%. whereas the last configuration parameter, which consisted of replacing the steel linkages between the S1 and S2 zones with CFRP sheet, revealed a cracking load that was 1.86 kN lower than the model (ST-50) with 43.4%, as shown in Fig. (4-26). Besides the fact that the CFRP bar is a linear material, it does not have the capacity for strain hardening as the steel reinforcement does. This enormous reduction was the result of replacing the link between S-zones, which is responsible for the specimen's ability to deflection beside the CFRP bar. There was a greater decrease in the ductility index as a result of wrapping the slabless staircases with CFRP sheet under the tread zone with multiple configurations. When the specimens were wrapped in CFRP strips measuring 5, 10, and 15 centimeters, it was discovered that the ductility index had drastically decreased in comparison to the control beam being used (ST-50). As can be seen in Fig. (4-26), the retrofitting of the models ST-CS-5, ST-CS-10, and ST-CS-15 with CFRP strips resulted in a reduction of the ductility index by 16.9%, 18.2%, and 22.2%, respectively. When compared to the control model, the ductility index was reduced by 30.5% when full wrapping was utilized.

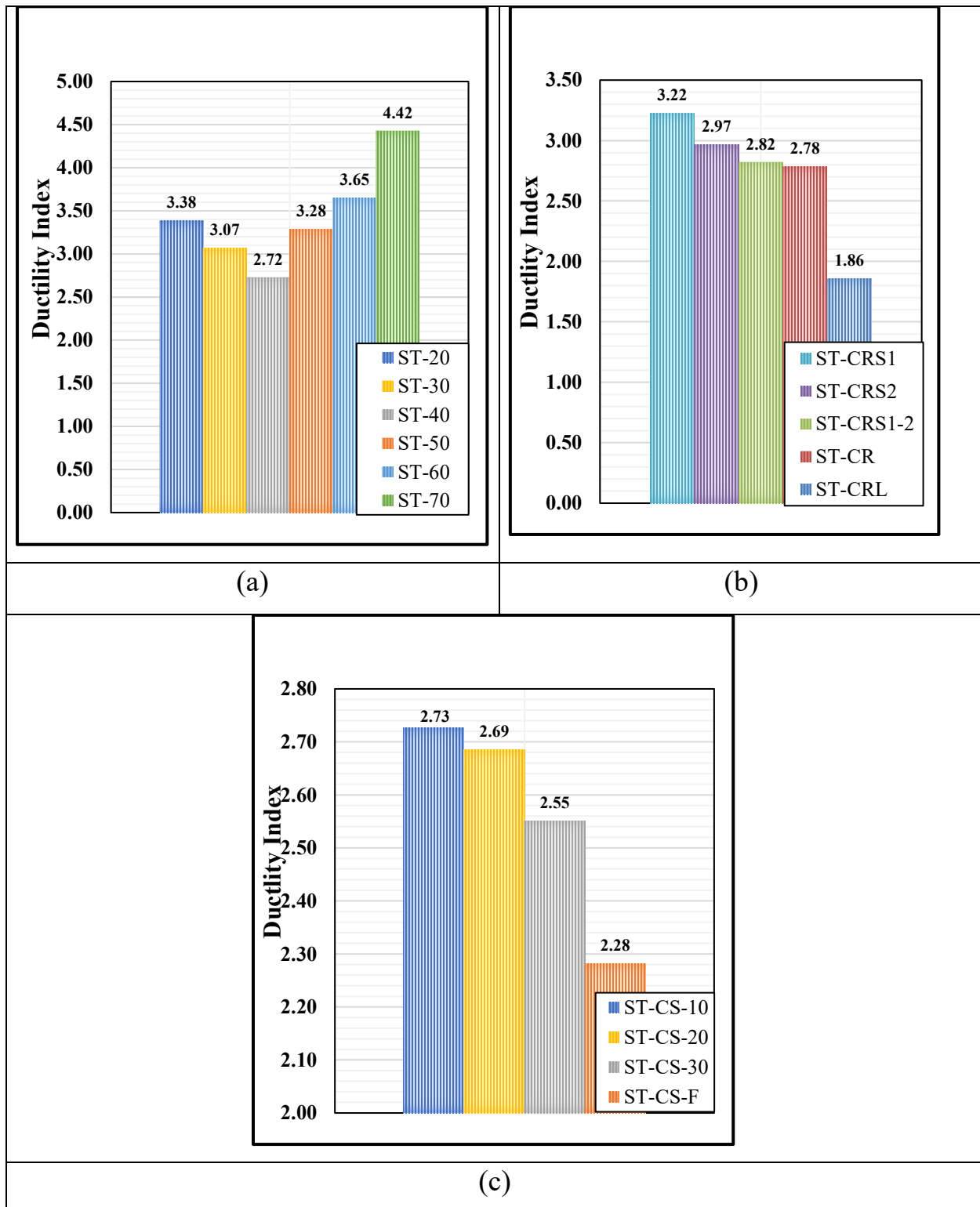


Figure 4-22 Ductility index of the slabless staircases.

F) Initial Stiffness

The initial stiffness is defined as the slope of the load-deflection curve's initial portion. The yield load (P_y) divided by the yield deflection (Δy) is the formula for its calculation [19]. The findings of the slabless staircases' initial stiffness are displayed in Table (4-5). In order to study how concrete compressive strength affects stair stiffness, the specimen involved a range of compressive strengths (20, 30, 40, 50, 60, and 70 MPa). In the instance of high strength concrete, where a high compressive strength combined with a high ratio of steel reinforcement provided greater resistance to flexure, the ductility index rose in tandem with the increase in concrete's compressive strength. Models with compressive strengths of 30, 40, and 50 MPa exhibited an initial stiffness increase of 66.1%, 127%, and 142.25 percent, respectively, when f_c was increased from 20 MPa to 30, 40, and 50 MPa. Figure 6 shows the effect of the high compressive strength (60 and 70 MPa) which resulted in a 4% increase in the initial stiffness, respectively. Reference specimens reinforced with steel offer less flexural strength than CFRP bar. By adopting the steel reinforcement in the S1 zone for a different arrangement, the initial stiffness increased from 23.31 kN/mm in the ST-CRS1 model to 43.23 kN/mm in the ST-CRS2 model, a 14% increase over the ST-50 model. The initial stiffness was dropped after replacing the steel reinforcing bar at the S2 zone (ST-CRS2) compared to the S1 zone, perhaps because the S2 zone is more vulnerable to flexural stresses. As shown in Fig. (4-27) , the initial stiffness was 58.32 kN/mm, or 185% greater than the model (ST-50), when the stirrups and steel links were retained as steel rebar and CFRP reinforcement was completely replaced in both zones. The model (ST-CR) showed a decrease in the initial stiffness of the reinforced slabless stairs by 286.2% when the steel rebar was replaced with CFRP bar, while keeping the steel stirrups intact. Fig. (4-27) demonstrates that the final configuration parameter, which substituted CFRP sheets for steel links between the S1 and S2 zones, led to an initial

stiffness that was 19.74 kN/mm lower than the ST-50 model, representing a decrease of 3.5%.

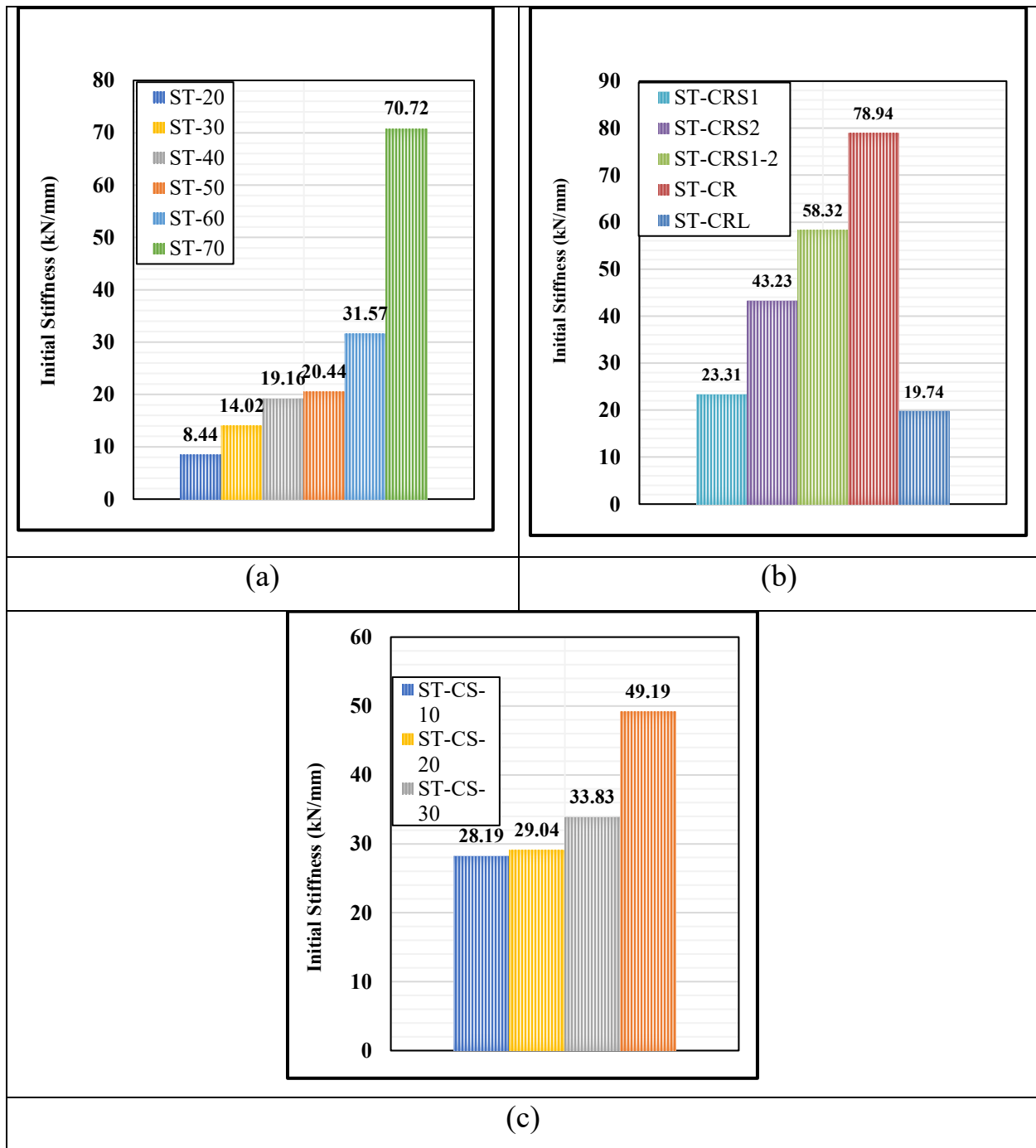


Figure 4-23 Initial stiffness of the tested slabless staircases.

The replacement of the link between S-zones, which is crucial for the specimen's deflection ability, with a linear material like CFRP bar which lacks the strain

hardening capability of steel led to this reduction. Additional reduction in the ductility index was seen after encasing the slabless staircases with CFRP sheet beneath the tread zone using multiple configurations. The initial stiffness was found to be greatly enhanced when the specimens were wrapped with CFRP strips (5, 10, and 15 cm) in comparison to the control beam (ST-50). As shown in Fig.(4- 27), the ST-CS-5, ST-CS-10, and ST-CS-15 models' initial stiffness was increased by 37.9%, 42.1%, and 65.5%, respectively, after being retrofitted with CFRP strips. By incorporating full wrapping into the final structure, the initial stiffness was increased by 1405 compared to the control model.

G) Cracking and failure mode

It was shown in Fig.(4-28) that the distribution of stresses did not alter as the compressive strength rose in models (ST-20) to (ST-70), which included simulating slabless staircases with varying compressive strengths. When CFRP rebar was used in place of steel reinforcement for some models, it the stress distribution. When steel rebar was substituted with CFRP rebar in the S1 zones, the results demonstrated that the stresses were concentrated most intensely there, with lower concentrations elsewhere. Compared to the control model, the concentration increased after replacing the steel rebar in the S2 zone. When carbon bars were used in place of steel in the S1 and S2 zones, it was found that additional stresses were generated along the tread, with the greatest concentration at the stepped area where the tread meets the riser. Fig. (4-28) shows that models made of CFRP had less stress concentration along the treads because the carbon sheet strips diffused the stresses across the model.

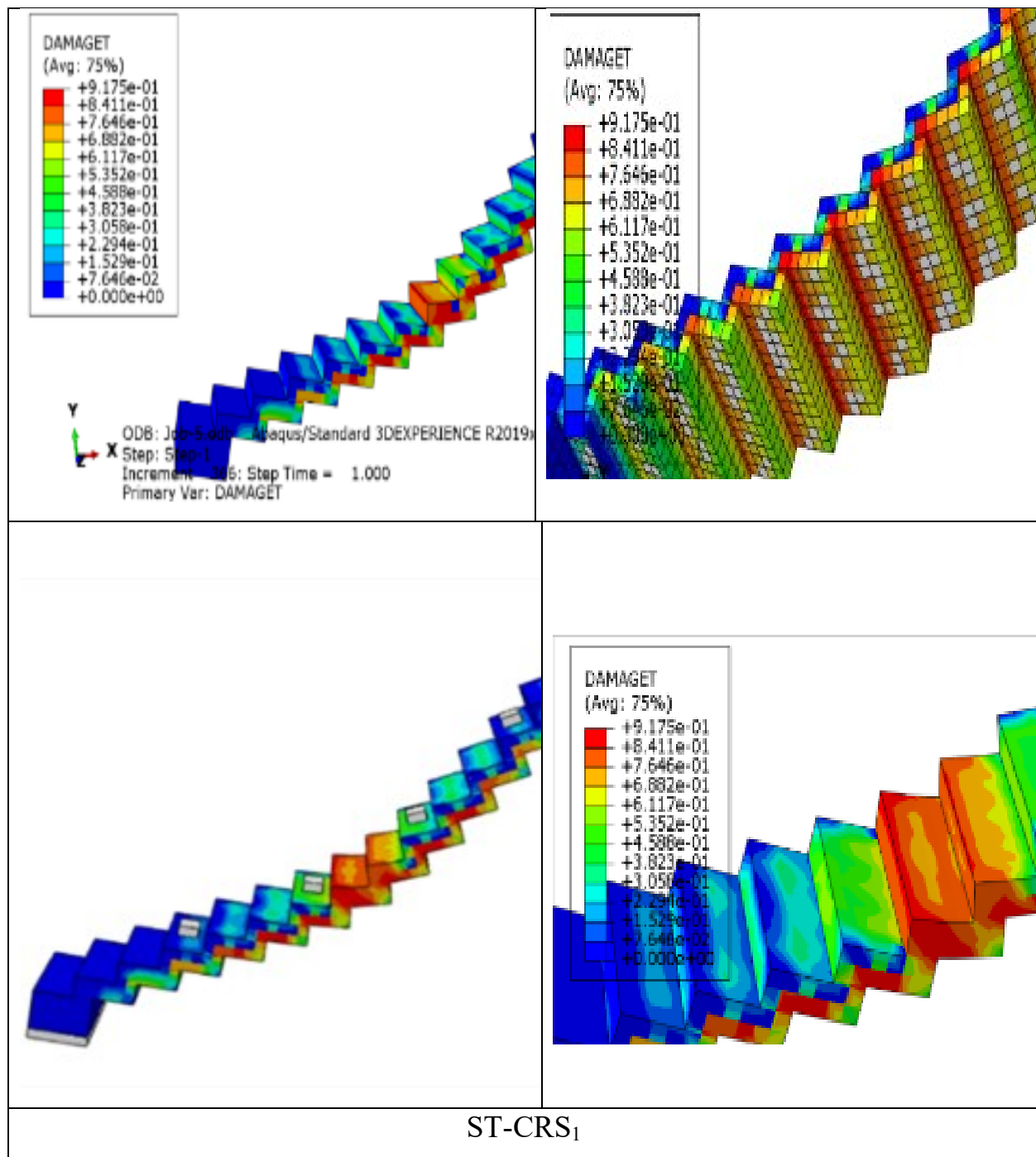
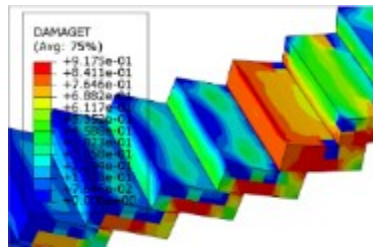
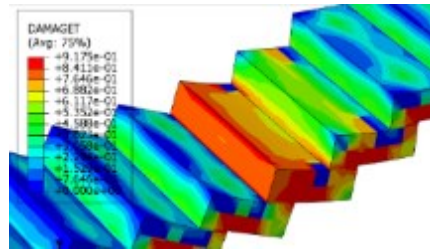


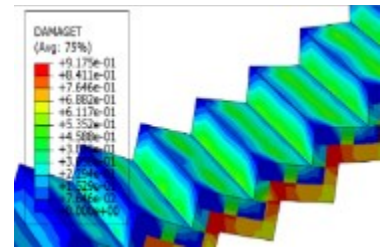
Figure 4-24 Cracks pattern for slabless staircases Series Two.



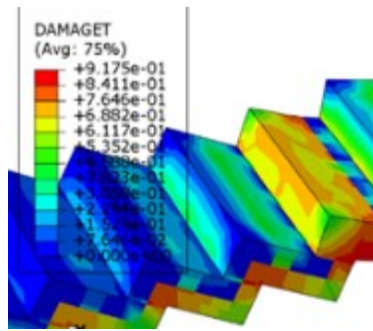
(b) ST-CRS₂



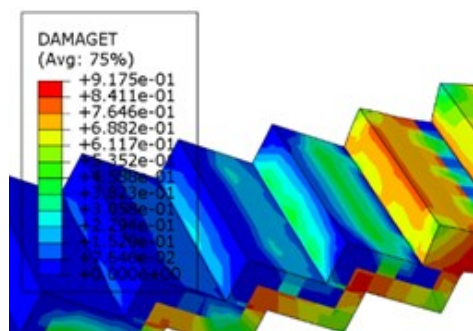
(c) ST-CRS₁₋₂



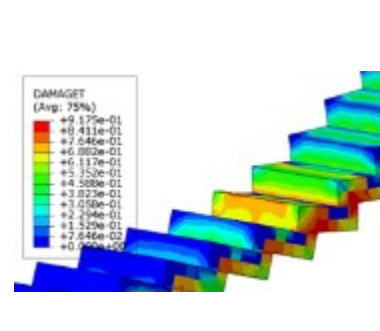
(d) ST-CS-5



(e) ST-CS-10



(f) ST-CS-15



(g) ST-CS-F

Figure 4-28 Continued.

4.4.3 Series Three

Regarding the geometrical effect on the flexural behavior of slabless staircases, change the geometry configuration to that staircases have landing with 1 meter in the midspan of the specimen as seen in Fig. (4-32) and Table (4-6)

Table 4-6 Description of Specimens

ID	f_c' (MPa)	Variable Details
ST	50	-
ST-Ln	50	Addition of landing to the staircases
ST-Ln-60	60	Change the compressive strength to 60 MPa
ST-Ln-70	70	Change the compressive strength to 70 MPa

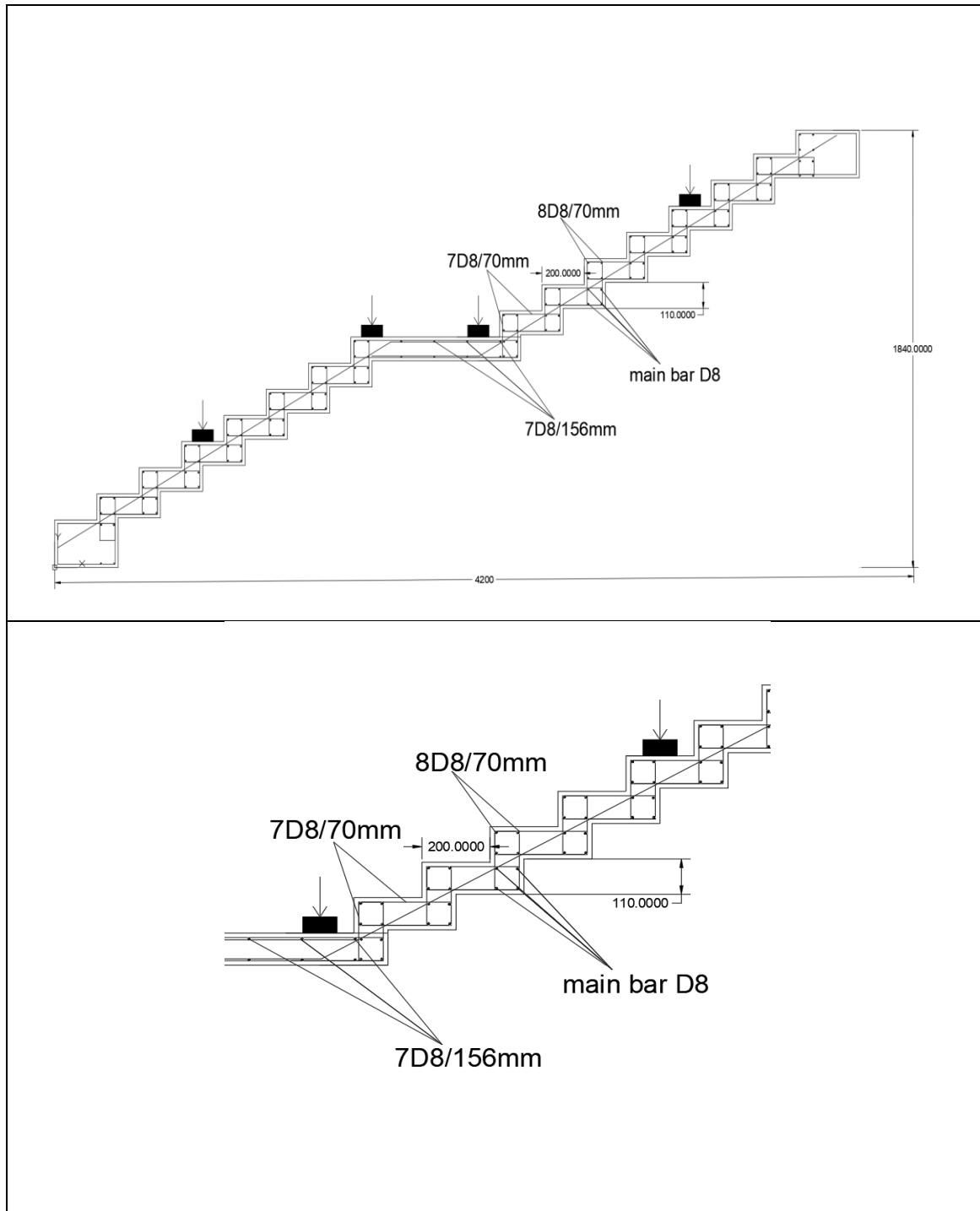


Figure 4-29 Demonstrations of geometry tests

4.4.3.1 Results and Discussion of Series Three

The cracking load of the model ST-Ln revealed a value of 8.53 kN which less the control slab without landing with 19% while the ultimate load carrying capacity

showed 27.31 kN which was less than reference slab with 29% as revealed in Table(4- 7). The load deflection relationship showed that the existence of the landing with one meter only exhibited higher deflection when the deflection increased from 148.33 mm to 172.14 mm as demonstrated in the Fig. (4-29). the increase of the compressive strength can enhance the weakness in the flexural which use of 60 and 70 MPa increased the cracking load from 8.53 kN for the landing staircases to 10.46 which equal to an enhancement of 22.6% and 50.3% respectively when compared with the staircases with landing (ST-Ln) model. The ultimate load carrying capacity demonstrated that enhancement in the flexural strength raised to 54.4% and 140.1% when compared with the staircases with landing (ST-Ln) model as revealed in Table (4-8) and Fig.(4-30). Load deflection curve revealed that increase the compressive strength decreased the deflection which resulted a higher flexural strength with less ductility as seen in Fig.(4-31)

Table 4-7 Test result of Load Deflection Curve

ID	Pcr kN	Δy mm	Pu kN	Δu mm	Initial Stiffness kN/mm	Ductilit y Index	Energy Absorpti on (kN.mm)
ST	10.48	28.68	38.61	148.33	1.10	5.17	281.65
ST-Ln	8.53	39.12	27.31	172.14	0.83	4.41	236.77
ST-Ln-60	10.46	32.98	42.60	139.43	1.12	4.23	280.10
ST-Ln-70	12.82	27.80	66.46	116.57	1.50	4.19	377.74

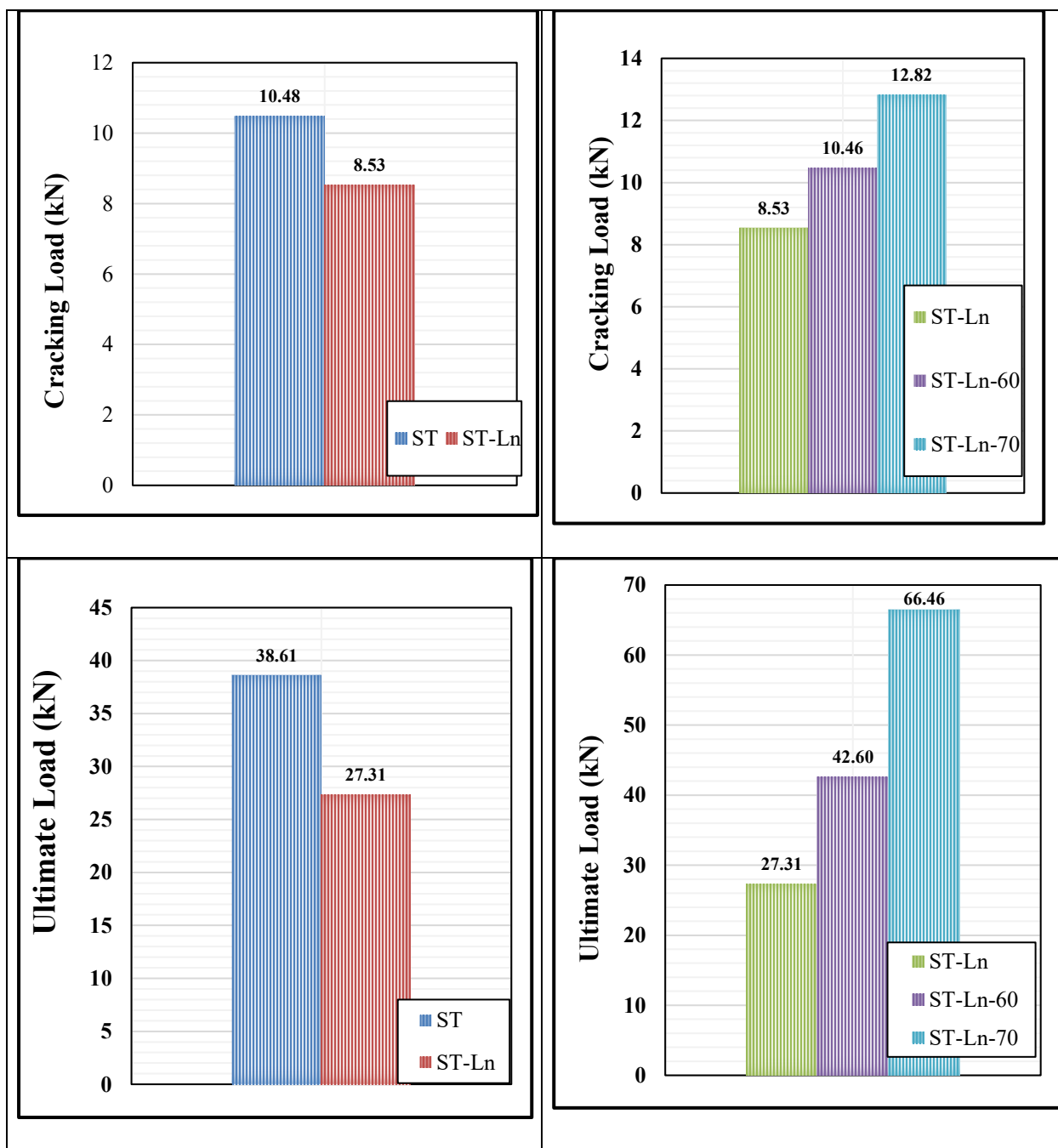


Figure 4-30 Ultimate and cracking load of slabsless staircases of Series Three

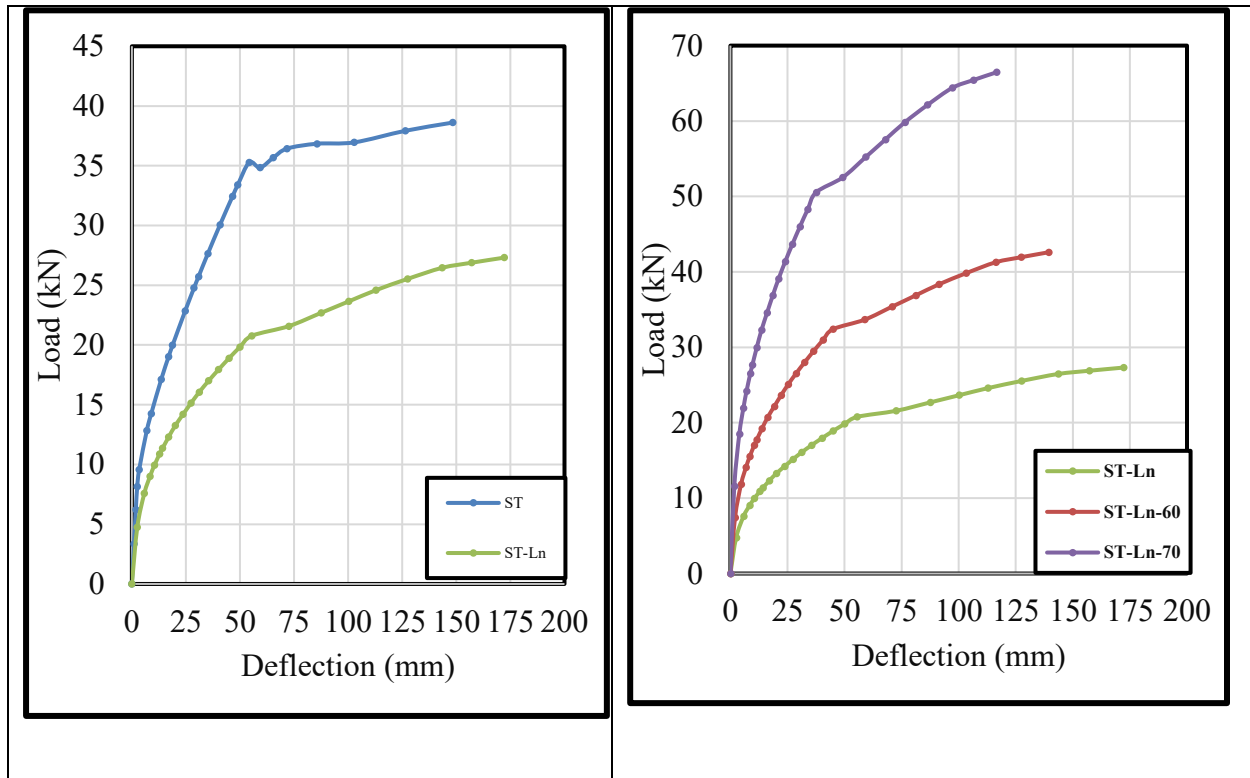


Figure 4-25 Load-deflection curve of ST-Ln-60 , ST-Ln-70 and ST-Ln slabless staircases.

A) Ductility and Stiffness .

The ductility of the model ST-Ln revealed a value of 4.41 which less the control slab without landing with 14.7%. The increase of the compressive strength reduced the ductility which use of 60 and 70 MPa decreased the ductility from 4.41 for the landing staircases to 4.23 and 4.19 which equal to an enhancement of 4.1% and 4.9% respectively when compared with the staircases with landing (ST-Ln) model as seen in Fig. (4-32).

The initial stiffness of the model ST-Ln revealed a value of 1.10 kN/mm which less the control slab without landing with 24.5%. The increase of the compressive strength increased the initial stiffness which use of 60 and 70 MPa increased the initial stiffness from 0.83 kN/mm for the landing staircases to 1.12 and 1.5 kN/mm

which equal to an enhancement of 34.4% and 80.6% respectively when compared with the staircases with landing (ST-Ln) model as seen in Fig. (4-33).

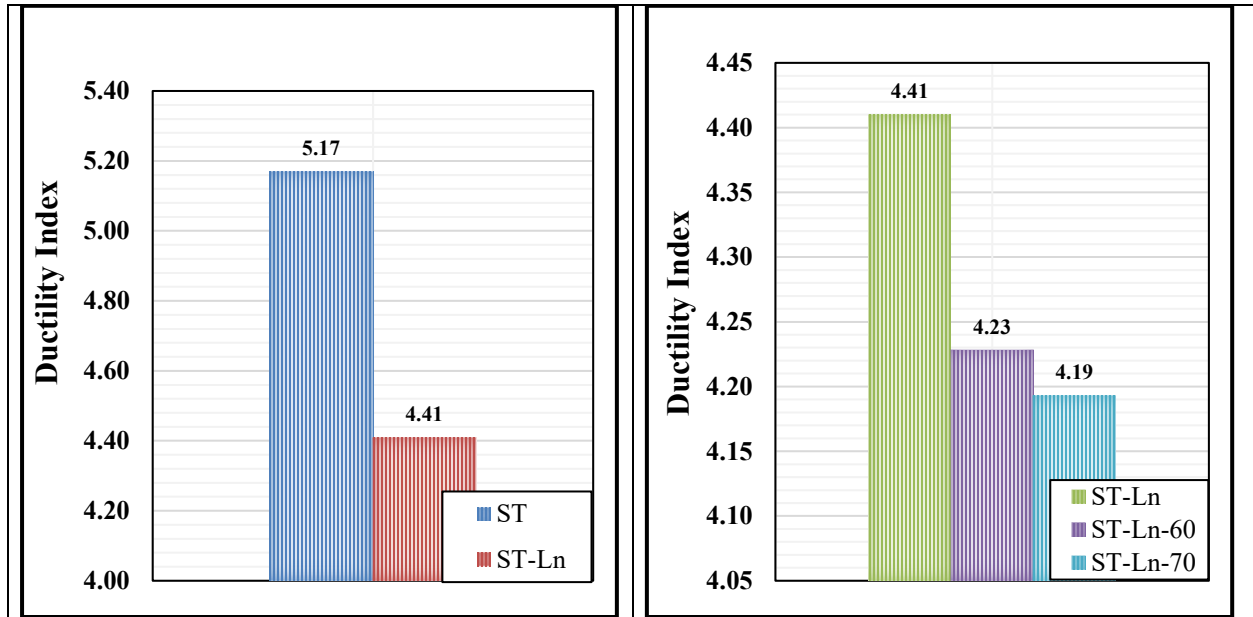


Figure 4-26 Ductility of slabsless staircases of Series Three

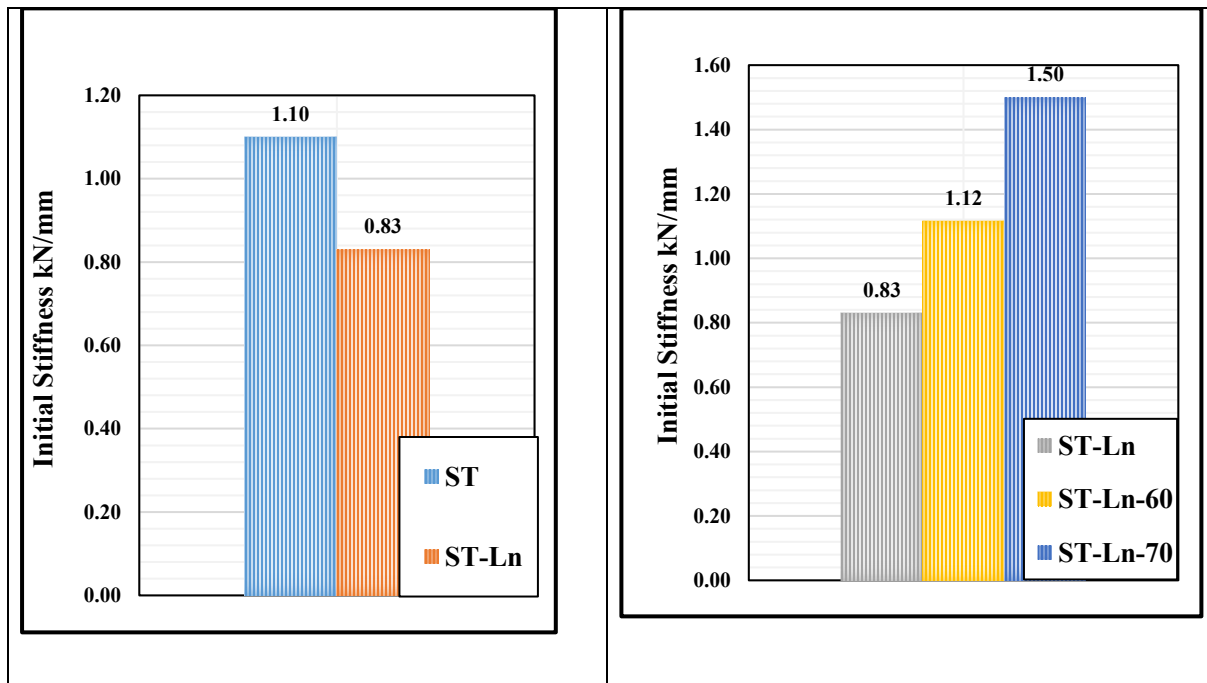


Figure 4-27 Initial Stiffness of of slabsless staircases Series Three

B) Cracking and failure mode

In this series which involved modeling of landing in the mid span. In the study of slabless staircases, particularly those with landings, the understanding of stress distribution is essential for evaluating their flexural behavior. When a load is applied to a slabless staircase, the stress distribution was influenced by the geometry and the presence of landings. In staircases without landings, the load is concentrated on the treads, which must resist both bending and shear forces. The absence of a slab means that the load transfer relies heavily on the individual treads and risers, leading to higher localized stresses. This feature increased the risk of cracking or failure, especially under concentrated loads. In contrast, the inclusion of a landing in a slabless staircase significantly alters the stress distribution. The landing acted as a redistribution point for the loads applied to the staircase. It provided additional support with less stiffness, which caused increasing of the bending moments experienced by the treads. The landing essentially served to spread the load over a larger area, reducing the peak stresses on the treads and risers. The flexural behavior of slabless staircases with landings was generally less to that of their counterparts without landings. Regarding the failure mode nad damaged (deformed area), the landing introduced a more stresses distribution along the staircase, as it could absorb some of the bending moments that would otherwise be concentrated at the edges of the treads in a staircase without a landing. This leads to a increase in deflection. Moreover, the landing provides a point of constraint that can alter the boundary conditions of the staircase. With the existence of a landing, the effective span of the treads is reduced, which increases the stresses on the boundary treads as seen in Fig.(4-38).

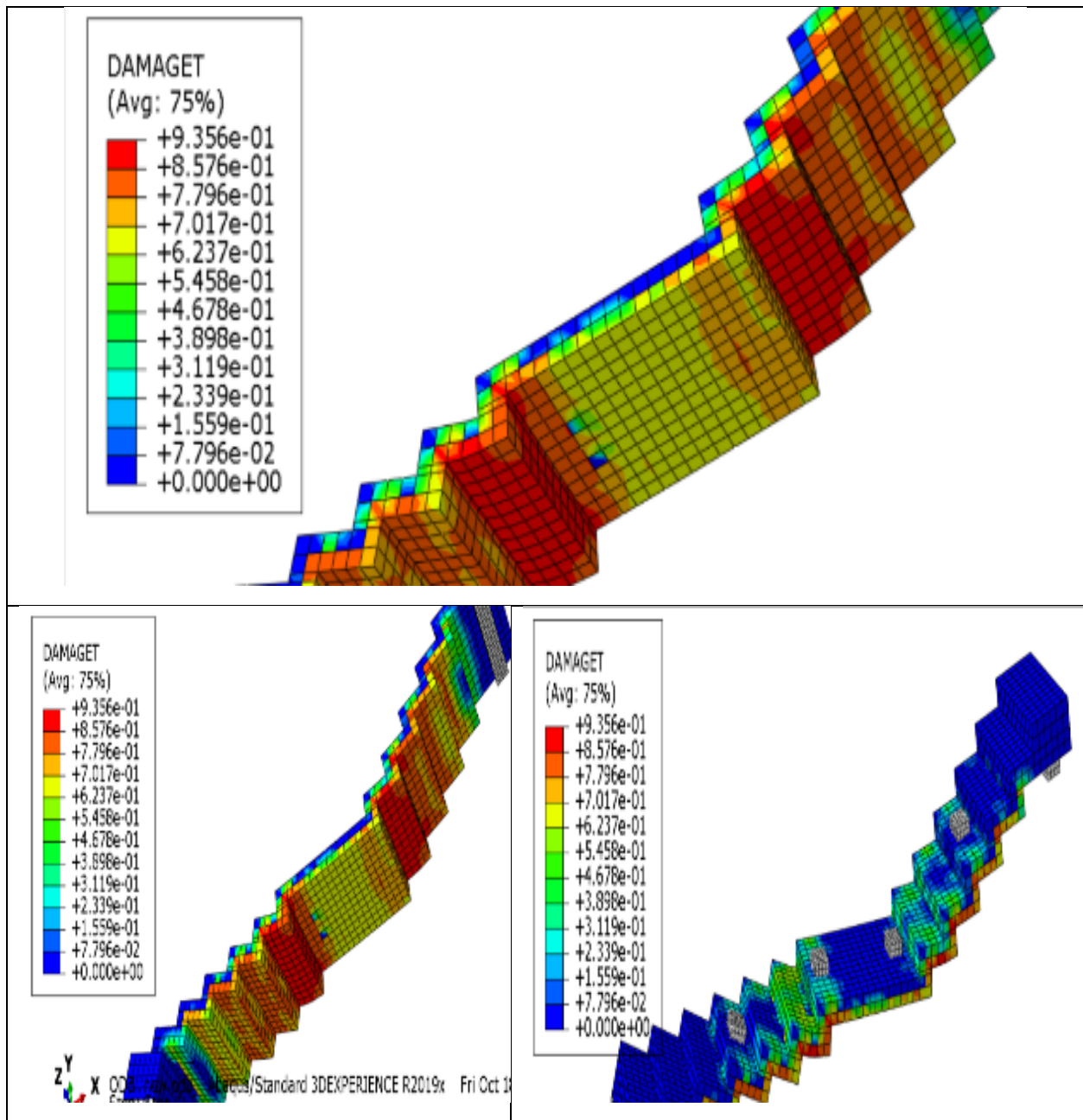


Figure 4-34 Cracks pattern for slabless staircases Series three.

CHAPTER FIVE:CONCLUSION AND RECOMNDATIONS

5.1 Conclusions

The current numerical analysis is centered on the behavior of slabless stairs with regard to their shear and flexural behavior in the presence of the parameters. As a consequence of the findings that were obtained from the finite element method (FEM) for the specimens, it has been shown that the manner in which shear and flexure failure takes place is highly variable. This effect can be stated as follows: the shear and flexural behavior of the beam at failure is significantly influenced by a number of factors, and these factors are as follows:

- 1) The developed finite element models using ABAQUS successfully replicated experimental results for slabless staircases, showing close agreement in load-deflection curves and crack patterns, with differences in ultimate load predictions ranging between 3% and 22%, demonstrating the reliability of FEM for analyzing such complex structural systems.
- 2) Although the FEM models matched experimental trends, they exhibited a stiffer response in the elastic zone, as evidenced by higher initial slopes in the load-deflection curves, particularly in specimens with triangular and staggered reinforcement configurations, highlighting the influence of modeling assumptions on stiffness estimation.
- 3) Introducing triangular steel reinforcement configurations significantly enhanced the structural capacity of slabless staircases; for example, repositioning steel bars into a triangular shape at the tread mid-span (ST-M) increased the cracking load from 10.48 kN to 13.12 kN, reflecting a 25.2% improvement, and also elevated the ultimate load by 4.8%.

- 4) Placing the triangular reinforcement in the S2 zone, at the end of the treads, proved more effective than in the S1 zone, achieving a 29.2% increase in cracking load versus 11.1% in S1, and an 18% rise in ultimate load versus 7.1%, confirming that stress concentrations are more critical at the tread ends under flexural action.
- 5) The staggered triangular reinforcement layouts (ST-L-R-1 and ST-L-R-4) delivered pronounced performance improvements, with ST-L-R-1 achieving a 43.2% increase in cracking load and a 14.5% increase in ultimate load, indicating that alternating triangular arrangements can better distribute stress and delay failure.
- 6) Removing planar steel reinforcement reduced performance, as seen in ST-M-WoP, where the cracking load dropped by 30.1% and the ultimate load decreased by 5.5% compared to ST-M, while deflections increased by up to 10.9%, underscoring the crucial role of planar reinforcement in controlling deformation and enhancing strength.
- 7) Increasing concrete compressive strength from 50 MPa to 70 MPa produced significant gains in both cracking and ultimate capacities; for instance, in ST-R, the cracking load rose by 78.9%, and the ultimate load more than doubled, increasing by 109.5%, demonstrating the direct benefit of higher concrete strength on flexural performance.
- 8) However, increased concrete strength led to a notable decrease in ductility; in the ST-L model, ductility dropped by 44% when moving from 50 MPa to 70 MPa concrete, highlighting the trade-off between higher load capacity and reduced deformation capability in high-strength concrete applications.
- 9) Partial replacement of steel reinforcement with CFRP bars in zones S1 and S2 significantly improved performance, with ST-CRS2 showing an 85.5% increase in cracking load and a 62.2% increase in ultimate load over ST-50,

confirming the effectiveness of CFRP in enhancing structural capacity where high stresses are concentrated.

- 10) Complete replacement of steel with CFRP bars, as in ST-CR, resulted in the highest gains, with cracking load improvements reaching 113.7% and ultimate load increases of 72.36%, validating CFRP bars as a viable alternative to steel for significantly boosting flexural strength in slabless staircases.
- 11) Applying CFRP sheets to the underside of stair treads enhanced both strength and stiffness, with full wrapping (ST-CS-F) increasing cracking load by 77.35% and ultimate load by 67.8%, while simultaneously reducing deflection by 48.2%, illustrating the benefits of CFRP sheets for strengthening and controlling deformations.
- 12) Nonetheless, CFRP applications generally reduced ductility; for example, full wrapping led to a 30.5% reduction in the ductility index compared to the control model ST-50, highlighting that while CFRP increases strength, it often results in a stiffer, less ductile behavior that must be considered in design.
- 13) Incorporating a mid-span landing (ST-Ln) into slabless staircases decreased performance, lowering cracking load by 19% and ultimate load by 29%, suggesting that geometric discontinuities such as landings can create stress concentrations and weaken overall structural capacity if not carefully reinforced.

5.2 Recommendation for Future Works

Extra investigation to understand the basic behavior of RC beams is required. The following suggestions are recommended:

- 1) Studying the torsion strength of slabless staircases
- 2) Investigation of the slabless staircases behavior when strengthened with CFRP sheet.

Appendix : Experimental Model Specifications for Verification

1.General

In this appendix, the simulation of slabless staircases, which was simulated by experimental method is discussed. The experimental model used for verification was designed to replicate the slabless reinforced concrete staircase configuration under flexural loading. The test setup was conducted in accordance with standard procedures to ensure accurate data collection and relevance to the numerical study.

2.Geometric Properties

Nine two-thirds-scaled RC slabless staircases were prepared within the scope of the study. The specimens were formed based on common dimensions used in practice and the limitations of the test setup as seen in Fig. 1. Because it was anticipated that this would affect strength and behavior, t_h and t_v were considered and investigated as test parameters. On the other hand, slabless stairs are constructed for aesthetic appeal. However, this fascination is lost if the thicknesses are excessive.

Number of Steps(N): 14 steps

Tread Width (t): 200 mm

Riser Height(r): 110 mm

Stair Width(b_w): 600 mm

Tread Thickness (t_h): 100 or 80 mm

Riser Thickness (t_v): 100 or 80mm

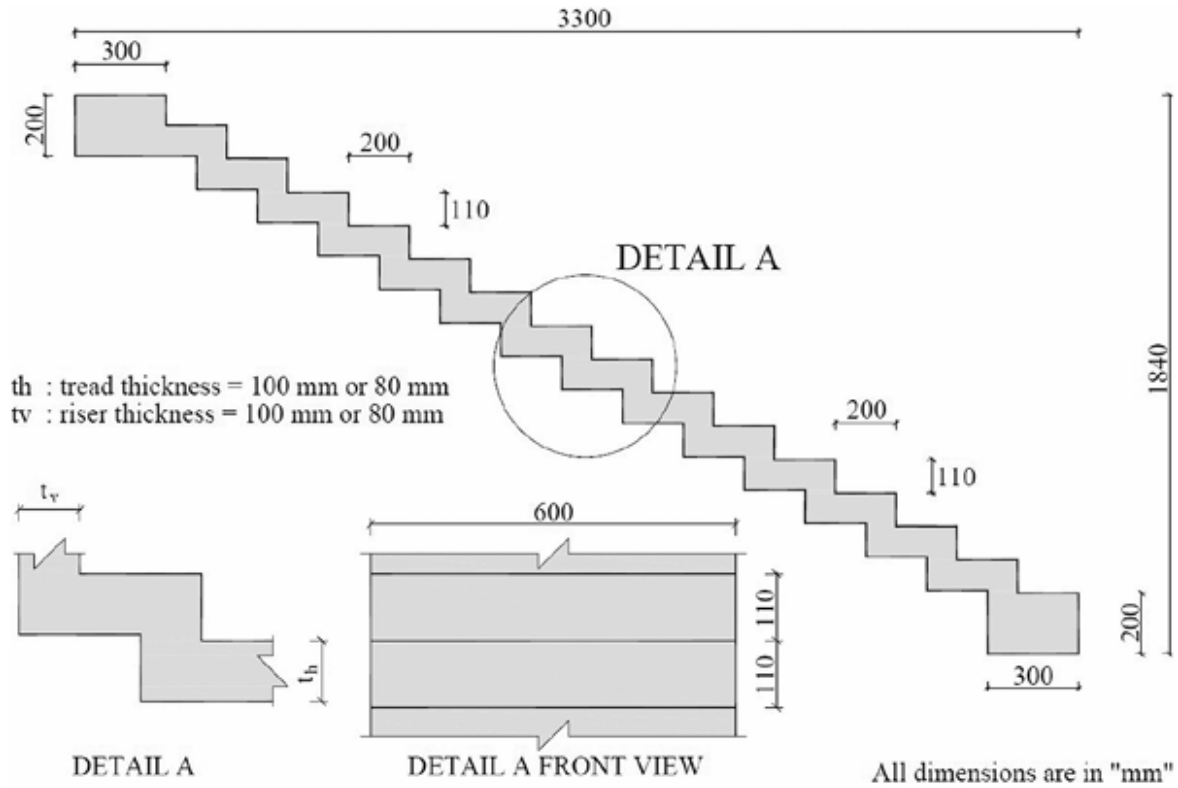


Fig. 1-Geometry of test specimens.

3.Materials

The 28-day average concrete compressive strength (f_c) of the specimens was 48 MPa, with a standard deviation of 3.7 MPa, based on 150 x 300 mm cylinder tests. On the other hand, the f_c of the specimens was 53 MPa, with a standard deviation of 2.8 MPa on the experiment day. A total of nine concrete specimens were taken for each staircase. Water- reducing admixtures were used to increase the strength and workability of concrete. Deformed steel bars were used for reinforcement. Ø8 reinforcing bars were of grade S420, which has a minimum yield strength (f_y) of 420 MPa and rupture strength (f_{su}) of 500 MPa. However, tensile tests indicated that the steel bars used in this research had f_y of 450 MPa and f_{su} of 520 MPa.

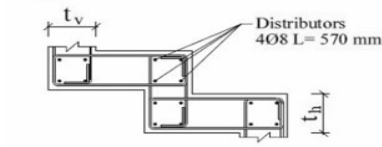
4.The reinforcement detailing

Previous research and structural reinforcement details on slabless stairs were investigated, and different reinforcement arrangements were proposed. Some of them were labor-intensive and nearly impossible to implement. For this reason, easy-to-implement reinforcement layouts were taken into consideration and four different reinforcement arrangements were selected among them as test parameters. They were called Type-t, Type-T, and Type-C

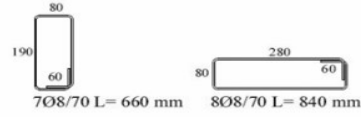
The most common and implemented reinforcement detailing was denoted by Type-t. The main reinforcements were in the form of closed loops (stirrups) for both treads and risers (Fig. 2). Closed loops were connected to each other at joints by 4Ø8 transversely located straight bars (distributors). Type-T had an alternate form of stirrup in addition to planar 6Ø8/90 straight bars. These planar bars were used to increase the stiffness and strength of stair joints (Fig. 2). Type-C was inspired from the local practice and easy to implement because closed loops were formed by two separate reinforcing bars. Distributors for 4Ø8 and planar straight bars 6Ø8/90 were also used (Fig. 3).

The location and cross-sectional area of the longitudinal reinforcement for treads and risers are summarized explicitly in Table 1 for more clarification. The test specimen notations were derived to summarize their properties. The first letter (t, T, and C) refers to the reinforcement detailing type of the specimen. The first following number, 80 or 100, stands for the thickness of the tread, and the second number, 80 or 100, stands for the thickness of the riser.

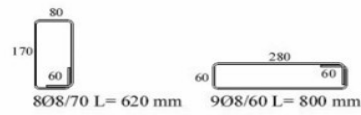
Type-t



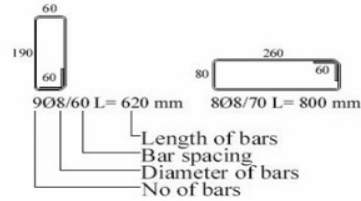
If $t_v=100$ mm and $t_h=100$ mm



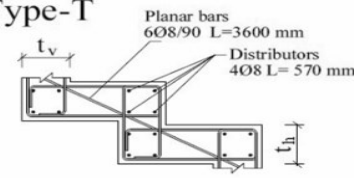
If $t_v=100$ mm and $t_h=80$ mm



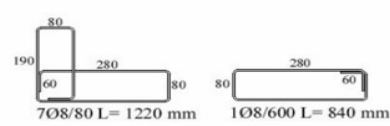
If $t_v=80$ mm and $t_h=100$ mm



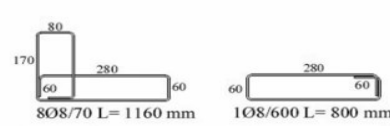
Type-T



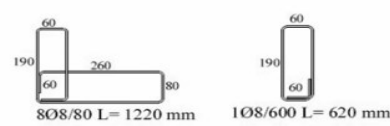
If $t_v=100$ mm and $t_h=100$ mm



If $t_v=100$ mm and $t_h=80$ mm



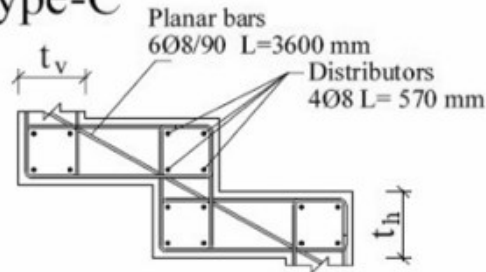
If $t_v=80$ mm and $t_h=100$ mm



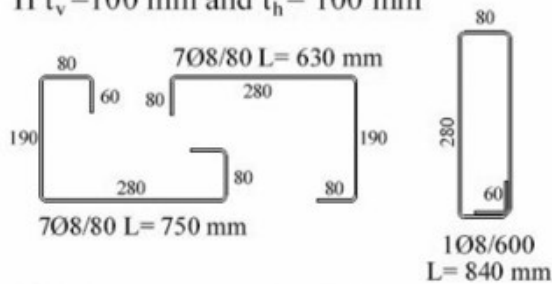
All dimensions are in "mm"

Fig. 2-Type-t and Type-T reinforcement details.

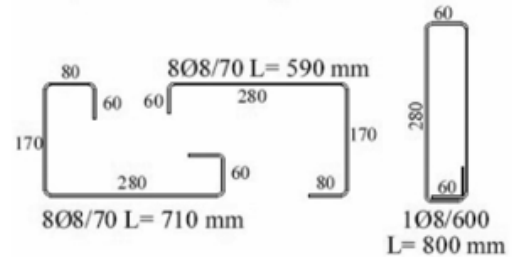
Type-C



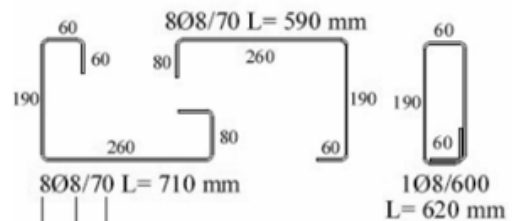
If $t_v=100$ mm and $t_h=100$ mm



If $t_v=100$ mm and $t_h=80$ mm



If $t_v=80$ mm and $t_h=100$ mm



Length of bars
Bar spacing
Diameter of bars
No of bars

Fig. 3-Type-C reinforcement details.

5. Test setup

Experiments were carried out in a closed steel frame, as illustrated in Fig. 4. Slabless staircases were positioned horizontally, different from the actual inclined position, and the test setup was designed considering this condition. Specific inclined steel pin and roller supports were provided to test specimens as simply supported. Four hydraulic jacks fed from a single source were evenly placed and positioned to apply the load perpendicular to the tread plane. Thus, the actual loading conditions were, to a large extent, simulated. Rubber pads were placed between the specimen and the hydraulic jacks to prevent local crushing. Rotations were released on the connection between the loading units and test frame so that the hydraulic jacks also rotated and kept transferring the load perpendicular to the tread surface, depending on the deformation of the specimen. The deformations perpendicular to the tread planes under each point of loading were measured with the help of linear variable differential transformers (LVDTs).

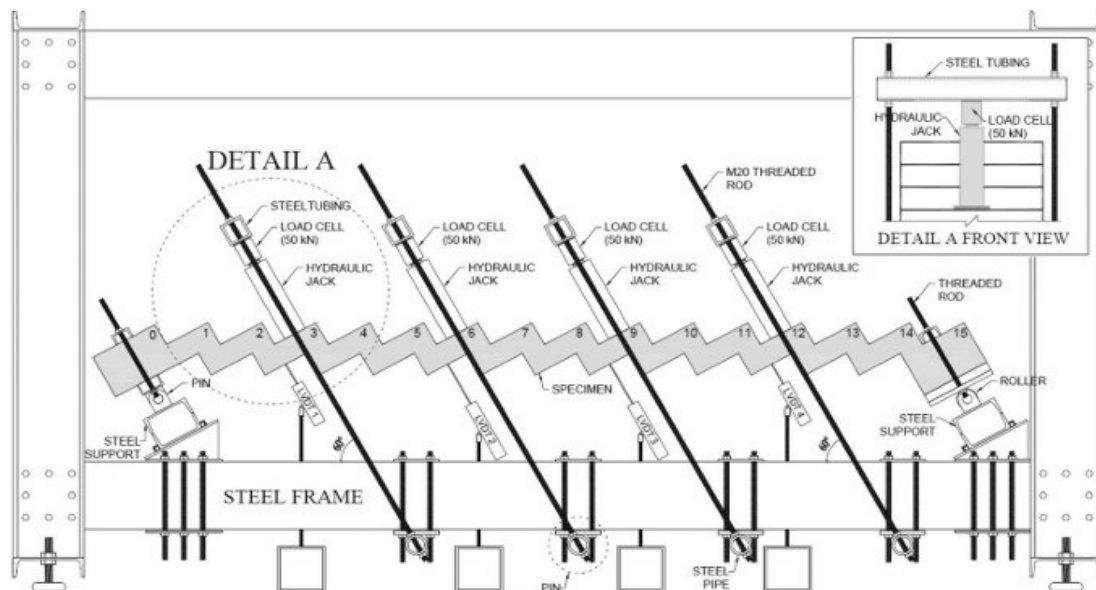


Fig. 4-Test setup.

A total of four load cells were used to measure the applied load.10 Specimens were subjected to the monotonic loading provided up to the stable stroke limit of the hydraulic jacks (approximately 130 mm) or until an abrupt decrease in the ultimate load (minimum 15%) took place within the stroke limits of the jack.

REFERENCES

- [1] Archea, J., Collins, B. L., & Stahl, F. I. (1979). *Guidelines for stair safety* (No. 120). The Bureau
- [2] Campbell, J. W., & Tutton, M. (Eds.). (2013). *Staircases: History, repair and conservation*. Routledge.
- [3] Bangash, M. Y. H. (2019). *Staircases-structural analysis and design*. Routledge.
- [4] Saenz, L. P., & Martin, I. (1961, October). Slabless tread-riser stairs. In *Journal Proceedings* (Vol. 58, No. 10, pp. 353-366).
- [5] Tegos, I. A., Panoskaltsis, V. P., & Tegou, S. D. (2013, June). Analysis and design of staircases against seismic loadings. In *4th ECCOMAS Thematic Conference on Computational Methods in Structural Dynamics and Earthquake Engineering*
- [6] Jiang, H. J., Gao, H. Y., & Wang, B. (2012). Seismic damage analyses of staircases in RC frame structures. *Advanced Materials Research*, 446, 2326-2330.
- [7] Smith, J. (2024). Orthopolygonal stair design: Principles and applications. Architectural .
- [8] Özbek, E., Kaya, Y., Bocek, M., & Aykaç, S. (2021). Flexural Behavior of Slabless Reinforced Concrete Staircases. *ACI Structural Journal*, 118(6).
- [9] <https://sl.bing.net/YLK0a048w8>
- [10] Code of practice for structural safety of building IS:875-1964, Indian Standard Institution, New Delhi
- [11] 2018 RESIDENTIAL STAIR GUIDE SECTION R311.7 STAIRWAYS R311.7.1

- [12] Sharma, S. (1993). Finite Element Analysis of Slabless Tread Riser Stairs. *Master's thesis, Department of Civil Engineering, University of Roorkee, Roorkee, India.*
- [13] Bishop, N. W. M., Willford, M., & Pumphrey, R. (1995). Human induced loading of flexible staircases. *Safety science*, 18(4), 261-276.
- [14] Saenz, J., & Martin, L. (1996). Design methodologies for slabless staircases. *Journal of Structural Engineering*, 122(5), 500-510
- [15] Solanki, H. T., "Free-Standing Stairs with Slabless Tread-Risers," *Journal of the Structural Division*, ASCE, V. 101, No. 8, 1975, pp. 1733-1738. doi: 10.1061/JSDEAG.0004150
- [16] Kerr, A., & Bishop, M. (2001). Differences in human-induced loading on floors and staircases. *Journal of Structural Engineering*, 127(4), 400-410.
- [17] Kerr, S. C., & Bishop, N. W. M. (2001). Human induced loading on flexible staircases. *Engineering structures*, 23(1), 37-45.
- [18] Kim, S. B., Lee, Y. H., Scanlon, A., Kim, H., & Hong, K. (2008). Experimental assessment of vibration serviceability of stair systems. *Journal of Constructional Steel Research*, 64(2), 253-259.
- [19] Cosenza, E., Verderame, G. M., & Zambrano, A. (2008, October). Seismic performance of stairs in the existing reinforced concrete building. In *14th world conference on earthquake engineering, Beijing, China* (pp. 12-13)
- [20] Davis, B., & Murray, T. M. (2009). Slender monumental stair vibration serviceability. *Journal of Architectural Engineering*, 15(4), 111-121.
- [21] Tegou, I. A., Panoskaltsis, V. P., & Tegou, S. D. (2013, June). Analysis and design of staircases against seismic loadings. In *4th ECCOMAS Thematic Conference on Computational Methods in Structural Dynamics and Earthquake Engineering*.
- [22] Baqi, A., & Mohammad, Z. (2013). Effect of U-Turn in Reinforced

- Concrete Dog-Legged Stair Slabs. *International Journal of Civil and Environmental Engineering*, 7(6), 479-484
- [23] Kumbhar, O. G., Kumar, R., & Adhikary, S. (2015). Effect of staircase on seismic performance of RC frame building. *Earthquakes and Structures*, 9(2), 375-390.
 - [24] Wang, X., & Hutchinson, T. C. (2018). Computational assessment of the seismic behavior of steel stairs. *Engineering Structures*, 166, 376-386.
 - [25] Özbek, E., Kaya, Y., Bocek, M., & Aykaç, S. (2021). Flexural Behavior of Slabless Reinforced Concrete Staircases. *ACI Structural Journal*, 118(6).
 - [26] Nespěšný, O., Pěňčík, J., Bečkovský, D., Vystrčil, J., & Šuhajda, K. (2021). Determination of material and elasticity constants of cement fibre boards to extend field of application. *Construction and Building Materials*, 306, 124821.
 - [27] Olivieri, C., Iannuzzo, A., Fortunato, A., & DeJong, M. J. (2022). The effect of concentrated loads on open-well masonry spiral stairs. *Engineering Structures*, 272, 114952.
 - [28] Shan, Y., Gong, Y., Wang, Y., Zhou, Q., Li, X., Ding, F., & Kuang, Y. (2024). Flexural behavior of ultra-high performance concrete (UHPC) shaped thin-plate ribbed staircases: an experimental and numerical study. *Materials and Structures*, 57(1), 18.
 - [29] Zhang, C., Huang, Z., Zhou, Y., Wang, G., Yu, T., & Huang, W. (2024). Seismic performance of novel low-damage stair system: Precast reinforced concrete stair isolated with a sliding joint. *Engineering Structures*, 298, 117061.
 - [30] Wang, Y., Sheng, D., & Wang, Y. (2024). Research on the Performance of Lightweight Prefabricated Concrete Stairs with a Special-Shaped Hollow Landing Slab. *Buildings*, 14(5), 1314.
 - [31] Hinton, E., and Owen, D.R.J., "An Introduction to Finite Element Computations", Pineridge Press limited, Swansea, U. K., 1979

- [32] Fanning, P., "Nonlinear Model of Reinforced and Post-Tensioned Concrete Beams", *Electronic Journal of Structural Engineering*, Vol.2, pp.111-119, 2001.
- [33] Kwak, H., and Filippou, F.C., "Finite Element Analysis of Reinforced Concrete Structures Under Monotonic Load", Department of Civil Engineering / University of California / Berkeley / California, USA, Report No. UCB SEMM-90/14, November, 1990.
- [34] Wischers, G., "Application of Effects of Compressive Loads on Concrete", *Betontechnische Berichte*, No.2 and 3, Duesseldorf, Germany, 1978.
- [35] Chen, W.F., "Plasticity in Reinforced Concrete", McGraw-Hill, 1982.
- [36] Hsu, L.S., and Hsu, C.T.T., "Complete Stress-Strain Behavior of High-Strength Concrete under Compression", *Magazine of Concrete Research (ASCE Journal)*, Vol.46, No.169, pp.301-312, 1994.
- [37] ASCE Committee on Concrete and Masonry Structures, "A State of the Art Report on the Finite Element Analysis of Reinforced Concrete structures", ASCE Special Publication, 1981.
- [38] Desayi, P., and Krishnan, S., "Equation for the Stress-Strain Curve of Concrete", *Journal of the American Concrete Institute*, Vol.61, No.3, pp.345-350, March, 1964.
- [39] Chen, W.F. and Saleeb, A.F., "Constitutive Equations for Engineering Materials", West Lafayette, Indiana, December 1981.
- [40] ABAQUS, "Theory Manual, User Manual and Example Manual. Version 6.10", Providence, RI. 2011.
- [41] Hillerborg, A., Modéer, M., & Petersson, P. E. (1976). Analysis of crack formation and crack growth in concrete by means of fracture mechanics and finite elements. *Cement and concrete research*, 6(6), 773-781.
- [42] Wang, T., & Hsu, T. T. (2001). Nonlinear finite element analysis of concrete structures using new constitutive models. *Computers & structures*, 79(32), 2781-2791.

- [43] Peterson P., "Riemannian Geometry". Springer: New York. 1996.
- [44] Al-Ahmed, A. H. A., Al-Zuhairi, A. H., & Hasan, A. M. (2022, March). Behavior of reinforced concrete tapered beams. In Structures (Vol. 37, pp. 1098-1118). Elsevier.
- [45] Abaqus, F. E. A. "ABAQUS analysis user's manual". Dassault Systemes, Vélizy-Villacoublay, France. 2009.
- [46] Karlsson, B.I. and Sorensen, E.P. ABAQUS, "Analysis user's guide volume II: Analysis", Pawtucket, Rhode Island, Hibbitt Publication, 2006c.
- [47] Karlsson, B.I. and Sorensen, E.P. ABAQUS, "Analysis user's guide volume IV: Elements", Pawtucket, Rhode Island, Hibbitt Publication, 2006c.
- [48] Karlsson, B.I. and Sorensen, E.P. ABAQUS, "Analysis user's manual volume V: Prescribed conditions", constraints and interactions, Pawtucket, Rhode Island, Hibbitt Publication, 2006c.
- [49] Tan, E.L. and Uy, B., "Experimental study on curved composite beams subjected to combined flexure and torsion", Journal of Constructional Steel Research. Vol.65, pp. 1855-1863, 2009.
- [50] Stolarski, T., Nakasone, Y., & Yoshimoto, S. (2018). Engineering analysis with ANSYS software. Butterworth-Heinemann.

الخلاصة

تقدم هذه الدراسة تحقيقاً عددياً شاملاً حول الأداء الانثنائي للسلالم الخرسانية المسلحة بدون بلاطات في البداية تم تطوير استراتيجية نمذجة بالعناصر المحددة (FE) والتحقق منها من خلال سلسلة من المحاكاة غير الخطية باستخدام برنامج ABAQUS. وقد تمت مقارنة هذه المحاكاة مع نتائج تجريبية مستخلصة من دراسات سابقة واردة في الأدبيات العلمية.

أظهرت نتائج التحقق وجود ارتباط قوي بين نماذج العناصر المحددة والنتائج التجريبية، لا سيما من حيث سلوك الحمل-الإزاحة وأنماط انتشار الشروخ. شملت الدراسة بشكل أساسي تأثير كل من مقاومة ضغط الخرسانة (f_c)، وأنظمة التدعيم باستخدام ألياف الكربون (CFRP)، ونوع مادة التسليح. أظهرت النتائج أن تكوينات التسليح الفولاذي المثلثية الجديدة أظهرت سلوكاً مختلفاً. حيث أدى وضع القضبان المثلثية في المنطقة S2 إلى زيادة حمل التشقق بنسبة 29.2% مقارنة بنسبة 11.1% عند وضعها في S1. بالنسبة للحمل الأقصى، تراوح الارتفاع من 38.61 كيلو نيوتن في النموذج ST إلى 40.47 كيلو نيوتن في النموذج ST-M (زيادة بنسبة 4.8%). وعند وضع التكوين المثلثي في منطقة S2، زاد الحمل الأقصى بنسبة 18% مقارنة بـ 7.1% في S1. كما أظهرت النماذج ST-L-R-1 و ST-L-R-4 زيادات في الحمل الأقصى بنسبة 14.5% و 12.9% على التوالي. زاد مقدار الإزاحة بنسبة 78.2% في منطقة S1 وبنسبة 69.2% في S2. وفي النماذج ST-L-R-1 و ST-L-R-4، ارتفع الحد الأقصى للإزاحة بنسبة 18.5% و 17.5% مقارنة بالنموذج ST. أدى إزالة القضبان المستوية إلى انخفاض حمل التشقق بنسبة 30.1% في ST-M-WoP مقارنة بالنموذج ST-M، وبنسبة 19.2% و 30.9% في النماذج ST-L-WoP و ST-R-WoP على التوالي. كما انخفض الحمل الأقصى بنسبة 5.5%، 2.1%، و 2.5% في النماذج ذاتها. في المقابل، زادت الإزاحة بنسبة 10.9%، 8.9%، و 14.2%.

أدى رفع مقاومة الخرسانة من 50 ميغاباسكال إلى 70 ميغاباسكال إلى تحسينات ملحوظة، إذ ارتفع حمل التشقق بنسبة 58.3% في النموذج ST-M-70، وبنسبة 43.4% في ST-L-70، و 78.9% في ST-R-70. كما ارتفع الحمل الأقصى بنسبة 63.8%، 79.2%، و 109.5% على التوالي.

تمت دراسة تأثير استبدال حديد التسليح بقضبان وأغشية CFRP. فقد أدى استخدام قضبان CFRP في S2 النموذج (ST-CRS2) إلى رفع حمل التشقق بنسبة 85.5% مقارنة بالنموذج ST-50، بينما أدى التدعيم المتزامن في منطقتي S1 و S2 النموذج (ST-CRS1-2) إلى زيادة حمل التشقق بنسبة 103.7%. كما أدى الاستبدال الكامل للحديد بقضبان CFRP النموذج (ST-CR) إلى تحسين حمل التشقق بنسبة 113.7%. أما

بالنسبة للحمل الأقصى، فقد زادت السعة بنسبة 62.2% في النموذج ST-CRS2 مقارنة بالنموذج ST-50 ، وارتفعت بنسبة 72.36% في النموذج ST-CR. أدى استبدال الروابط الفولاذية بين منطقتي S1 و S2 بقضبان CFRP النموذج (ST-CRL) إلى زيادة بنسبة 8.9%.

كما أسهم استخدام أغشية CFRP في تحقيق مكاسب ملحوظة، إذ أظهرت النماذج ST-CS-5 ، ST-CS-10 ، ST-CS-15 و ST-CS-15 زيادات في حمل التشقق بنسبة 28.9%، 31.84%، و 44.5% على التوالي، في حين أدى التغليف الكامل النموذج (ST-CS-F) إلى زيادة حمل التشقق بنسبة 77.35% والحمل الأقصى بنسبة 67.8%. كما انخفضت الإزاحة بشكل كبير بنسبة 48.2% مع التغليف الكامل. أدى إضافة هبوط بار ترفع متر في منتصف السلم النموذج (ST-Ln) إلى خفض حمل التشقق بنسبة 19% والحمل الأقصى بنسبة 29% مقارنة بالنموذج المرجعي بدون هبوط.

أعلى مؤشر مطيلية (5.17) سُجِّل في النموذج ST. وأدى رفع مقاومة الخرسانة إلى انخفاض المطيلية بنسبة 14.4%، 44%، و 42.3% في النماذج ST-M-70 ، ST-L-70 ، و ST-R-70 على التوالي. كما أدى استبدال الحديد بقضبان CFRP إلى خفض المطيلية بنسبة تتراوح بين 14.1% و 15.1%. وأسهمت أغشية CFRP في خفض إضافي للمطيلية بنسبة تراوحت بين 16.9% و 30.5%. ارتفعت الصلابة الابتدائية بنسبة 66.1%، 127%، و 142.25% مع رفع مقاومة الخرسانة إلى 50 ميغاباسكال، وبنسبة 185% عند استبدال الحديد بالكامل بتسليح CFRP مع الإبقاء على الركائب الفولاذية.

خلص هذا البحث إلى أن استراتيجيات التسليح الجديدة، لا سيما CFRP ، أثبتت فعاليتها في تحسين السعة الانثنائية للسلالم الخرسانية بدون بلاطات، رغم ما يصاحبها من انخفاض نسبي في المطيلية.



جمهورية العراق
وزارة التعليم العالي والبحث العلمي
كلية الهندسة/ جامعة ميسان
قسم الهندسة المدنية

دراسة عددية على سلوك الانحناء للسلالم الخرسانية المسلحة بدون بلاطات

اعداد الطالبة

رفل سعيد صبيح

بكلوريوس هندسة مدني 2020

رسالة

مقدمة الى كلية الهندسة في جامعة ميسان
كجزء من متطلبات الحصول على درجة الماجستير في علوم الهندسة المدنية / الانشاءات

2025

المشرف على الرسالة:

أ.د عبدالخالق عبد اليمه جعفر